Scaling Proprioceptor Gene Transcription by Retrograde NT3 Signaling

Inauguraldissertation

zur

Erlangung der Würde eines Doktors der Philosophie

vorgelegt der

Philosophisch-Naturwissenschaftlichen Fakultät

der Universität Basel

Von

Jun Lee

aus Wiesbaden, Deutschland

Basel, 2011

Genehmigt von der Philosophisch-Naturwissenschaftlichen Fakultät
auf Antrag von:

Prof. Dr. Silvia Arber

(Dissertationsleitung)

Prof. Dr. Pico Caroni

(Korreferat)

Basel, den 21. Juni 2011

Prof. Dr. Martin Spiess

(Dekan)

For Sarah, who is always there.

For Dieter Schade, who left too sudden.

For Grandma.

Table of Contents

Thesis Summary

The assembly of neuronal circuits depends critically on the sequential activation of transcriptional programs in distinct neuronal subpopulations. In the spinal cord, retrograde signaling interactions from the periphery have been shown to be essential for the onset of these programs and the establishment of specific sensory-motor connectivity (Lin et al., 1998; Wenner and Frank, 1995). Target-induced transcriptional programs of the ETS transcription factor family control several important aspects of late motor circuit assembly in the spinal cord, both in spinal motor neurons as well as in proprioceptive sensory neurons, two neuronal subpopulations connected in the spinal monosynaptic reflex circuit (Arber et al., 2000; Livet et al., 2002; Patel et al., 2003; Vrieseling and Arber, 2006).

This study provides a genome-wide analysis of target-induced gene cascades in proprioceptive afferents and defines in an unbiased way the pathways linking target-derived factors to central motor circuit assembly. We used gene expression profiling of purified proprioceptive afferents in combination with Affymetrix chip technology to study genes regulated by peripheral neurotrophin 3 (NT3). Data mining of our results demonstrates that several parallel signaling pathways influence differentiation of proprioceptive afferents retrogradely. Thus these findings suggest that NT3 does not solely induce the transcriptional program orchestrated by the ETS transcription factor Er81 in proprioceptive afferents, but also triggers additional pathways, which may influence connectivity of motor circuits in the spinal cord in a retrograde manner.

In addition to its expression in proprioceptors, Er81 has also been shown to be expressed in a subpopulation developing cortical neurons. In a collaborative study with the laboratory of Francois Guillemot, the second part of this thesis focuses at elucidating the role of *Er81* in these neurons and our results provide deeper insights into the specification of rostral Cajal-Retzius cells in the developing cortex.

1. Aim of the Thesis

Biology, especially the field of neurobiology, has benefited greatly from the recent advantages in molecular biology and cellular imaging and thus has brought us closer to understanding the molecular and functional logic of neuronal circuits. Sophisticated labeling techniques as well as state of the art loss-of-function or gain-of-function analysis are enabling us to dissect specific neuronal circuits at great detail. However, targeted manipulation of cell types not only requires knowledge about individual functional or morphological properties, but for this work, the identification of specific molecular markers is of key importance.

The aim of this thesis was to reveal genes involved in the specification of distinct primary sensory afferent populations during development, with an emphasis on characterizing the genetic pathways activated by target derived retrograde signaling interactions in the monosynaptic stretch reflex circuit of the spinal cord. In doing so, we were especially interested in late aspects of neuronal circuit development, specifying the functional and synaptic properties of this circuit. Furthermore, we investigated the plastic properties of the system in the adult by asking how exercise might reshape the molecular information of the involved sensory neurons. The information gained through the present work will provide many novel entry points into studying the connectivity of spinal cord networks throughout development.

2. Introduction

The nervous system is composed of interconnected neuronal circuits, which ultimately orchestrate our perception and behavior. Individual neuronal circuits are specialized in specific neuronal functions ranging from sensory perception, simple reflexes and rhythmic movement control to cognitive processes such as emotion, learning and memory. The function of neuronal circuits is largely determined by the integrity of the circuit architecture, which is based on selective synaptic connections between neurons. The main layout for neuronal circuits is established early during embryogenesis and early development and is generated by the specification of distinct neuronal types and subsequent circuit assembly. The development of the nervous system is a continuous process, which is highly organized and underlies the initial formation of neuronal circuits. During development, the connections between subpopulations of neurons are established through multiple coordinated events. These developmental processes are organized both spatially and temporally and form the basis for the formation of specific neuronal circuits in the adulthood.

Neuronal circuit assembly is characterized by a series of interdependent and characteristic developmental steps ((Albright et al., 2000; Dasen, 2009; Jessell and Sanes, 2000; Ladle et al., 2007), **Fig.1**). First of all, the generation of neurons is a critical step for later circuit assembly, which involves processes such as neural induction and neurogenesis. In the following stages, newly born neurons become progressively specified to give rise to a particular neuronal cell types. This process of neuronal specification is regulated in a spatio-temporal manner by extrinsic and intrinsic factors, which initially define the progenitor and subsequently postmitotic identity of neuronal cells arising from these progenitors.
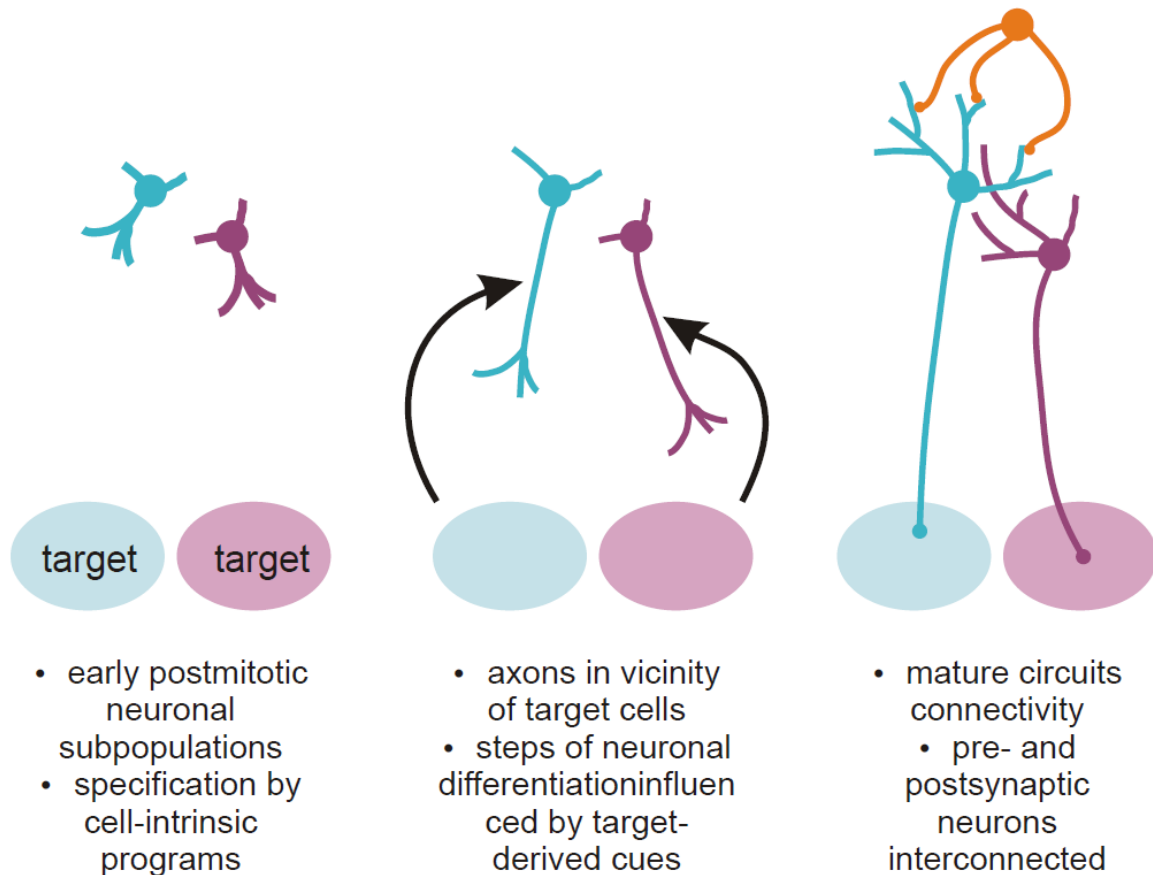
Fig. 1: Sequential steps in neuronal differentiation and connectivity

Postmitotic neurons migrate to specific locations in the central nervous system and also initiate neurite outgrowth. Neurons extend axonal projections towards the target region, a process followed by selection of the appropriate target neurons within the termination zone. In parallel, neurons develop highly specific dendritic trees receive synaptic connections. All these steps are essential to set up selective connectivity between individual neurons and are likely to be orchestrated by interactions of cell autonomous as well as extrinsic factors during development. In general, the phases of circuit assembly such as axonal path finding and dendritic patterning are activity-independent and are controlled by a variety of axon guidance molecules as well as neurotrophic factors. Finally, the process of synaptogenesis occurs between the neurons. Synaptogenesis includes the formation of a presynaptic neurotransmitter release site,

postsynaptic density assembly as well as the alignment of the newly formed pre- and post-synaptic specializations.

Over the last decades, studies at the molecular level have revealed a large array of evolutionarily conserved genes, which have critical roles in the development of the nervous system and during the described steps of neuronal circuit assembly. A particular advantageous system to assay the involvement of specific molecules in specified developmental steps of neuronal circuit assembly is the monosynaptic reflex circuit in the spinal cord. This is mainly due to the simple reflex circuit architecture, in its most simple description comprising two neuronal classes. A large body of work characterizes this circuitry at the level of both circuit organization as well as physiological function in great detail. At present, the monosynaptic stretch reflex circuit in the spinal cord is one of the best-understood neuronal circuits within the vertebrate nervous system (Brown, 1981; Eccles et al., 1957; Glover, 2000; Sherrington, 1910).

2.1 Development of the proprioceptive reflex circuit

2.1.1 Basic Anatomy and connectivity in the spinal cord

In the spinal cord, the axons of sensory neurons of dorsal root ganglia (DRG) terminate in distinct layers, depending on their functional characteristics. Cutaneous afferents are passing on cutaneous and noxious stimuli from the periphery to the central nervous system, terminating in the superficial layers of the dorsal horn (Mirnics and Koerber, 1995; Molliver et al., 1995). Mechanoreceptive afferents convey pressure-related information towards the deeper layers of the dorsal horn (Mirnics and Koerber, 1995; Sanes and Yamagata, 1999). Proprioceptive afferents, receiving feedback from sensory organs in individual muscles, are the most ventrally projecting sensory neurons,

with group Ia and II proprioceptive afferents forming connections to interneurons in the intermediate zone of the spinal cord and to motor neurons in the deep ventral horn and group Ib proprioceptive afferents projecting to the intermediate zone of the spinal cord (Maier, 1997; Ozaki and Snider, 1997; Sanes and Yamagata, 1999; Zelena, 1994; Zelena and Soukup, 1977).

Interestingly, different classes of DRG sensory neurons do not only exhibit unique central and peripheral connectivity. They also can be distinguished by selective expression of neurotrophic factor receptors (Farinas, 1999). Cutaneous afferents are marked by the tyrosine kinase receptor TrkA (Minichiello et al., 1995; Molliver et al., 1995). In contrast, mechanoreceptive neurons express the receptor TrkB and proprioceptive afferents are marked by the expression of TrkC (Klein et al., 1994; Marmigere and Ernfors, 2007; Minichiello et al., 1995). These different receptors bind to different ligands present in the corresponding peripheral targets of these neurons. Nerve growth factor (NGF) binds to TrkA, brain-derived neurotrophic factor (BDNF) binds to TrkB, and neurotrophin 3 (NT3) mainly activates TrkC with some crossing activities to TrkA and B (Bibel and Barde, 2000; Huang and Reichardt, 2001; Reichardt, 2006). In addition, distinct subpopulations of DRG neurons coexpress the low affinity receptor p75, which – either alone or in combination with a Trk receptor - also interacts with all neurotrophins (Reichardt, 2006), adding another layer of complexity to the system. It should be mentioned that an additional population of DRG neurons expresses the receptor tyrosine kinase Ret, which signals through glia cell line derived neurotrophic factor (GDNF) (Luo et al., 2007).

2.1.2 Development and diversity of sensory neurons

Developmentally, all DRG sensory neurons arise from neural crest cells (NCC) whose induction involves bone morphogenetic protein (BMP) and Wnt signaling (Lee et al., 2004; Marmigere and Ernfors, 2007). Expressing the common

transcription factor islet1 (*Isl1*) (Avivi and Goldstein, 1999; Pfaff et al., 1996), these cells derive from the dorsal neural tube during early embryonic development and subsequently settle next to the neural tube to form the developing DRG (Marmigere and Ernfors, 2007). During proliferation, neurogenesis occurs in three successive waves. The first two waves depend on the joint activities of the basic-helix-loop-helix transcription factors neurogenin 1 (*ngn1*) and neurogenin 2 (*ngn2*), with ngn2 initiating the first wave giving only rise to TrkB/TrkC proprioceptive and mechanoreceptive sensory neurons. The second wave is being initiated by ngn1 and results in the generation of TrkA nociceptive and thermoreceptive sensory neurons as well as TrkB/TrkC neurons (Frank and Sanes, 1991; Ma et al., 1999). Cells of the third wave originate from boundary cap cells and result almost exclusively in a small population of TrkA DRG neurons as well as peripheral glia (Maro et al., 2004). However, it should be noted that these steps only define the fate of DRG neurons, not their competence.

2.1.3 Target derived mechanisms of sensory neuron development

The assembly of neuronal circuits represents a sequential process, during which neuronal subpopulations initiate the establishment of cell-type specific axonal trajectories, project towards their postsynaptic neuronal targets, elaborate terminal branches and establish synaptic connections. Many aspects of neuronal differentiation are regulated by cell-intrinsic programs, which are set up at stages when progenitor cells proliferate and give rise to postmitotic neuronal populations (Marmigere and Ernfors, 2007). These intrinsic cell type specific differences are often known to be reflected at the level of gene expression, where an individual cell type expresses a unique set of genes, allowing it to steer the initial axon guidance decisions toward the target region without additional interventions and adjustments at the gene expression level.

As axons extend towards their target region, they have to interpret and integrate various axon guidance cues along their path (Dickson, 2002). While many of the downstream responses occur only locally (Huber et al., 2003), there are however signals acting retrogradely on the cell body (Hippenmeyer et al., 2004). For example, primary sensory neurons in somato-sensory systems project to innervate various types of peripheral sense organs and relay information measured at these sensory terminals directly to distinct neuronal populations in the central nervous system. This principle applies to many different types of primary sensory neurons, including trigeminal sensory neurons innervating whiskers or dorsal root ganglia (DRG) sensory neurons innervating end organs in the skin and muscle among other targets (Hodge et al., 2007; Patel et al., 2003). Sensory neurons detect and relay functionally distinct information. These differential properties also manifest themselves at the level of gene expression, leading to the expression of distinct transcriptional factors and transmembrane receptors in functionally diverse sensory neuron subsets (Ernsberger, 2009; Luo et al., 2007; Patel et al., 2003). One of the most well studied receptor families in

the context of sensory neuron diversification are transmembrane receptors binding to neurotrophic factors (Bibel and Barde, 2000; Reichardt, 2006).

A distinct group of neurotrophic factors are the neurotrophins, four closely related proteins sharing homologies in sequence and structure: NGF (Levi-Montalcini and Booker, 1960), BDNF (Barde et al., 1982; Hofer and Barde, 1988), NT3 and NT4 (Hohn et al., 1990; Ip et al., 1992; Maisonpierre et al., 1990). Acting through activation of the previously mentioned Trk receptors as well as the receptor p75 the neurotrophins play an essential role in survival and development of neurons (Bibel and Barde, 2000; Reichardt, 2006; Tucker et al., 2001). For instance, the tyrosine kinase receptors TrkA and TrkC are expressed by functionally distinct DRG sensory neuron populations and during development, survival of these neurons is regulated by the target-derived factors nerve growth factor (NGF) and Neurotrophin-3 (NT3). More specifically, NGF provided by target structures in the skin regulates neuronal survival of TrkA expressing small diameter sensory neurons (Crowley et al., 1994), whereas NT3 plays important roles in promoting neuronal survival of TrkC expressing proprioceptors projecting to mechanoreceptive sense organs embedded within skeletal muscles (Ernfors et al., 1994; Farinas et al., 1994; Tessarollo et al., 1994).

Notably, peripheral neurotrophic signals are known to induce expression of the ETS transcription factors Er81 and Pea3 in distinct subpopulations of DRG neurons (Sharrocks, 2001) as well as motor neuron pools several days after these neurons become postmitotic (Arber et al., 2000; Haase et al., 2002; Lin et al., 1998; Livet et al., 2002; Patel et al., 2003). Within the spinal cord both transcription factors control distinct aspects of monosynaptic circuit assembly (Arber et al., 2000; Livet et al., 2002; Vrieseling and Arber, 2006). Induction of Er81 in proprioceptive DRG neurons is mediated by peripheral NT3 (Patel et al., 2003) and in *Er81* or in *NT-3/Bax* mutant mice, Ia proprioceptive afferents fail to invade the ventral horn of the spinal cord, thus resulting in an absence of synaptic connections to motor neurons (Arber et al., 2000; Patel et al., 2003). In addition, induction of Pea3 in MNs is mediated by target derived Glial cell line

derived neurotrophic factor (GDNF) (Haase et al., 2002; Livet et al., 2002) and in distinct cervical MN pools, Pea3 was shown to be necessary for the control of dendrite patterning and the selectivity of group Ia afferent connectivity (Vrieseling and Arber, 2006). These results imply that Er81 and Pea3 both control certain aspects of late sensory or motor neuron differentiation at stages when DRG and MNs become dependent on target derived signals, suggesting that controlled induction of Er81 and Pea3 in distinct subpopulations could be necessary for the control of late aspects of neuronal differentiation, such as invasion and branching within a target region.

Interestingly, other parts of the CNS also express Er81 and Pea3 in distinct subpopulations of cells. But their role during development in these regions has not been analyzed in more detail. Nevertheless, a growing body of work has been dedicated towards the involvement of neurotrophins in the late aspects of neuronal differentiation, which intersect with the initial transcriptional profiles in neuronal subpopulations (Huang and Reichardt, 2001; Lu et al., 2005; Sharma et al., 2010a). However, information about how profound these changes are at the gene expression level in identified neuronal populations at the genome-wide level is currently sparse and filling this gap is one of the main goals of this thesis.

2.2 Introduction to the monosynaptic stretch reflex circuit

A critical action of spinal reflexes is the linkage of sensory information from the periphery to central motor units in order to achieve coordination of movement. This important "body sense" is called proprioception, which provides central feedback on how one own limbs are oriented in space. In more detail, proprioception is an internal representation of static positions of the body as well as changes in body movement. Loss of proprioception is typically associated with impairments in postural stability, motor planning and motor control, showing that specific sensory input is central for the regulation and control of coordinated

movements. This was first proposed by Charles Sherrington in the beginning of the 20th century when he stated that complex movements were based on basic units of elemental and stereotypic movement units that get recruited upon activation of sensory receptors in the periphery (Sherrington, 1906). As a famous example, the monosynaptic stretch reflex circuit controls stereotyped sensory-motor behavior (Brown, 1981; Eccles et al., 1957).

A standard test to assay the stretch reflex circuitry is a so called 'functionality test', in which one taps on the patellar tendon, which connects the kneecap to the shin bone. This tapping in turn results in the reflexive extension of the lower leg. This spinal reflex involves the interplay of a sensory and a motor unit, which causes a contraction of muscle as a result of changes in the length and/or tension of the respective muscle. The sensory information on the current state of muscle contraction is transmitted from the periphery from intrafusal muscle fibers to the central motor unit through the proprioceptive afferents of the DRG (Brown, 1981; Eccles et al., 1957), which provide the basis for this kind of sensory integration in the spinal cord.

The motor unit in the spinal cord comprises α-motor neurons and the corresponding innervated extrafusal muscle fibers at the neuromuscular junction (NMJ) of the respective muscle. The cell bodies or α-motor neurons are located in the ventral horn of the spinal cord where they form characteristic cell clusters referred to as motor neuron pools (Landmesser, 2001). Proprioceptive sensory neurons consist of two major classes, which are distinguished by their axonal projection into the spinal cord and their specific association peripheral transduction cells (**Fig. 2**; (Brown, 1981; Zelena, 1994)). The first group - Ia afferents - form two major termination zones: A) in the ventral spinal cord where Ia proprioceptive afferents form direct excitatory connections to α-motor neurons (Brown, 1981; Eccles et al., 1957; Frank and Wenner, 1993; Glover, 2000); B) in the intermediate spinal cord where group Ia collaterals establish synapses onto interneurons of the Clarke's column which in turn project to granule cells in the

cerebellum (Hantman and Jessell, 2010). Notably, only group Ia and II proprioceptive afferents form direct monosynaptic connections with α-motor neurons and these connections are known to exhibit a high degree of selectivity with respect to the contacted motor neuron pool (Brown, 1981; Eccles et al., 1957; Frank and Wenner, 1993; Glover, 2000). In the periphery, group Ia proprioceptive afferents innervate intrafusal muscle spindles, small encapsulated spindle-like shaped sensory mechanoreceptors. Muscle spindles are sensitive to changes in muscle length and are embedded in parallel within extrafusal muscle fibers (Maier, 1997; Zelena, 1994). The second group - Ib proprioceptive afferents - innervate Golgi tendon organs (GTOs) which are located at the junction between muscle fibers and tendon. Golgi tendon organs are sensitive to changes in muscle tension (Zelena and Soukup, 1977).
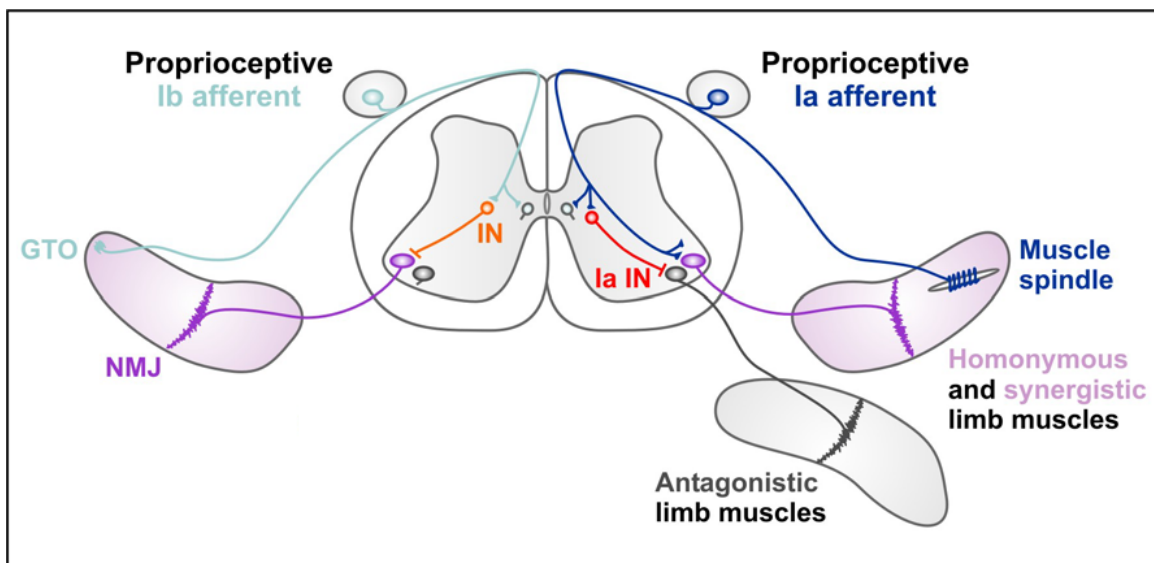
Fig. 2: Spinal reflex circuitry of proprioceptive sensory neurons

Central and peripheral projections of group Ia (blue) and Ib (light blue) proprioceptive DRG neurons. Left: group Ib afferents innervate Golgi tendon organs (GTO) in the periphery at the myo-tendinous junctions of skeletal limb muscles and project centrally to the intermediate spinal cord to form synapses with interneurons (orange), thus indirectly connecting with spinal α-motor neurons (purple). Right: group Ia afferents innervate muscle spindles at the periphery and form centraly direct monosynaptic connections to homo- and heteronymous α-motor neurons (purple). α-motor neurons projecting to antagonistic muscles (grey) are innervated in a disynaptic fashion through Ia inhibitory interneurons (red). Abbreviations: GTO = Golgi Tendon Organ; IN = interneuron; NMJ = neuromuscular junction. (Adapted from Arber et al., 2000.)

At the circuit level, group Ia afferents form specific central synapses with α-motor neurons innervating the same muscle, which is referred to as homonymous connections. In addition, group Ia afferents connect to motor neurons innervating muscles with a similar mechanical function, representing heteronymous connections. In contrast, so called 'antagonistic' α-motor neurons do not receive direct excitatory input from group Ia afferents from these two functionally related muscle groups, but instead receive indirect inhibitory input through group Ia afferents that synapse onto GABAergic interneurons in the spinal cord (Frank and Wenner, 1993; Glover, 2000; Wenner and Frank, 1995). Notably, the specificity of this neuronal connectivity is crucial for appropriate sensory-motor processing in order to control the contraction of specific muscles. The characteristic developmental phases of the monosynaptic stretch-reflex circuit assembly comprise the initial axon outgrowth to muscle targets in the periphery (Tessier-Lavigne and Goodman, 1996), the specific selection of the termination zone within the corresponding target regions (Sanes and Yamagata, 1999) as well as the selective synapse formation in the spinal cord (Smith and Frank, 1988). Activity of this circuit is not needed to establish specific synaptic connections (Mendelson and Frank, 1991), suggesting molecular cues at work in the formation of this circuit.

In summary, the spinal monosynaptic reflex circuit in its most simple illustration is composed of two neuronal classes, namely the α-motor neurons and group Ia proprioceptive afferents. This simple stretch reflex circuit contributes critically to motor behavior by controlling the appropriate movement and its feedback at any given time. Altogether, the monosynaptic stretch reflex circuit therefore represents an optimal system to investigate the molecular basis of circuit assembly during development.

3. Target derived effect of NT3 on transcriptional regulation in the spinal monosynaptic reflex circuit

3.1 Introduction

The prominent role of NGF and NT3 in regulating DRG sensory neuron survival has prevented genetic studies on elucidating possible other roles of neurotrophin signaling pathways in neuronal differentiation and connectivity. However, elegant studies and the insightful observation that cell death of DRG sensory neurons can be successfully prevented by coincident mutation of neurotrophins and the proapoptotic gene Bax, have opened new avenues allowing studies on non-survival functions of NGF and NT3 signaling pathways (Patel et al., 2000; Patel et al., 2003). Analysis of $NGF^{-/-}Bax^{-/-}$ mutant mice for example revealed an important role of NGF signaling in peripheral target invasion and branching, but no role in the establishment of central trajectories of TrkA^{on} sensory neurons (Patel et al., 2000). In contrast, retrograde NT3 signaling to proprioceptive sensory neurons innervating muscular sense organs is instrumental in setting up the appropriate central trajectory of group Ia proprioceptive afferents to project and establish connections with motor neurons in the ventral spinal cord (Patel et al., 2003). Together, these findings provide evidence that retrograde signaling by peripheral neurotrophic factors influences the maturation of sensory circuits in pronounced ways, and raise the question of the identity of the transcriptional pathways in DRG sensory neuron populations downstream of Neurotrophins implementing the various cell-type specific morphological programs and connections.

Small diameter TrkA expressing DRG sensory neurons make up the majority of all neurons within a DRG (~80-90%; (Ernsberger, 2009; Farinas et al., 1998; Snider, 1994)), and it has therefore been possible to carry out gene expression profiling experiments by direct isolation and comparison of entire wild-type and

NGF$^{-/-}$Bax$^{-/-}$ mutant DRG in order to characterize transcriptional pathways downstream of NGF signaling (Guo et al., 2011). It is now known that intricate transcriptional signaling programs are central players in reading out and translating retrograde NGF-signaling in TrkA^{on} sensory neurons (Guo et al., 2011; Luo et al., 2007). TrkC^{on} proprioceptive afferents make up a minority of all DRG neurons (~10-20% depending on the spinal level (Ernsberger, 2009; Farinas et al., 1998; Snider, 1994))) and it has therefore not been feasible to acquire good transcriptional profiles by simple comparison of entire DRG from wild-type and *NT3$^{-/-}$Bax$^{-/-}$* mutant mice. Nevertheless, a study on candidate genes with known roles in proprioceptor differentiation showed that the expression of the ETS transcription factor Etv1 is induced by retrograde NT3 signaling in proprioceptive afferents (Patel et al., 2003) and *Etv1* mutant mice show defects in the establishment of proprioceptive afferent trajectories into the ventral spinal cord (Arber et al., 2000). It remains unknown however how proprioceptive afferents respond more generally to retrograde NT3 signaling by adjusting transcriptional pathways and whether variation in the levels of peripheral NT3 is able to modulate gene expression specifically within proprioceptive afferents.

In this study, we establish a strategy to dissociate and purify proprioceptive afferents using a genetic green fluorescent protein (GFP) tag selectively expressed in DRG proprioceptive afferents but not in non-proprioceptive cells of the DRG. We exploit this genetic tool to compare genome-wide transcriptomes of purified proprioceptors isolated from different *NT3* signaling mutant mouse strains by Affymetrix chip technology. Taken together, our study aims at identifying genome-wide transcriptional cascades in proprioceptors, specifically regulated by NT3 signaling and thereby providing evidence for the pronounced regulatory roles of target-derived factors in the regulation of neuronal subtype specific transcriptional programs.

3.2 Results

3.2.1 TrkC Bac line as a reporter line for TrkCon proprioceptive neurons

To isolate genes with enriched expression in DRG proprioceptive afferents, we made use of a GENSAT BAC transgenic mouse line, in which the expression of enhanced green fluorescent protein (GFP) is controlled by genomic regulatory elements of the neurotrophic factor receptor TrkC ($TrkC^{GFP}$) (Gong et al., 2003). We first determined the faithfulness of transgene expression in order to verify its association with proprioceptive afferents in the DRG. Costaining with antibodies targeting GFP and TrkC revealed that only a subpopulation of TrkC neurons are GFP positive (**Fig. 3B**), suggesting that only the proprioceptive population of TrkC neurons might be labeled. Because the expression of the Runt domain transcription factor Runx3 has previously been shown to be highly restricted to proprioceptive DRG neurons (Chen et al., 2006; Kramer et al., 2006), we next determined the overlap between Runx3 and GFP expression in $TrkC^{GFP}$ transgenic mice. We found that in p0 lumbar DRG, the majority of GFP^{on} DRG neurons coexpressed Runx3, and conversely, also most $Runx3^{on}$ neurons were associated with GFP expression (**Fig. 3A**), providing support for the selective expression of the GFP transgene in proprioceptors.

With this knowledge in hand, we crossbred our GFP line with NT3 transgene (Taylor et al., 2001) and mutant (Farinas et al., 1994) mouse lines in order to specifically label proprioceptive DRG neurons in these mouse lines for FACS purification and subsequent Affymetrix analysis (Haeberle et al., 2004; Okaty et al., 2011). In addition, we harvested wild type cells ($TrkC^{GFP}$ only) at additional time points - namely E14, E16 and p4 - enabling us to generate a wild type time course profile of genes of interest (**Fig. 4**).

16
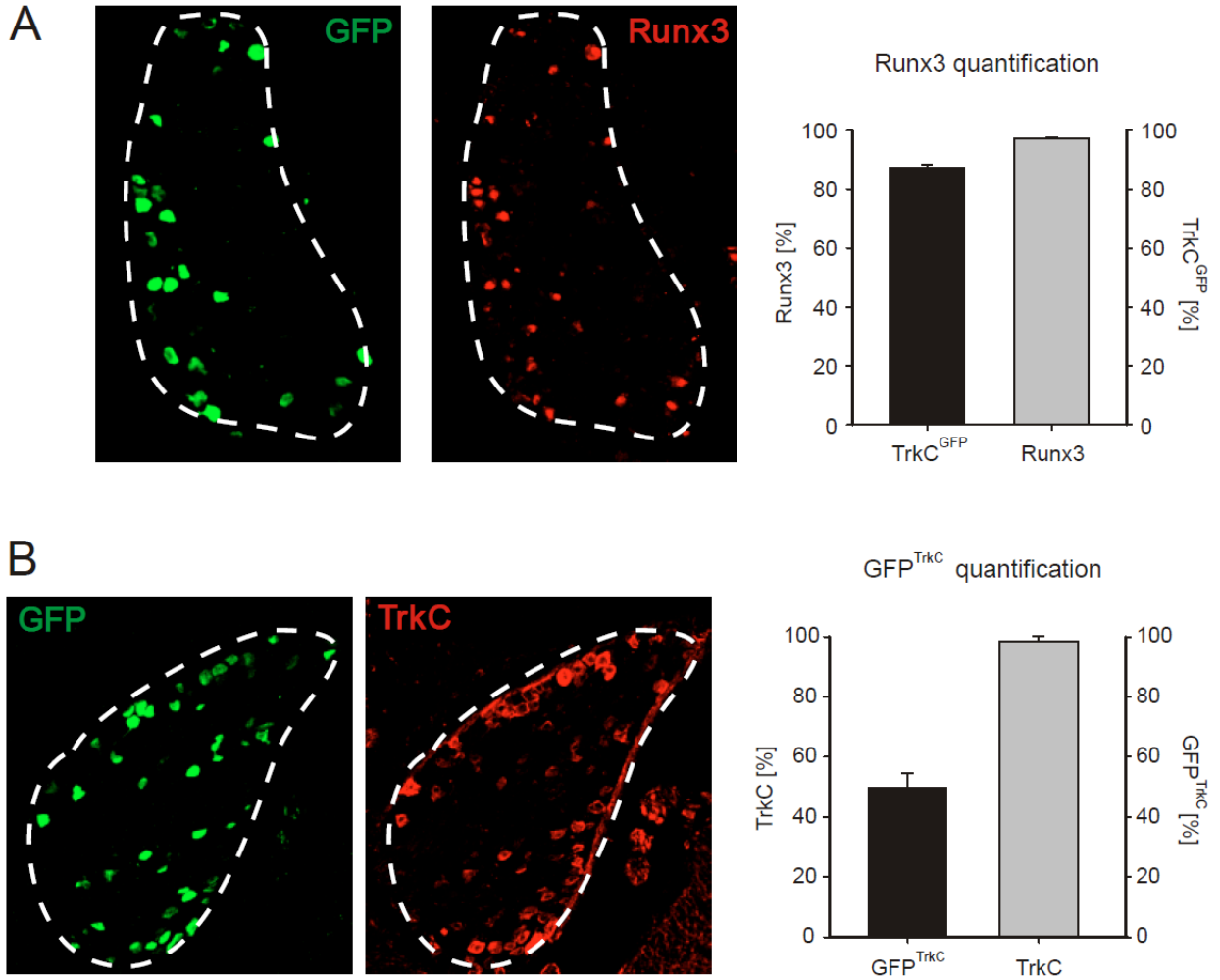
Fig. 3: *TrkC^GFP* BAC line shows enriched expression in proprioceptors
(A) Immunohistochemisty to quantify GFP (left) and Runx3 (right) on representative lumbar DRG section from p0 *TrkC^GFP* BAC transgenic mouse line. Quantification of percentage of Runx3^on cells co-expressing GFP (black bar: 86.4% ± SEM) and of percentage of GFP^on neurons co-expressing Runx3 (grey bar: 97.6% ± SEM) in p0 *TrkC^GFP* mice (n=3 animals; >20 sections each)
(B) Immunohistochemisty to quantify GFP (left) and TrkC (right) on representative lumbar DRG section from p0 *TrkC^GFP* BAC transgenic mouse line. Quantification of percentage of TrkC^on cells co-expressing GFP (black bar: 49.6% ± SEM) and of percentage of GFP^on neurons co-expressing TrkC (grey bar: 98.5% ± SEM) in p0 *TrkC^GFP* mice (n=3 animals; >20 sections each)
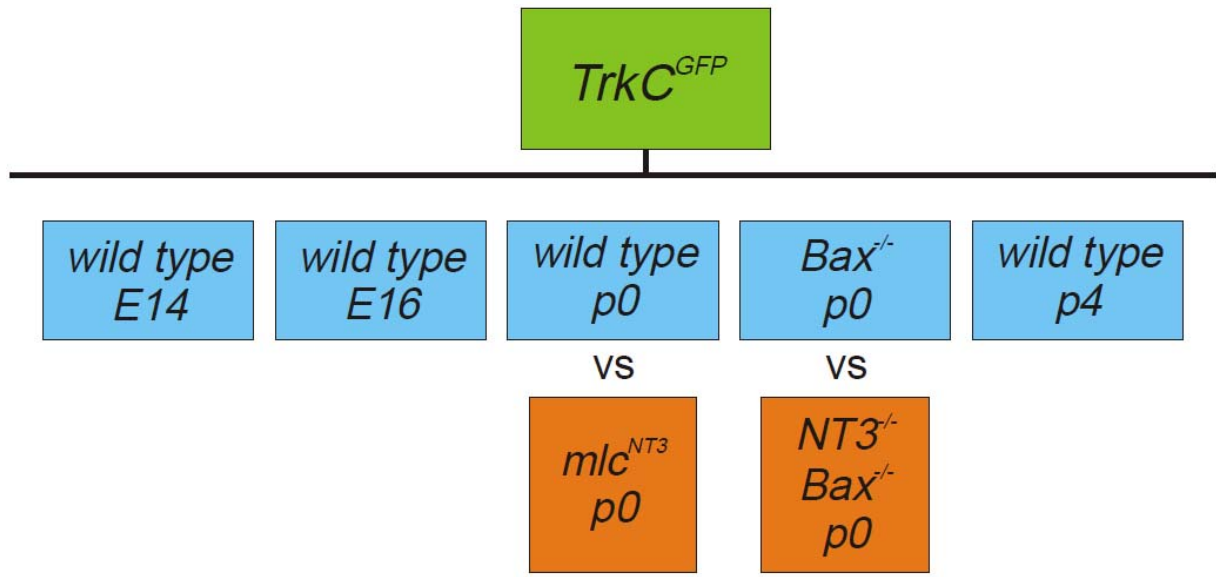
Fig. 4: Breeding scheme

Displaying the various conditions generated for FACS and subsequent Affymetrix genechip analysis.

3.2.2 Distribution of Trk receptors among DRG sensory neurons

While we expected that the absence of NT3 would have the biggest impact on neurons within the population of TrkC positive population, we were also aware of the fact that NT3 is able to activate other Trk receptors as well as the p75 receptor (Bibel and Barde, 2000; Reichardt, 2006). However, whereas the distribution of the Trk receptors has been well documented for the embryonic stages (Ernsberger, 2009), the postnatal distribution of the Trk receptors and the p75 receptor within the DRG has been less well studied. Bearing in mind the fact that p75 is coexpressed with a certain percentage of Trk receptors we considered the postnatal distribution of p75 to be important. To quantify it we co-stained p4 wild type DRG with antibodies targeting different Trk receptors and p75 **(Fig. 5)**.

The quantification of the relative population size of each receptor revealed that the percentage of TrkC and TrkB neurons postnatally is in line with previously published ratios at earlier developmental stages (Ernsberger, 2009). However, the percentage of TrkA neurons is smaller than at earlier stages (**Fig. 5B**), most likely due to an increase in Ret+ neurons at these later stages (Luo et al., 2007; Molliver and Snider, 1997). While within the TrkA and TrkC population, only a subgroup of neurons coexpresses the p75 receptor, almost all TrkB neurons were p75 positive (Fig. **5A**). In general, the distribution of p75 and the nonTrkC receptors implies that NT3 might carry out its effect differently in various non-proprioceptive subpopulations in addition to its activity on proprioceptors.
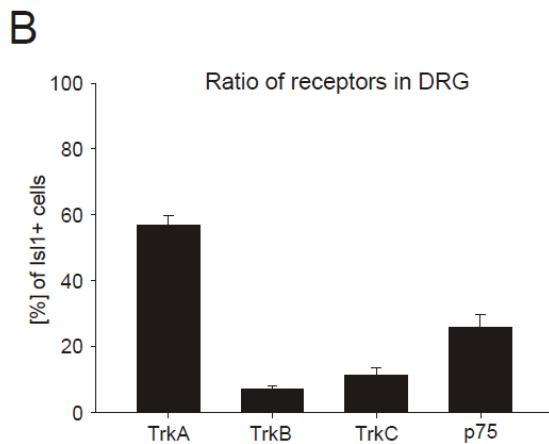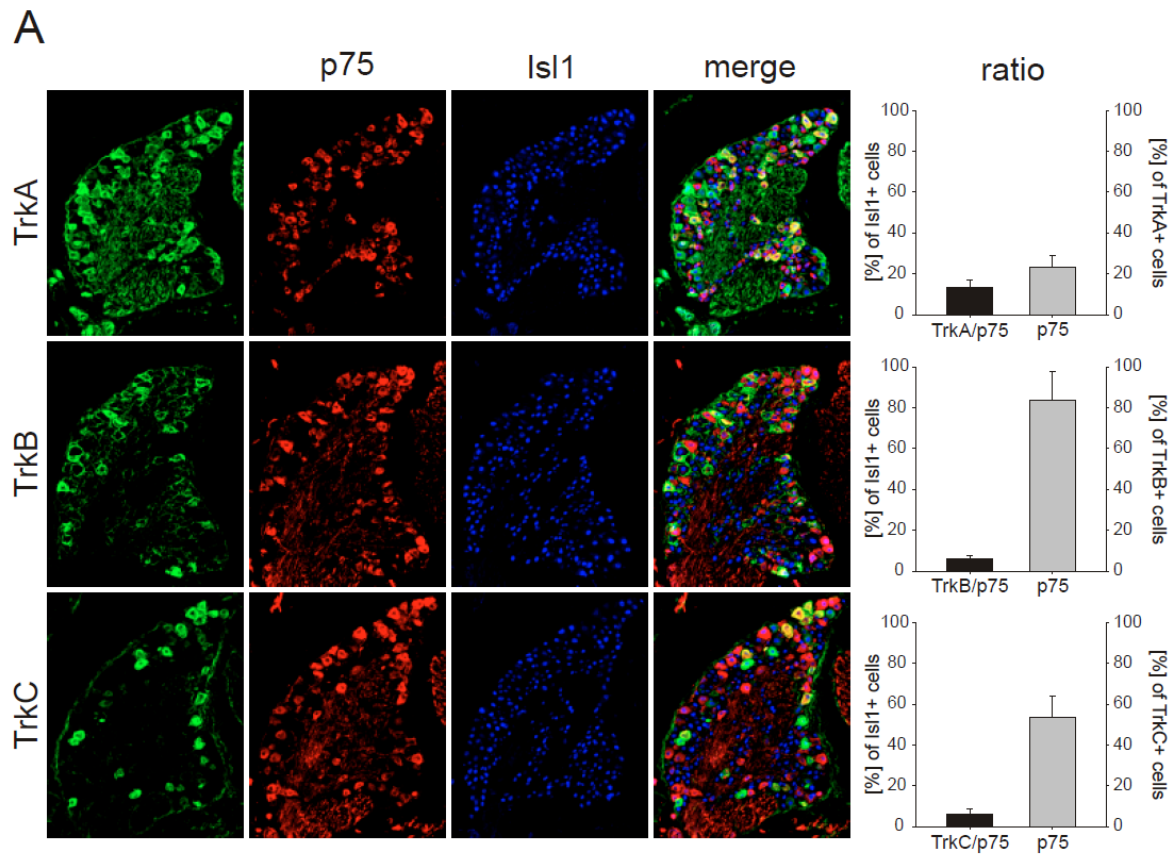
Fig. 5: Quantification of Trk and p75 receptor distribution in wild type DRG
(**A**) Immunohistochemistry to quantify the ratio of Trk and p75 receptor expressing cells. Ratio of TrkA/p75 coexpressing cells: 13.2% ± SEM; 29.9% (± SEM) of all TrkA cells expressed p75. Ratio of TrkB/p75 coexpressing cells: 5.9% ± SEM; 84% (± SEM) of all TrkB cells expressed p75. Ratio of TrkC/p75 coexpressing cells: 6.2% ± SEM; 53.7% (± SEM) of all TrkC cells expressed p75. (**B**) Quantification of total receptor distribution with p4 wild type DRG: TrkA = 57% (± SEM); TrkB = 7% (± SEM) ; TrkC = 11.3% (± SEM); p75 = 25.6% (± SEM); (n>3 animals; >5 sections each)

3.2.3 Validation of FACS result and identification of marker for all proprioceptive neurons or subsets

We next dissociated bilaterally collected p0 lumbar DRG (levels L1-L6) into single cell suspensions, and separated GFP^{on} proprioceptive from GFP^{off} non-proprioceptive populations by Fluorescent Activated Cell Sorting (FACS).

To determine possible gene expression differences between these two populations, we performed Affymetrix microarray experiments comparing genome-wide transcriptional differences (Haeberle et al., 2004; Okaty et al., 2011). These experiments revealed many genes with significant expression differences between the two populations. In order to get a first impression of how efficient this approach is in detecting genes with proprioceptor-enriched gene expression, we analyzed expression profiles of four genes with previously known association to proprioceptors. Confirming the selective expression of GFP in TrkC^{on} proprioceptors, the expression of *TrkC* was highly enriched in the GFP^{on} population when compared to the non-proprioceptor GFP^{off} population. Similarly, the transcription factors *Runx3* and *Er81*, as well as the gene encoding for the calcium binding protein Parvalbumin (*Pvalb*) scored as highly enriched in our analysis (**Supp. 1**).
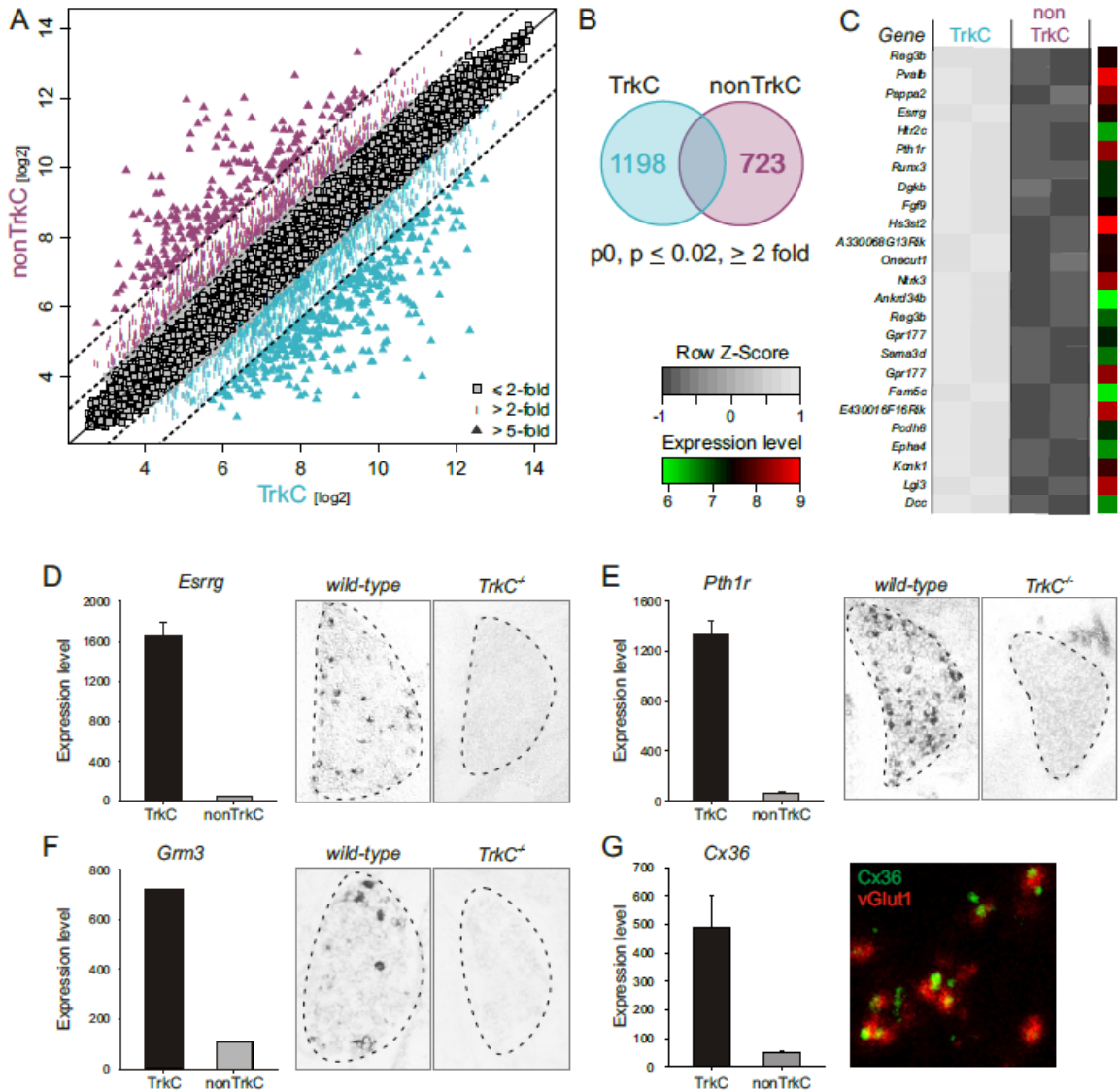
Fig. 6: Isolation of genes with enriched expression in proprioceptors

(A) Affymetrix gene expression profiling data showing genes enriched in *TrkC*[on] proprioceptors and *TrkC*[off] non-proprioceptors. Diagonal lines indicate cut-off for genes with expression values >5 fold change (outermost dotted lines), >2 fold change (middle dotted lines) and ≤2 fold change (grey squares around central diagonal line). TrkC[on] proprioceptor data points with enrichment ≥2 fold are displayed in turquoise and TrkC[off] non-proprioceptors with the same criteria in purple. **(B)** Venn diagram illustrating the number of genes enriched ≥2 fold in proprioceptors and non-proprioceptors respectively. **(C)** Analysis of the 25 genes with highest fold changes displayed in detail. Values of two samples of each p0 TrkC[on] proprioceptors (left) and TrkC[off] non-proprioceptors (right) are shown. Grey scale values represent row z-score values and log2 unit average expression values are shown to the right of each probe (scales plotted bottom left). Gene names are displayed to the left of each row. **(D-G)** Four examples of individual genes with highly enriched expression in proprioceptors (TrkC) when compared to non-proprioceptors (non-TrkC) are displayed. Each panel shows Affymetrix expression values to the left (y-scale expression values; ± SEM) and verification by either *in situ* hybridization on wild-type and *TrkC* mutant lumbar DRG sections (**D-F**) or immunohistochemistry in ventral spinal cord lamina IX (**G**; green: Cx36; red: vGlut1, p20 wild type tissue) to the right.

22

To perform a quantitative genome-wide analysis of gene expression differences between TrkC^{on} and TrkC^{off} populations, we used a significance threshold of p≤0.02 and an enrichment factor of ≥2 fold. Using these criteria, we found that 1198 of ~45K expressed probes on the Affymetrix chip set used were enriched in TrkC^{on} proprioceptors, and conversely, 723 probes exhibited clear enrichment in the TrkC^{off} non-proprioceptor population (**Fig. 6A,B**). We were able to this analysis at all observed time points consistently (**Supp. 2**).

We next analyzed in more detail the 25 probes with the highest observed expression differences based on fold changes between TrkC^{on} and TrkC^{off} populations (**Fig. 6C**), and found that these genes encompassed genes of various expression levels, indicating no particular bias towards a specific expression level as a contributing factor to enrichment. In addition, and in agreement with the high fold changes detected, z-score analysis reveals a strong deviation of the two populations from the distribution mean (**Fig. 6C**). These findings demonstrate that many genes show enriched expression in proprioceptors.

To further probe the reliability of our data at the single gene level, we picked four genes not previously known to exhibit proprioceptor-enriched gene expression profiles and performed *in situ* hybridization or immunohistochemical experiments on DRG at lumbar spinal levels (**Fig. 6D-G**). To verify the selective expression pattern of these genes, we carried out *in situ* hybridization experiments on tissue from both wild-type and *TrkC* mutant mice, in which proprioceptors are eliminated at early developmental stages due to the absence of neurotrophic factor signaling essential for proprioceptor survival (Klein et al., 1994). The orphan transcription factor estrogen related receptor Esrrg, with previously shown expression in gamma motor neurons in the ventral spinal cord (Friese et al., 2009), also exhibited highly selective enrichment in proprioceptors by the Affymetrix gene expression profiles and *in situ* hybridization verified the complete absence of expression in *TrkC* mutant mice (**Fig. 6D**). Parathyroid hormone 1

receptor (*Pth1r*), a receptor with prominent role in bone formation (Guo et al., 2002) and currently unknown function in the nervous system, also exhibited highly enriched expression in proprioceptors within the DRG and displayed complete absence of expression in *TrkC* mutant mice (**Fig. 6E**). Metabotropic glutamate receptor 3 (*Grm3*), a gene with significant gene variant associations linked to memory performance in humans (de Quervain and Papassotiropoulos, 2006), revealed scattered cells within the DRG by *in situ* hybridization, a pattern absent in *TrkC* mutant mice (**Fig. 6F**). In contrast to *Esrr3* and *Pth1r* however, *Grm3* exhibited a much sparser labeling density within the DRG, indicating that its expression is confined to only a restricted subset of proprioceptors. These findings demonstrate that our approach not only picks up genes expressed by all TrkC[on] DRG neurons, but is sensitive enough to isolate genes with expression in subsets of proprioceptors, a feature further exploited later in this study. Lastly, we also determined whether genes expressed by proprioceptors produce proteins transported to central synapses, exploiting the example of connexin 36 (*Cx36*), a gap junction protein with known neuronal expression and required for gap junction function in several systems (Allen et al., 2011; Deans et al., 2001; Van Der Giessen et al., 2008) (**Fig. 6G**). Using an antibody to Cx36, we determined whether proprioceptor terminals in the ventral spinal cord marked by the selective accumulation of vesicular glutamate transporter 1 (vGlut1) (Vrieseling and Arber, 2006) exhibit colocalization with the gap junction protein Cx36. We found association of vGlut1[on] proprioceptive terminals in spinal lamina IX with Cx36[on] signal, suggesting that gap junction proteins are present and might play a role at proprioceptive central synapses. Together, these findings demonstrate the reliability of our Affymetrix gene expression experiments in isolating genes with highly enriched expression in proprioceptive afferents when compared to non-proprioceptor populations, and allow us to exploit this method further to study the regulation of these genes by perturbation of peripheral neurotrophic factor signaling cascades.

3.2.4 Identification of NT3 dependent gene regulation in proprioceptive afferents

Since *NT3* mutant mice exhibit pronounced neuronal cell death in DRG at early developmental stages due to an essential role of NT3 in promoting neuronal survival (Ernfors et al., 1994; Farinas et al., 1994; Tessarollo et al., 1994), we made use of the observation that concurrent elimination of the proaptototic gene *Bax* in mice circumvents DRG neuronal cell death and allows studying a role of NT3 other than the regulation of neuronal survival (Patel et al., 2003).

To determine the effect of absence of NT3 on gene expression in DRG neurons, we compared genome-wide expression profiles of proprioceptors and non-proprioceptors isolated through the *TrkC^{GFP}* BAC allele, in each of the three genetic backgrounds of wild-type, *NT3$^{-/-}$Bax$^{-/-}$*, and *Bax$^{-/-}$* DRG. This three-way comparison would allow us to avoid isolating genes affected in expression solely due to *Bax* mutation (**Fig. 7**). Comparison of gene expression data from these three different genotypes and the two separate cell populations each, revealed that 473 probe sets (328 genes) were significantly enriched in p0 proprioceptors, and also significantly downregulated in proprioceptors of *NT3$^{-/-}$Bax$^{-/-}$* but not affected in *Bax$^{-/-}$* mice (fig; p≤0.02; regulation ≥2 fold) (**Fig. 7A**). In contrast, only a small fraction of genes (33 probes; 29 genes) with proprioceptor-enriched expression profile were upregulated in *NT3$^{-/-}$Bax$^{-/-}$* proprioceptors (**Fig. 7B**; p≤0.02; regulation ≥2 fold). To probe the reliability of these results, we determined the expression profiles of several individual genes in more detail. We first analyzed the expression profiles of *Etv1*, a member of the ETS transcription factor family with previously described regulation by peripheral NT3 (Patel et al., 2003). We found that *Etv1* expression was highly enriched in proprioceptors of both wild-type and *Bax$^{-/-}$* mice, much in contrast to the observed expression in *NT3$^{-/-}$Bax$^{-/-}$* mice, where *Etv1* expression was very low, a pattern which was also confirmed by *in situ* hybridization on DRG sections (**Fig. 7C**).
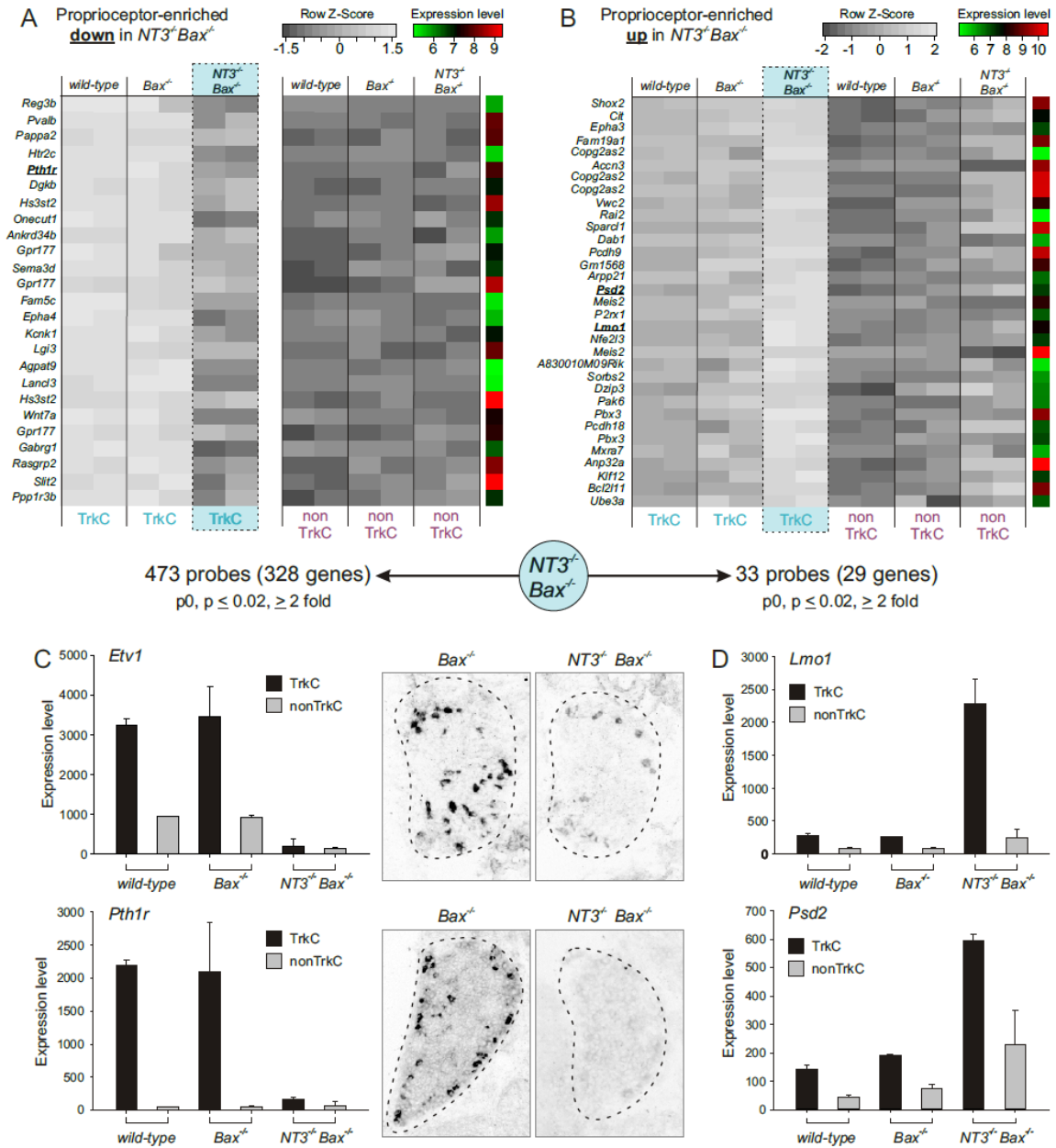
Fig. 7: NT3 deletion alters proprioceptor gene expression

(**A, B**) Analysis of the 25 most downregulated (A) or 33 most upregulated (B) genes with highest fold changes in $NT3^{-/-}Bax^{-/-}$ mice is displayed. Values of two samples of each p0 TrkC^{on} proprioceptors (left; TrkC) and TrkC^{off} non-proprioceptors (right; non-TrkC) isolated from wild-type, $Bax^{-/-}$ and $NT3^{-/-}Bax^{-/-}$ mice are shown. Grey scale values represent row z-score values and log2 unit average expression values are shown to the right of each probe (scales plotted top right of each panel). Gene names are displayed to the left of each row, and genes analyzed below shown in bold. The number of probes and genes regulated in proprioceptors (p≤0.02; regulation ≥2 fold) is shown below the plots. (**C, D**) Detailed expression analysis of two individual genes downregulated (*Etv1* and *Pth1r*) and two genes upregulated (*Lmo1* and *Psd2*) in proprioceptors of $NT3^{-/-}Bax^{-/-}$ but not in $Bax^{-/-}$ mice is shown (Affymetrix analysis: y-scale displays expression values; ± SEM). For *Etv1* and *Pthr1*, also confirmation by i*n situ* hybridization on p0 lumbar DRG of in $Bax^{-/-}$ and $NT3^{-/-}Bax^{-/-}$ mice is displayed to the right.

26

Moreover, we also determined the expression of *Pth1r*, a gene which scored amongst the highest-fold genes regulated by NT3 based on the analysis of *NT3^{-/-} Bax^{-/-}* profiles. We found that its expression in proprioceptors is high in wild-type and *Bax^{-/-}* mice, but dramatically downregulated in *NT3^{-/-}Bax^{-/-}* mice (**Fig. 7C**). Conversely, the gene encoding the Lim-domain containing protein Lmo1 exhibited only low-level expression and enrichment in proprioceptors in wild-type and *Bax^{-/-}* mice, but showed striking upregulation in *NT3^{-/-}Bax^{-/-}* proprioceptors, similar to the gene encoding Pleckstrin and Sec7 domain containing protein 2 (*Psd2*) (**Fig. 7D**). Together, these findings demonstrate that genetic elimination of *NT3* affects gene expression of a selective subset of genes with enriched expression in proprioceptors, and of the genes affected, most genes with significant changes in expression levels in isolated proprioceptive afferents are downregulated by developmental genetic deprivation of NT3.

Since complete genetic elimination of NT3 by virtue of studying *NT3^{-/-}Bax^{-/-}* mice revealed pronounced effects on gene expression in proprioceptors, we next sought to determine whether raising NT3 levels in skeletal muscles would also affect proprioceptor gene expression. Previous work demonstrated that altering NT3 levels genetically to abnormally high values by transgenic expression of NT3 using the skeletal muscle promoter myosin light chain (mlc) leads to a dramatic breakdown of the specificity in central connectivity between proprioceptors of the group Ia afferent subtype with motor neuron pools (Wang et al., 2007), suggesting that accurate NT3 levels in the muscle might be influential in controlling central connectivity by retrograde signaling.

To study whether gene expression in proprioceptors cannot only be influenced by complete elimination of NT3 signaling, but also by raising peripheral NT3 levels, we compared gene expression profiles in *TrkC^{GFP}* proprioceptors to the non-proprioceptive population in *mlc^{NT3}* mice (Wang et al., 2007) (**Fig. 8**). A genome-wide analysis of gene expression differences showed 88 probe sets (78 genes) with significant upregulation of expression in proprioceptors, but without any

coincident expression changes in non-proprioceptive populations (fig; p≤0.02; regulation ≥1.5 fold). Conversely, 180 probe sets (168 genes) scored as significantly downregulated in proprioceptors of *mlc*^{NT3} mice (fig; p≤0.02; regulation ≥1.5 fold) (**Fig. 8A, B**). Again, these gene expression changes could be confirmed at the level of individual genes (**Fig. 8C, D**), where for example the genes encoding for insulin-growth factor 1 (*Igf1*) and Src homology 2 domain containing family member 4 (*Shc4*) were upregulated in *mlc*^{NT3} mice (**Fig. 8C**), whereas Tachykinin receptor 3 (*Tacr3*) and Myoblastosis oncogene (*Myb*) were downregulated (**Fig. 8D**). Together, these findings demonstrate that not only complete elimination of *NT3* affects gene expression in proprioceptors, but even the more subtle genetic manipulation to raise NT3 levels in skeletal muscles leads to profound and significant gene expression changes in proprioceptors, yielding possible molecular entry points to understand the observed central connectivity defects in *mlc*^{NT3} mice (Wang et al., 2007). Not unexpectedly though, expression changes detected in *mlc*^{NT3} mice were less dramatic and numerous than in *NT3*$^{-/-}$*Bax*$^{-/-}$ mice, we had therefore lowered our fold change cut off from 2 fold to 1.5 fold and focused in future experiments on the analysis of the *NT3*$^{-/-}$ *Bax*$^{-/-}$ mice.

We next performed an analysis of genes with enriched and altered expression in proprioceptors by combining the two strategies of genetic manipulations, the elimination of NT3 expression in *NT3*$^{-/-}$*Bax*$^{-/-}$ mice and the rise in endogenous NT3 expression in *mlc*^{NT3} mice (**Fig. 9**). We reasoned that genes with anticorrelative expression profiles in proprioceptors would likely be those most perceptive in sensing changes in endogenous NT3 levels, and therefore reacting in opposite directions in adjusting expression levels in response to peripheral signals. Since most genes with significant changes in expression changes in *NT3*$^{-/-}$*Bax*$^{-/-}$ mice were downregulated in proprioceptors (328 down vs 29 up), we were most interested in which ones of these genes were upregulated in *mlc*^{NT3} mice. In this anti-correlative analysis, we found 41 genes matching these criteria. These findings indicate that almost 50% of all genes upregulated upon rising
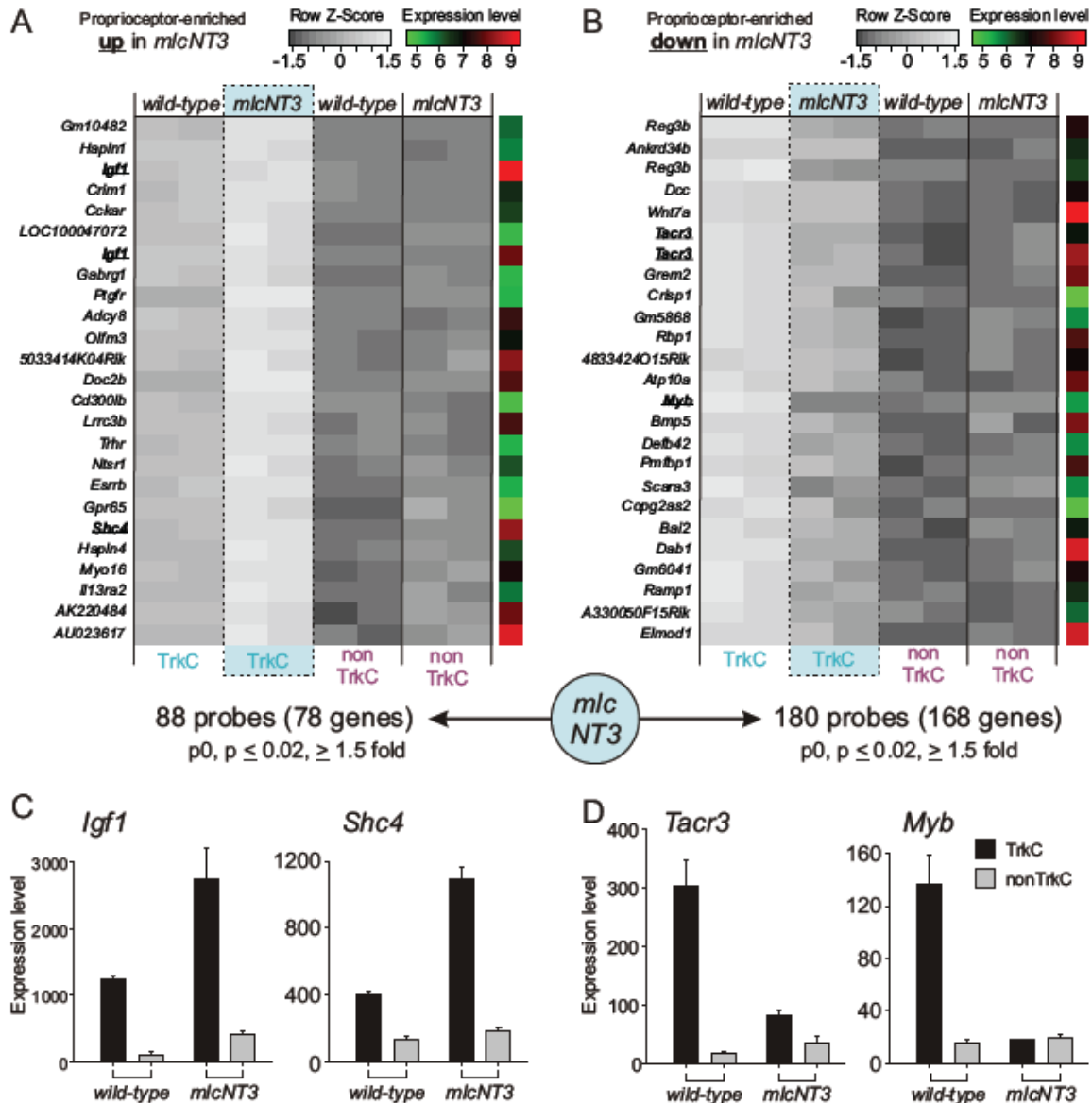
Fig. 8: Surplus skeletal muscle NT3 alters proprioceptor gene expression

(**A, B**) Analysis of the 25 most upregulated (**A**) or downregulated (**B**) genes with highest fold changes in mlc^{NT3} mice is displayed. Values of two samples of each p0 TrkC^{on} proprioceptors (left; TrkC) and TrkC^{off} non-proprioceptors (right; non-TrkC) isolated from wild-type and mlc^{NT3} mice are shown. Grey scale values represent row z-score values and log2 unit average expression values are shown to the right of each probe (scales plotted top right of each panel). Gene names are displayed to the left of each row, and genes analyzed below shown in bold. The number of probes and genes regulated in proprioceptors (p≤0.02; regulation ≥1.5 fold) is shown below the plots. Because the transcriptional changes in these samples were less numerous compared to the $NT3^{-/-}Bax^{-/-}$ data (**Fig. 7**) we had lowered our fold change cut off from 2 fold to 1.5 fold. (**C, D**) Detailed expression analysis of two individual genes upregulated (*Igf1* and *Shc4*) and two genes downregulated (*Tacr3* and *Myb*) in proprioceptors of mlc^{NT3} mice is shown (Affymetrix analysis: y-scale displays expression values; ± SEM).

peripheral NT3 were regulated in the opposite direction upon complete genetic elimination of NT3, whereas the majority of genes downregulated in $NT3^{-/-}Bax^{-/-}$ mice were not altered in mlc^{NT3} mice. The opposite anticorrelative analysis was less rewarding, but nevertheless, we identified 11 genes with increased expression in $NT3^{-/-}Bax^{-/-}$ mice and decrease in mlc^{NT3} mice.
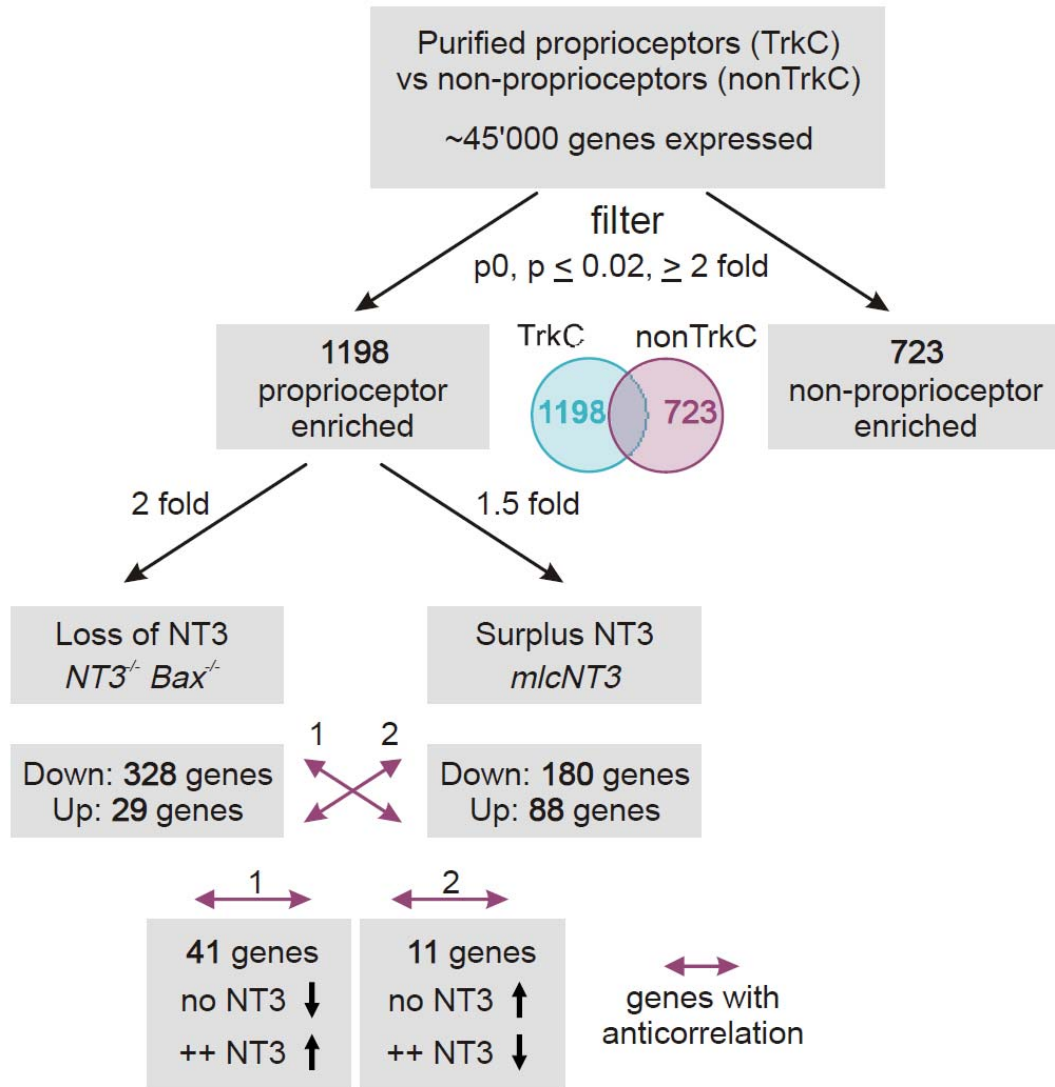
Fig. 9: Identification of anticorrelative gene populations
By comparing the populations significantly regulated in $NT3^{-/-}Bax^{-/-}$ mice and mlc^{NT3} mice we isolated genes with an anticorrelative behavior. 41 genes (purple arrow no. 1) were significantly down regulated in the absence of NT3 and upregulated by surplus NT3. In contrast to that only 11 genes which were upregulated in the absence of NT3 were downregulated by surplus NT3.

3.2.5 Identification of NT3 dependent gene regulation in non-proprioceptive afferents

While NT3 might not be necessary for the survival of non-proprioceptive DRG neurons, there is evidence suggesting that NT3 plays a role for their further specification postnatally (Airaksinen et al., 1996; Krimm et al., 2004; McIlwrath et al., 2007). Consistent with this possibility, NT3 also seems to be able to weakly activate the TrkA and TrkB receptors (Bibel and Barde, 2000; Reichardt, 2006). In addition, its effect on the p75 receptor is also well documented (Bibel and Barde, 2000; Lu et al., 2005; Reichardt, 2006). Taken together we had to assume that deletion of NT3 would also affect transcriptional regulation in non-proprioceptive DRG neurons. To identify the transcriptional changes of NT3 removal upon non-proprioceptive afferents we filtered the previously established list of probe sets with an enrichment in the wild type TrkC^{off} population (p ≤ 0.02, at least 2 fold change difference), asking how many of those probe sets were significantly changed at least 2 fold upon removal of NT3. Arguing that the removal of *NT3* seemed to have a more pronounced effect upon the transcriptional regulation of DRG neurons, we focused on the analysis of *NT3$^{-/-}$ Bax$^{-/-}$* mutants.

We found that 105 wild type TrkC^{off} marker (100 genes) were downregulated using these filter settings (Fig. 10). In contrast, 32 wild type TrkC^{off} marker (32 genes) were upregulated significantly, demonstrating that the genetic elimination of *NT3* affects gene expression of a selective subset of genes with enriched expression in non proprioceptive afferents. The question remain open, how and when these neurons switch to a dependency on NT3 expression.
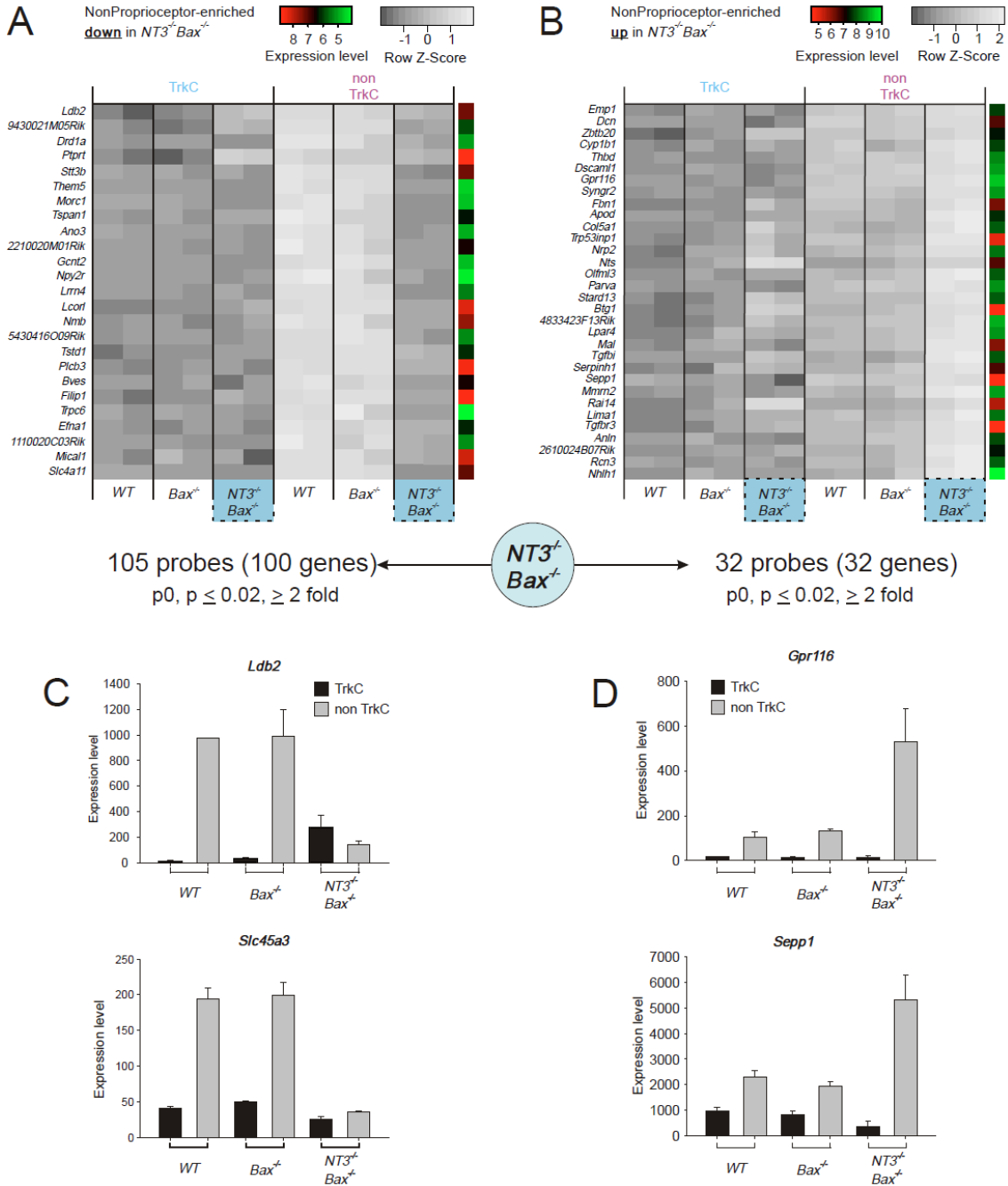
Fig. 10: Identification of NT3 dependent gene regulation in non-proprioceptive afferents
(**A, B**) Analysis of the 25 most downregulated (A) or 32 most upregulated (B) genes with highest fold changes in $NT3^{-/-}Bax^{-/-}$ mice is displayed. Values of two samples of each p0 TrkC[on] proprioceptors (turquoise; TrkC) and TrkC[off] non-proprioceptors (purple; non-TrkC) isolated from wild-type, $Bax^{-/-}$ and $NT3^{-/-}Bax^{-/-}$ mice are shown. Grey scale values represent row z-score values and log2 unit average expression values are shown to the right of each probe (scales plotted top right of each panel). Gene names are displayed to the left of each row, and genes analyzed below shown in bold. The number of probes and genes regulated in proprioceptors ($p \leq 0.02$; regulation ≥ 2 fold) is shown below the plots. (**C, D**) Detailed expression analysis of two individual genes downregulated (*Ldb2* and *Slc45a3*) and two genes upregulated (*Gpr116* and *Sepp1*) in non-proprioceptors of $NT3^{-/-}Bax^{-/-}$ but not in $Bax^{-/-}$ mice is shown (Affymetrix analysis: y-scale displays expression values; ± SEM).

3.2.6 Comparison between gene expression of target-dependent and target-independent phase of sensory neuron development

As mentioned in the introduction, the development of sensory neurons can be divided into a target independent (Marmigere and Ernfors, 2007) and dependent phase (Hippenmeyer et al., 2004). Consistent with this, we know of proprioceptive marker genes, which are target independent (Kramer et al., 2006) and target-dependent (Arber et al., 2000; Patel et al., 2003). As was the case for the analysis of $NT3^{-/-}Bax^{-/-}$ mice (**Fig. 7**), also in mlc^{NT3} mice (**Fig. 8**), we observed many genes with enriched expression in proprioceptors, but which did not show a perturbation in expression by raising peripheral NT3 levels.

While we previously filtered our screens for proprioceptive markers, which are target-dependent, our current data also allows us to filter for genes, which are enriched in proprioceptive populations but not dependent on NT3 expression. Assuming that these target independent proprioceptive marker genes should already be enriched in TrkC^{on} neurons at early developmental stages, we cross-filtered those NT3 independent markers with our E14 TrkC marker list. This filtering resulted in a list of 29 probe sets (26 genes) (**Fig. 11**).
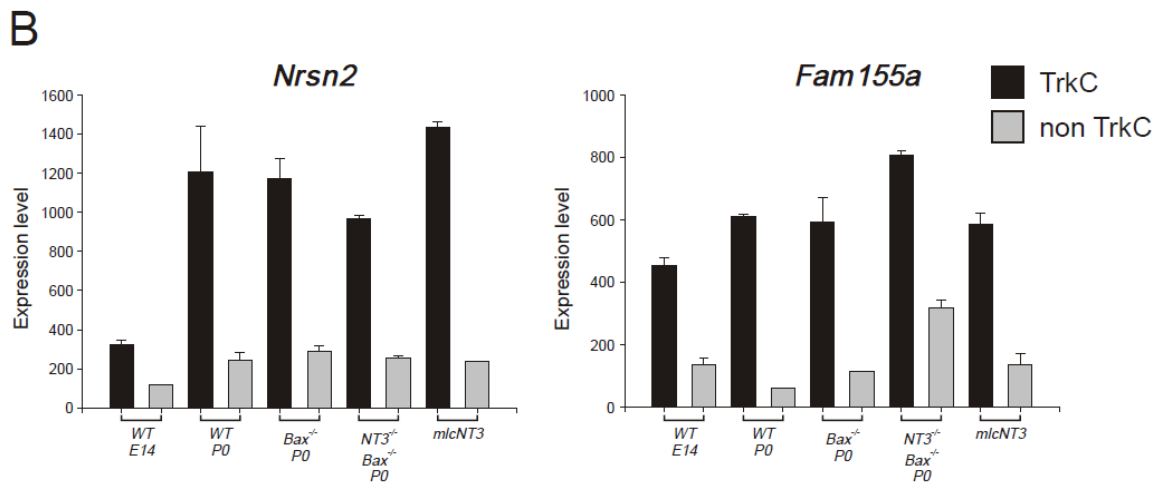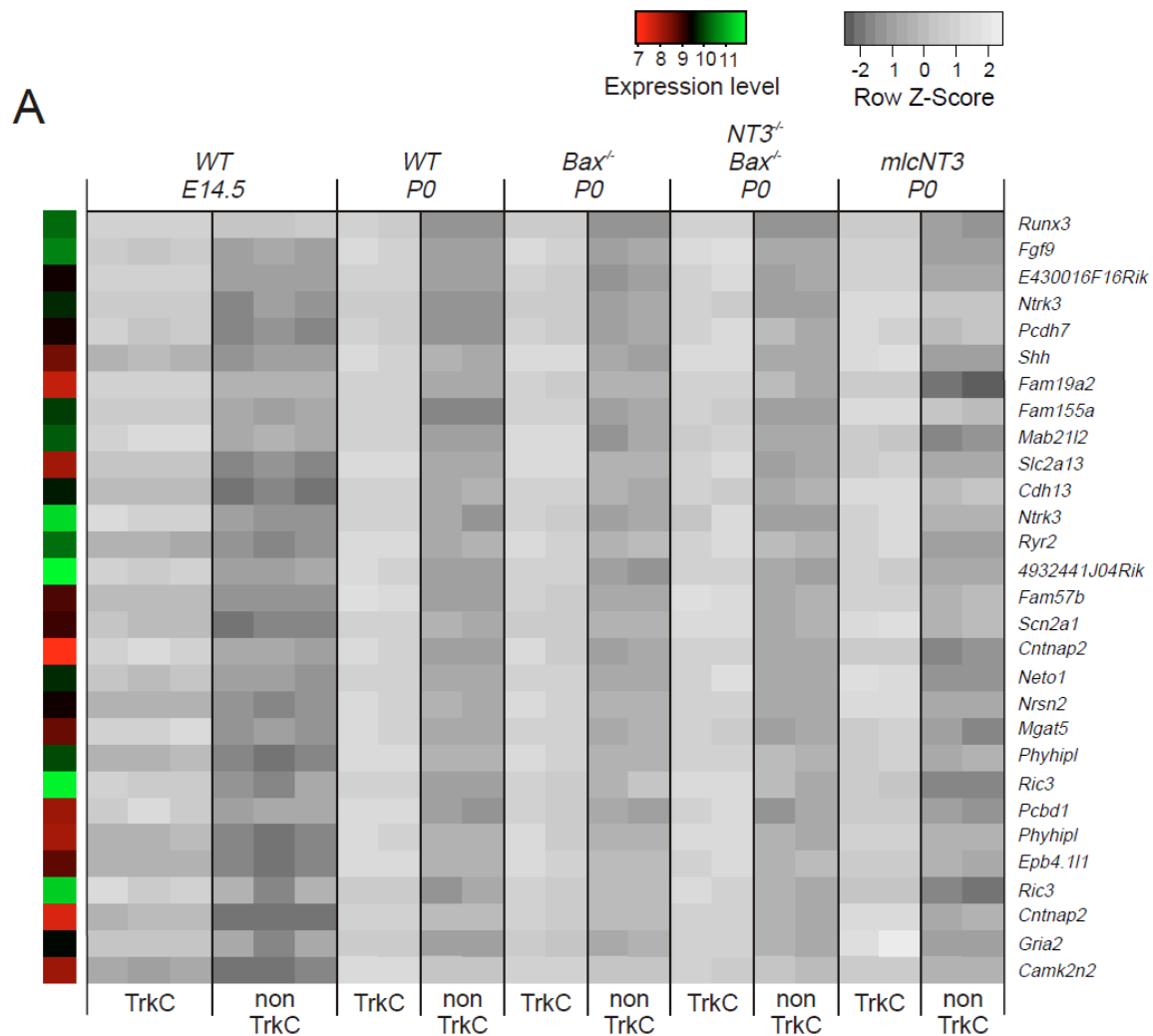
Fig. 11: Target independent gene expression in DRG sensory neurons
(**A**) 26 genes (29 probe sets) with potentially target independent expression were identified. Values of p0 TrkC^{on} proprioceptors and TrkC^{off} non-proprioceptors isolated from wild-type, *Bax$^{-/-}$*, *NT3$^{-/-}$Bax$^{-/-}$* and *mlc^{NT3}* mice are shown. Grey scale values represent row z-score values and log2 unit average expression values are shown to the left of each probe (scales plotted top right of

panel). Gene names are displayed to the right of each row, and genes analyzed below shown in bold (p≤0.02; regulation ≥2 fold). (**B**) Detailed expression analysis of two individual genes (*Nrsn2* and *Fam155a*) enriched in proprioceptors of all mutant backgrounds and at E14 is shown (Affymetrix analysis: y-scale displays expression values; ± SEM).

The list includes *Ntrk3* (TrkC) and *Runx3,* two known target independent genes of the proprioceptive population (**Supp. 1**), thus validating our way of filtering for genes expressed in a target independent manner. Interestingly, the list also contains markers for genes encoding functionally relevant proteins such as Scn2a1 (Boiko et al., 2001; Kaplan et al., 2001), a voltage gated sodium channel or Gria2 (Meng et al., 2003), an ionotropic glutamate receptor. While at this point we can only tell that the transcription for these genes is activated, we have no evidence for possible translational effects at the observed time points.

In summary, the expression phase for target independent and target dependent genes do not seem to be temporally separated but tightly interlinked with each other, suggesting that the target independent gene population might also take over additional roles in later developmental stages.

:

3.2.7 Identification of Er81 dependent gene expression

Previous work from our lab had focused on changes in the transcriptional profile upon *Er81* mutation in mice (Friese, 2010). Since Er81 expression is dependent on NT3 (Patel et al., 2003), comparing these previous data with our results was an interesting avenue to pursue, in particular with respect to the following aspects:

1. Identify genes in our *NT3* mutant proprioceptor analysis, which are also regulated by Er81, to map how pronounced the transcriptional pathway downstream of *Er81* is in relation to all genes regulated by NT3 signaling.
2. Having the same gene downregulated in two independent screens made a comparison between the two screens very interesting in terms of consistency.

Ideally we would expect all downregulated genes from the *Er81* mutant proprioceptor data also to be downregulated in proprioceptors isolated from *NT3* mutant mice, considering the fact that Er81 is a downstream target of NT3 signaling. However, one should bear in mind that the methodology applied in the two sets of experiments is not identical. While the *NT3* mutant proprioceptor profiling described in this thesis was performed at p0, the *Er81* mutant analysis was carried out at E16 (Friese, 2010). Additionally, Friese et al used a *PVCre::Tau^{GFP}* binary transgenic line to label proprioceptive afferents, while the *NT3* mutant screen in my thesis utilized a BAC *TrkC^{GFP}* transgene approach.

Filtering for probes, which were significantly downregulated ($p \leq 0.02$) at least 2 fold in both conditions (*Er81$^{-/-}$* and *NT3$^{-/-}$Bax$^{-/-}$* mice) led to the identification of 29 probe sets (29 genes) (**Fig. 12A**). Among the hits identified, we also isolated *Er81* (*Etv1*) (**Fig. 12B**), confirming previously published findings (Patel et al., 2003). While we did not expect a high number of probe sets to be shared between the two datasets, we were also surprised to only identify 29 common
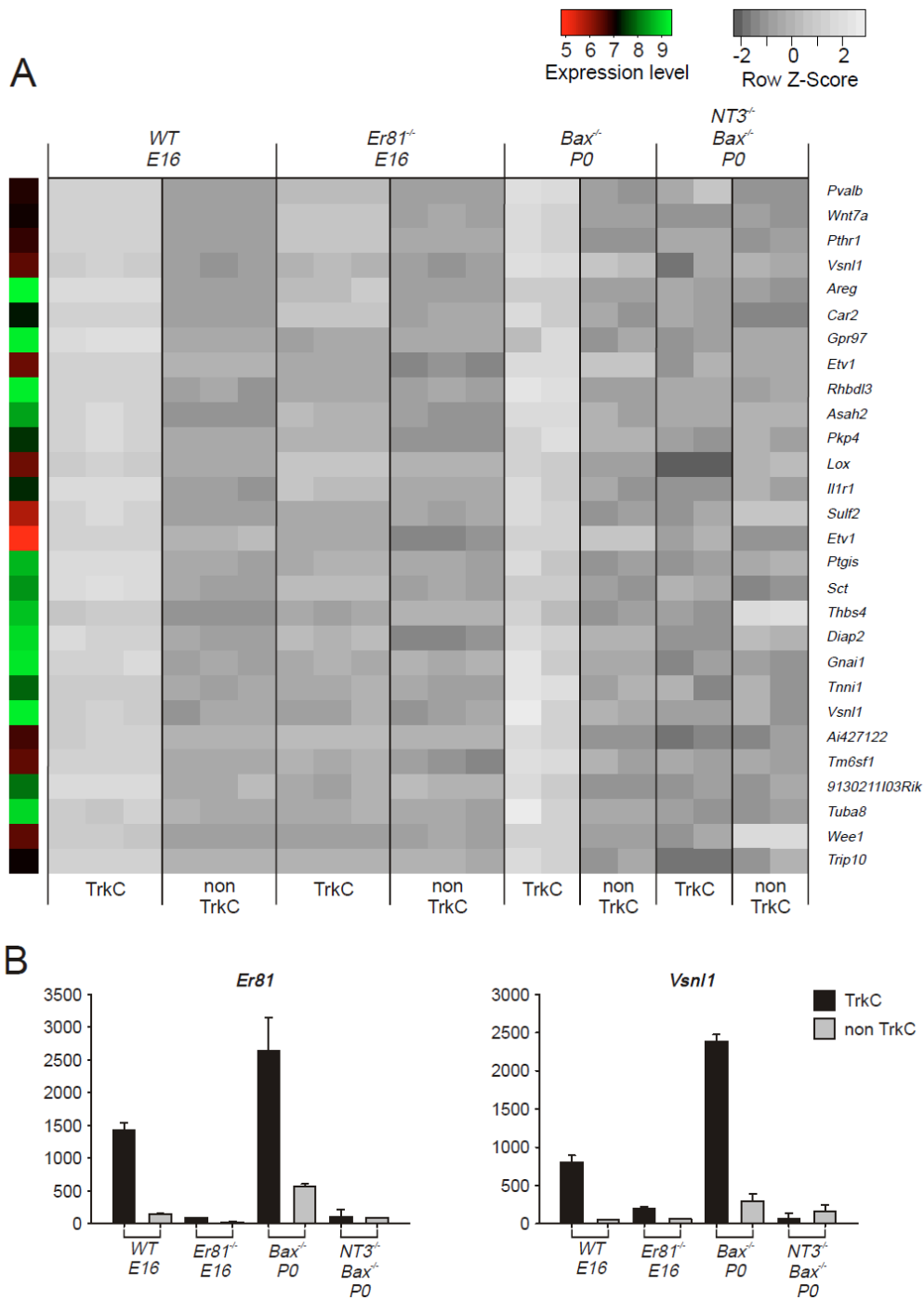
Fig. 12: **Identification of Er81 dependent gene expression**
(**A**) 29 genes (29 probe sets) potentially downstream the NT3-Er81 signaling pathway were identified. Values of p0 TrkC^on proprioceptors and TrkC^off non-proprioceptors isolated from wild-type E16, E16 *Er81*^-/-^, p0 *Bax*^-/-^ and p0 *NT3*^-/-^*Bax*^-/-^ mice are shown. Grey scale values represent row z-score values and log2 unit average expression values are shown to the left of each probe (scales plotted top right of panel). Gene names are displayed to the right of each row, and genes analyzed below shown in bold (p≤0.02; regulation ≥2 fold). (**B**) Detailed expression analysis of two individual genes (*Er81* and *Vsnl1*) is shown (Affymetrix analysis: y-scale displays expression values; ± SEM).

genes, suggesting that our different technical approaches might have played a bigger role than expected. Alternatively, only a small fraction of genes regulated by NT3 are in fact downstream of Er81 and/or the developmental differences in the profiling experiments influences the gene lists identified.

3.3 Discussion

In this study, we use genome-wide gene expression profiling to determine the transcriptional consequences of NT3 signaling in proprioceptive sensory neurons. By transgenic fluorescent tagging of proprioceptors in order to specifically purify this minor DRG sensory neuron subpopulation, we identify genes with highly enriched expression profiles in proprioceptors when compared to non-proprioceptive sensory neurons. The expression level of many of these proprioceptor-enriched genes is dramatically regulated by genetic elimination of *NT3* in the absence of neuronal cell death, leading to the identification of genes dependent on NT3 signaling but not involved in neuronal survival related activities. Combined with analysis of mice with surplus NT3 expression in skeletal muscles, we identify a specifically anticorrelated gene subset reacting in opposite directions to lower or higher NT3 levels in proprioceptors.

Transgenic marking of proprioceptors in mice allowed us to isolate a large number of genes with highly enriched expression in proprioceptors of the DRG. Neuronal purification was a prerequisite to success since proprioceptors only make up a minority of all neurons in the DRG. Our observations add to a number of studies on gene expression profiling in the nervous system demonstrating that genes with highly enriched expression in defined neuronal cell types making up small fractions of a sampled structure can be isolated with much higher success rates upon neuronal purification (Okaty et al., 2011). Nevertheless, the proprioceptor population studied here does not represent a functionally unique

neuronal population. It can be further subdivided into group Ia/II afferents innervating muscle spindles and group Ib afferents targeting Golgi tendon organs in the periphery (Chen et al., 2003; Zelena, 1994; Zelena and Soukup, 1977). Each individual proprioceptive neuron also only targets one peripheral muscle and mechanisms controlling the establishment of axonal trajectories peripherally as well as the selection of specific central target neurons are currently unknown. The identification of genes expressed by subpopulations of proprioceptors may therefore provide an important entry point to study further cell type diversification amongst the proprioceptor population, both with respect to functional subtypes as well as projection targets. Taking motor neurons in the ventral spinal cord as an example, recent work provides evidence for dedicated molecular programs acting at the level of motor neuron pools projecting to distinct peripheral muscles as well as within functional subtypes of motor neurons innervating intra- and extrafusal muscle fibers (Bonanomi and Pfaff, 2010; Dalla Torre di Sanguinetto, 2009; Friese, 2010). Similar mechanistic insight is missing on DRG sensory neuron subpopulations, most likely due to the scattered neuronal cell body distribution within the DRG, in contrast to the highly organized and clustered organization of motor neuron pools. Our study now provides a database to mine for genes expressed in all proprioceptors or subpopulations thereof, and we already provide evidence for at least some genes with clearly non-panproprioceptor expression profiles.

Cellular and transcriptional effects of retrograde signaling in neuronal subpopulations

The approach of isolating specific neuronal populations in genetic mouse mutants has allowed us to study in detail the effect of the NT3 signaling pathway on transcription in proprioceptors. NT3 represents an important signaling system not only for the control of proprioceptor cell survival (Klein et al., 1994; Oakley et al., 1995; Tessarollo et al., 1994), but from loss-of-function experiments

preventing cell death phenotypes has also been shown to play a role in the establishment of the central trajectory of group Ia afferents towards motor neurons (Patel et al., 2003) and by studies overexpressing NT3 in skeletal muscles is known to influence the selection process of synaptic connections between group Ia afferents and specific motor neuron pools (Wang et al., 2007). Our study provides insight into the transcriptional consequences of these NT3 level manipulations at the cell type specific level. We found that NT3 elimination in $NT3^{-/-}Bax^{-/-}$ mice elicits a much more prominent downregulatory effect on proprioceptor gene expression than further raising their expression, suggesting that the normal role of NT3 is to mainly promote and/or enhance proprioceptor gene expression. Changes in gene expression upon raising muscular NT3 levels were more modest, most likely reflecting the fact that not all genes have the ability to scale expression gradually in response to differing NT3 levels, and may instead already reach saturating expression levels in the wild-type. It is the anticorrelative combinatorial analysis carried out in this study, which may point specifically to genes sensitive to gradual changes in NT3 levels.

Our study has specifically focused on genes with enriched expression in wild-type proprioceptors and analyzed the effect of NT3 signaling on these genes. However, we also observed transcriptional effects of NT3 on non-proprioceptors. These findings are not surprising, since in addition to TrkC, NT3 can also signal through p75 and to a minor extent through TrkA and TrkB, all three expressed in subpopulations of DRG sensory neurons (Bibel and Barde, 2000; Reichardt, 2006). It will therefore also be interesting in the future to determine which transcriptional effects of NT3 signaling can be attributed to which receptor in non-proprioceptor subpopulations.

Keeping in mind the fact that certain non-proprioceptive DRG neurons survive the deletion of $NT3$ until birth (Patel et al., 2003), but die within the first postnatal weeks (in $NT3+^{/-}$ animals, (Airaksinen et al., 1996)), one has to consider the possibility that subpopulations of DRG neurons are initially not target dependent

but then undergo a switch to target dependency. This in turn suggests that target derived NT3 might play additional roles in late stages of spinal circuit development, a possibility which will be explored further in this thesis.

An emerging feature in studies on the influence of target-derived retrograde neuronal responses is the observation that postmitotic neurons are capable to adjust their transcriptional programs in the cell body in order to react to these signals by changing specifically their cellular phenotypes. These changes can become apparent by a variety of different readouts. Studies on retrograde signaling pathways in NGF-responsive TrkA expressing DRG sensory neurons have provided evidence that retrograde NGF signaling promotes a switch to the emergence of non-peptidergic Ret-expressing sensory neurons, by virtue of inducing expression of Ret and GFRalpha coreceptors as well as other characteristic receptor genes in these neurons (Luo et al., 2007). Non-peptidergic Ret neurons gradually lose NGF-responsiveness at postnatal stages, providing evidence that retrograde signaling pathways can profoundly alter neuronal phenotypes as circuits mature. In the trigeminal somatosensory system, retrograde signaling by TGFbeta family members also acts to change transcriptional profiles in these whisker innervating sensory neurons, inducing the transcription factor *Onecut2*, which in turn is involved in the regulation of central projections (Hodge et al., 2007). The genome-wide analysis performed on proprioceptive afferents in this study lends support to the notion that retrograde signaling from the target area intersects in a very profound way with the transcriptional programs set up at stages before axons invade their targets. It also demonstrates however the parallel existence of proprioceptor-specific gene programs not influenced by target-derived cues, exemplified by TrkC and Runx3.

4. Inhibitory control of the monosynaptic reflex circuit

4.1 Introduction

Considering the vast amount of information relayed by sensory neurons towards motor output circuitry, it can be assumed that incoming impulses are modulated in order for the system to adapt and focus on certain inputs. Most commonly, inhibitory mechanisms act at the postsynaptic side, mediated by GABAergic or glycinergic synapses, which are either axo-dendritic or axo-somatic. However, seminal work in the monosynaptic stretch reflex circuit of the spinal cord described a depression of the excitatory postsynaptic potential (EPSP) occurring without any change in the postsynaptic potential or any change in motoneuronal excitability (Frank and Fuortes, 1957), initially termed "remote inhibition". Subsequent observations confirmed these findings (Eccles et al., 1961) and led to the concept of "presynaptic inhibition", where in so-called axo-axonic synapses, GABAergic terminals contact proprioceptive afferents, their postsynaptic partners in this synapse, in order to cause a primary afferent depolarization (PAD). In the motor nuclei of the spinal cord, the involved boutons are presynaptic to Ia afferent terminals (Conradi et al., 1983; Fyffe and Light, 1984; Pierce and Mendell, 1993; Watson and Bazzaz, 2001). Additionally, these presynaptic boutons are immunoreactive for an isoform of glutamic acid decarboxylase (GAD65) (Hughes et al., 2005) as well as its synthesis product GABA (Destombes et al., 1996; Holstege and Calkoen, 1990; Ornung et al., 1996; Watson and Bazzaz, 2001), strongly supporting the idea that these boutons are the source of presynaptic inhibition on Ia proprioceptive afferents. The involved inhibitory interneurons are generated by two populations of neurons: DI4 and DILA, both specified by the *Ptf1a* and *Lbx1* transcription factors (Betley et al., 2009; Glasgow et al., 2005; Gross et al., 2002; Muller et al., 2002).

An open question in the field of presynaptic inhibition of this circuit concerns the composition of the $GABA_A$ receptors involved in presynaptic inhibition located in Ia afferent synapses postsynaptically. $GABA_A$ receptors are a heterogeneous group of ionotropic receptors and ligand gated ion channels mediating the main synaptic actions of the dominant inhibitory neurotransmitter GABA (Luscher et al., 2011). Once activated, the $GABA_A$ receptor changes conformation, allowing Cl- to pass which ultimately usually leads to a hyperpolarization of the cells' resting potential. Because excitation through depolarization now is less likely, the end result is inhibitory. However, DRG neurons have a high intracellular Cl⁻ concentration (Sung et al., 2000) and as a result $GABA_A$ receptor activation there has a depolarizing effect, thus decreasing the effect of the incoming axonal spike. Hence the term "primary afferent depolarization" (PAD). The high attention these receptors receive arises from their diverse response patterns towards a broad range of psychopharmaca. $GABA_A$ receptors are composed of five subunits (two homomers, one monomer) and so far, 19 subunits have been identified (Luscher et al., 2011). Their diverse composition provides the basis for their flexibility in signal transduction and drug induced modulation (Fritschy and Mohler, 1995; Levitan et al., 1988; Olsen, 1982). Generally, a combination of α-, β- and γ-subunit seem to be required in order to form a fully functional $GABA_A$ receptor (Luscher et al., 2011), but depending on the subunit composition, the channel will exhibit different functional features.

So far, the rules underlying the assembly of $GABA_A$ receptors are poorly understood. Some data suggests that the composition might be a mass-driven event, regulated by the rate of translation of compatible subunits: The deletion of $\alpha 1$ subunit is compensated by the upregulation of receptors containing other subunits (Kralic et al., 2002a; Kralic et al., 2002b; Kralic et al., 2006; Sur et al., 2001). Mice expressing ectopic $\alpha 6$ subunits in pyramidal cells of the hippocampus gained more $\alpha 6 \beta \gamma 2$ receptors at the cost of other postsynaptic receptors (Wisden 2002).

The data described in this PhD thesis provides an entry point to closer investigation of GABA$_A$ receptor composition in proprioceptive afferents. In addition, it provides deeper insight into the molecular pathways involved in synaptic development and/or functionality of proprioceptive afferents by means of regulation by target derived mechanisms.

4.2 Results

4.2.1 NT3 dependent expression of functionally relevant proprioceptive marker genes

The validation of our proprioceptor enriched geneset data revealed among others also functionally relevant genes such as *Cx36* (**Fig. 6G**). While it is well known that neurotrophins play a role in development and survival, the notion that they retrogradely induce the expression of functionally relevant genes is quite recent. Even though recent data has shown that for example retrograde NGF is necessary to induce pre- and postsynaptic structures (Sharma et al., 2010a), there is so far still no data about the involved genetic pathways.

We therefore addressed the question, which genes with a known role in synaptic structure and function might be regulated by the expression of NT3 (**Fig. 13**). Filtering our list of proprioceptor enriched genes for the appropriate GO terms, we compiled a list of 168 probe sets (120 genes, blue ring, **Fig. 13A**) with a known role in synaptic structure or function. Consistent with our previous cut off values, we again selected those probe sets with a significance of p ≤ 0.02 and a 2 fold expression difference between the wild type TrkC^{on} and TrkC^{off} population. Within this group,
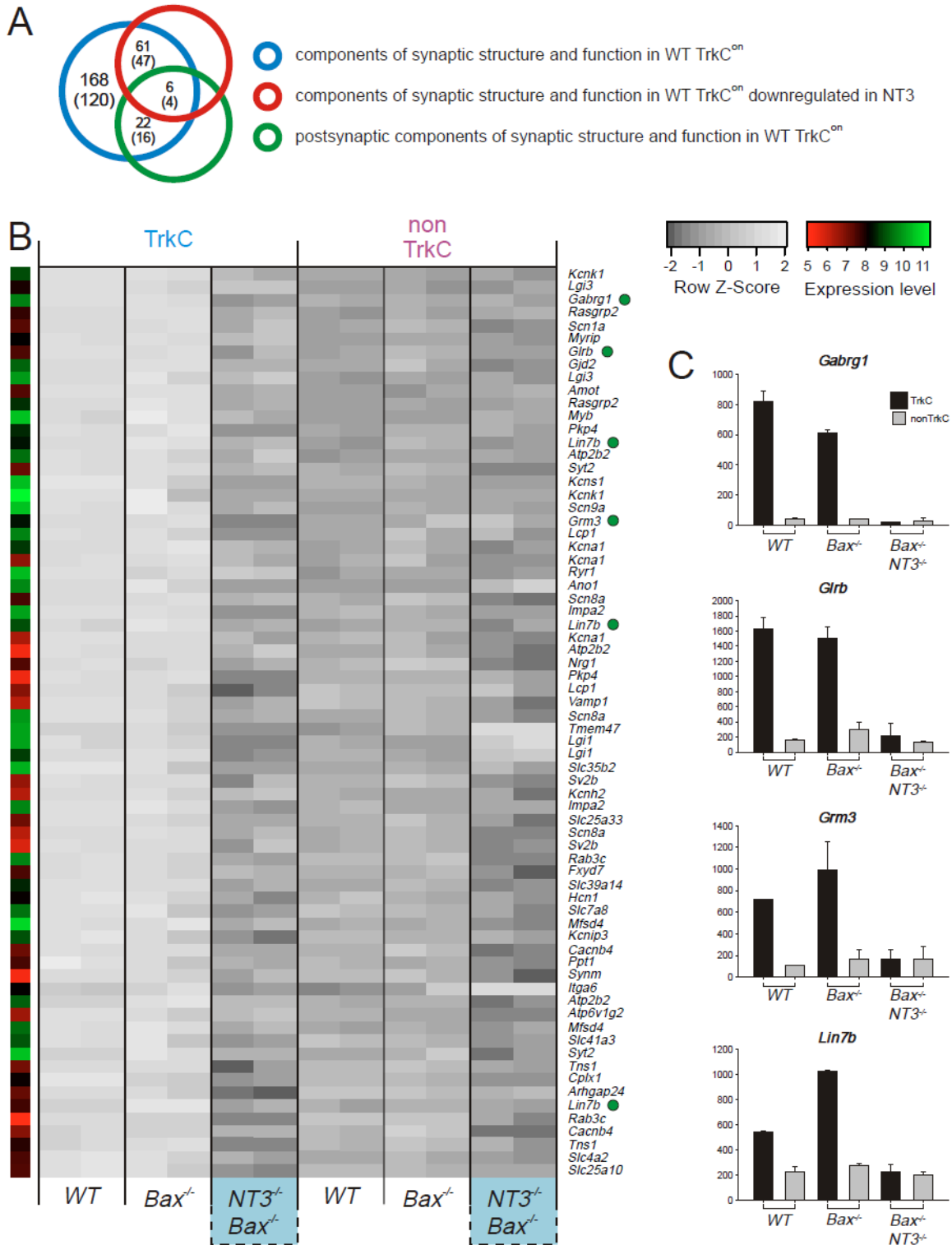
Fig. 13: **NT3 dependent expression of functionally relevant proprioceptive marker genes**
(**A**) Venn diagram of GO term analysis: 168 probe sets (120 genes, blue ring) encoded components of synaptic structure and function and were enriched in the wild type TrkC[on] population. Within this group 67 probe sets (51 genes, red ring) are downregulated in the absence of NT3. 28 probe sets (20 genes, green ring) encode postsynaptic components of synaptic structure and function. GO = Gene Ontology

(**B**) Visualization of the 67 NT3 regulated probe sets (51 genes, red ring, **Fig. 13A**) encoding components of synaptic structure and function. Values of p0 TrkC^{on} proprioceptors (turquoise) and TrkC^{off} non-proprioceptors (purple) isolated from wild-type, $Bax^{-/-}$ and $NT3^{-/-}Bax^{-/-}$ mice are shown. Grey scale values represent row z-score values and log2 unit average expression values are shown to the left of each probe (scales plotted top right of panel). Gene names are displayed to the right of each row, and genes analyzed below shown in bold (p≤0.02; regulation ≥2 fold). Green dots correspond with the postsynaptic probe sets in the green ring (**Fig. 13A**). (**C**) Detailed expression analysis of the four TrkC^{on} specific, NT3 regulated, postsynaptic marker genes: *Gabrg1, Glrb, Grm3* and *Lin7b* is shown (Affymetrix analysis: y-scale displays expression values; ± SEM).

61 probe sets (47 genes, red ring, **Fig. 13A, B**) showed an NT3 dependent expression profile, analyzing the loss of function data set. While the vast majority of those NT3 dependent genes play a role in various aspect of the function of presynaptic sites, four genes encoded proteins usually found at postsynaptic sites: Gabrg1, Grm3, Glrb, Lin7b (**Fig. 13C**) and could therefore play a role in presynaptic modulation or inhibition. Especially the expression of *Gabrg1* is interesting, as it encodes the γ1 subunit of the GABA$_A$ receptor, implying that target derived NT3 is taking part in the regulation of GABA$_A$ receptor composition.

4.2.2 Only the regulation of *Gabrg1* is NT3 dependent

Because GABA$_A$ receptors consist of several subunits, we next wondered whether other GABA$_A$ receptor subunits might be expressed in a NT3 dependent manner. Though we were able to identify several GABA$_A$ receptor subunits specific for the proprioceptive population, only *Gabrg1* is regulated in an NT3 dependent manner (**Fig. 14**). Its expression is downregulated in *NT3* mutant proprioceptors and also significantly upregulated in mice with ectopic skeletal muscle expression of NT3. Upon removal of *NT3*, we did not detect changes in the expression of α5 and an increased expression of α3 and β2 receptors. In the cases of alpha 2 and alpha 4 receptor subunits, no reliable statement can be made, since it seems that part of the effect is a result of the deletion of *Bax*.

Considering the fact that we have also analyzed proprioceptor enriched gene expression at several time points throughout development, the question arises whether TrkC specificity of those $GABA_A$ receptor subunits marks only a transient stage or is a consistent phenomenon throughout development. We therefore sought to map the expression time course of all $GABA_A$ receptor subunits, we are able to detect at p0 in wild type. 40 subunits were detected this way and are displayed according to their expression fold change in proprioceptors in a descending ranking order (**Fig. 15**). Several subunits – namely those, which were identified to be expressed in a proprioceptor-enriched manner – show consistent specificity throughout the developmental stages, though it should be noted that at E14, in some cases the specificity is not fully recognizable.

Interestingly, we do not observe clear enrichment amongst the GABA receptor subgroup for the non-proprioceptive DRG populations, an observation which might be explained by the fact that this population is not homogeneous and also still in a state of afferent remodeling in the dorsal horn from p0 on (Airaksinen et al., 1996; Krimm et al., 2004; Luo et al., 2007).
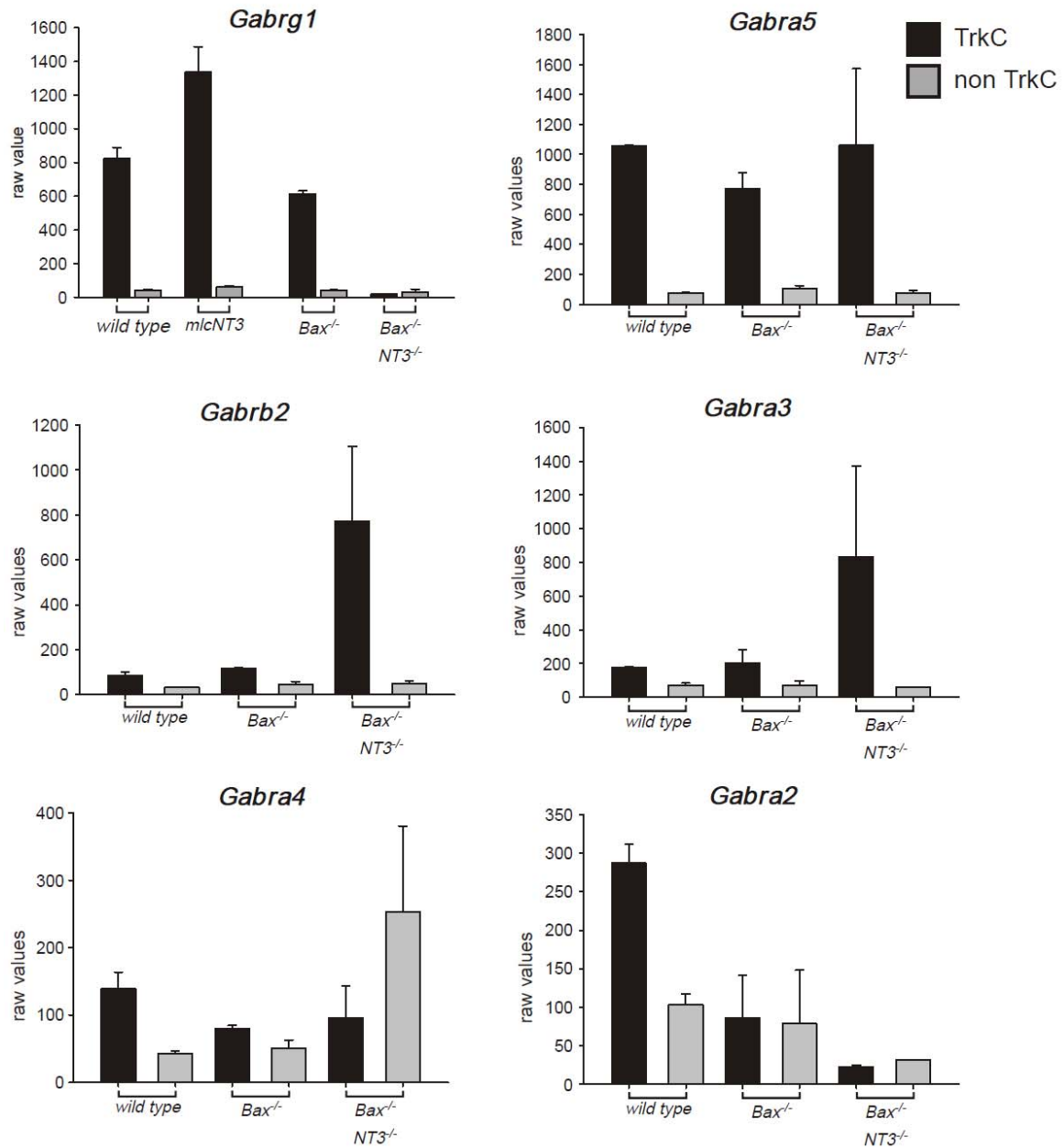
Fig. 14: **TrkC**[on] **enriched GABA**[A] **receptor subunits and their expression in absence of NT3**

Six **GABA**[A] receptor subunits with an enrichment in wild type TrkC[on] cells were identified: *Gabrg1, Gabra5, Gabrb2, Gabra3, Gabra4* and *Gabra2*. Only *Gabrg1* seems to be downregulated in absence of NT3. Black bar: TrkC[on] cells; grey bar: TrkC[off] cells
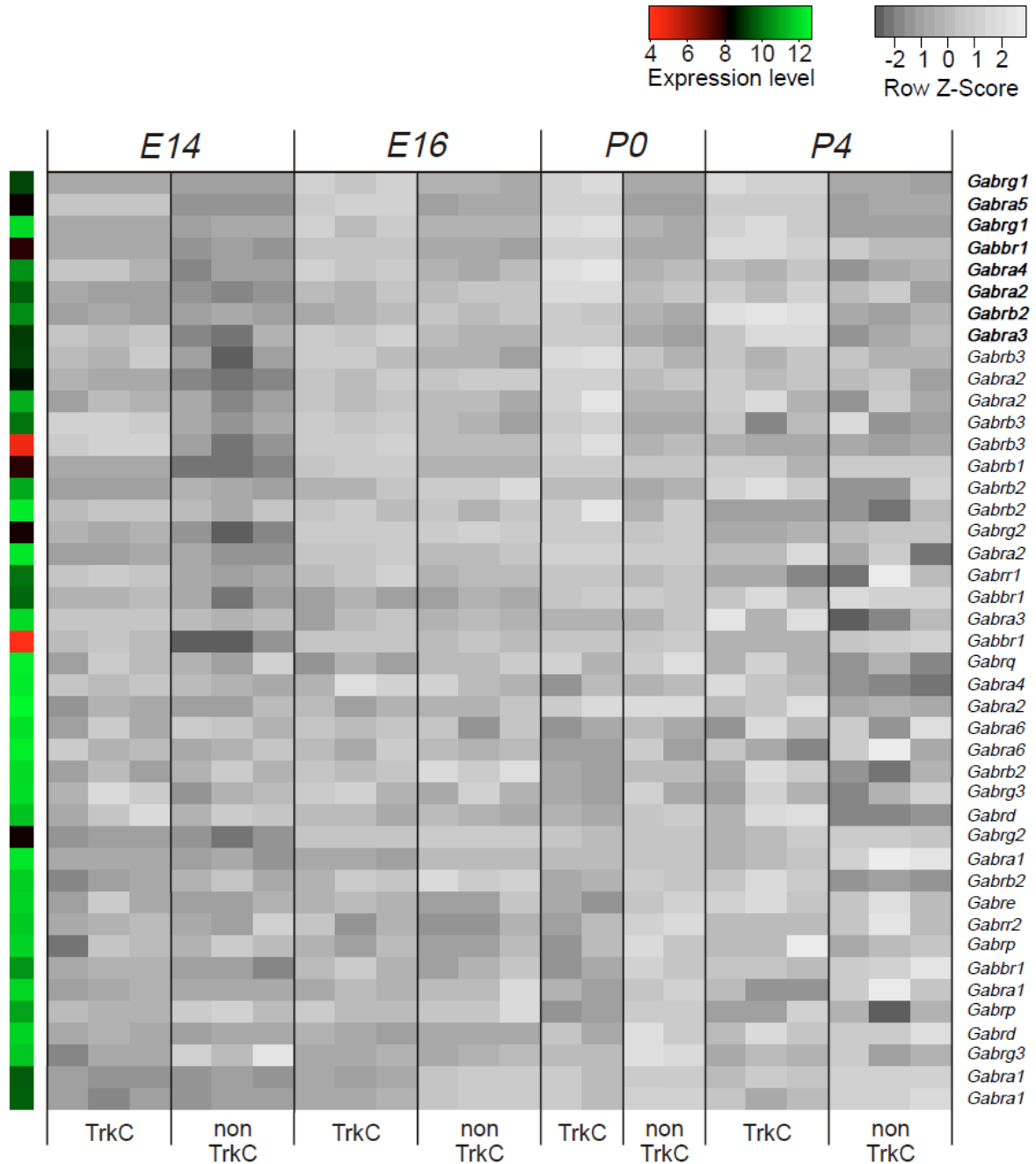
Fig. 15: **Time course analysis of all GABA$_A$ receptor subunits expressed at wild type p0**
Wild type p0 screen data was filtered for **GABA$_A$** receptor subunits. Bold printed names mark subunits with an enriched expression in TrkC^{on} cells (see also **Fig. 14**). Values of wild type E14, E16, p0 and p4 TrkC^{on} proprioceptors and TrkC^{off} non-proprioceptors are shown. Grey scale values represent row z-score values and log2 unit average expression values are shown to the left of each probe (scales plotted top right of panel). Gene names are displayed to the right of each row, and genes analyzed below shown in bold (p≤0.02; regulation ≥2 fold). Note the low average expression value (log2) of most probes.

While in some cases, in individual time points specificity for the *TrkC^{on}* or *TrkC^{off}* population can be observed, it is usually only a transient temporal effect. However, we see receptor subunits with ubiquitous expression in either DRG population, e.g. *Gabrg2*, a prominent GABA$_A$ receptor subunit (Luscher et al., 2011) or *Gabrb1*. It should be pointed out that even though we detect many subunits, the actual expression value of many of those is rather low (see colored bar at the side). This does not necessarily mean that we measure noise but leaves room for speculation about the DRG cell subtypes with unique GABA$_A$ receptor signatures at the level of individual cells.

4.2.3 Gabrg1 expression is confined to subsets of TrkC neurons and exhibits rostro-caudal gradient

Because *Gabrg1* showed a very striking expression profile across all mutants, it prompted us to analyze its expression in more detail. We first confirmed its high enrichment in *TrkC^{on}* proprioceptors of lumbar DRG when compared to non-proprioceptors as predicted from the Affymetrix expression profile data (**Fig. 16A**). Using *in situ* hybridization on DRG of wild-type and *TrkC* mutant mice, we found an almost complete absence of *Gabrg1* expression in *TrkC* mutant DRG. Moreover, assessing individual Affymetrix microarray profiles of *Gabrg1*, we found that its expression was nearly completely downregulated in *NT3^{-/-}Bax^{-/-}* mice while increased significantly and selectively in proprioceptors of *mlc^{NT3}* mice (**Fig. 16B**). Expression in non-proprioceptor populations was not altered in any of the mutants and was at low levels throughout.
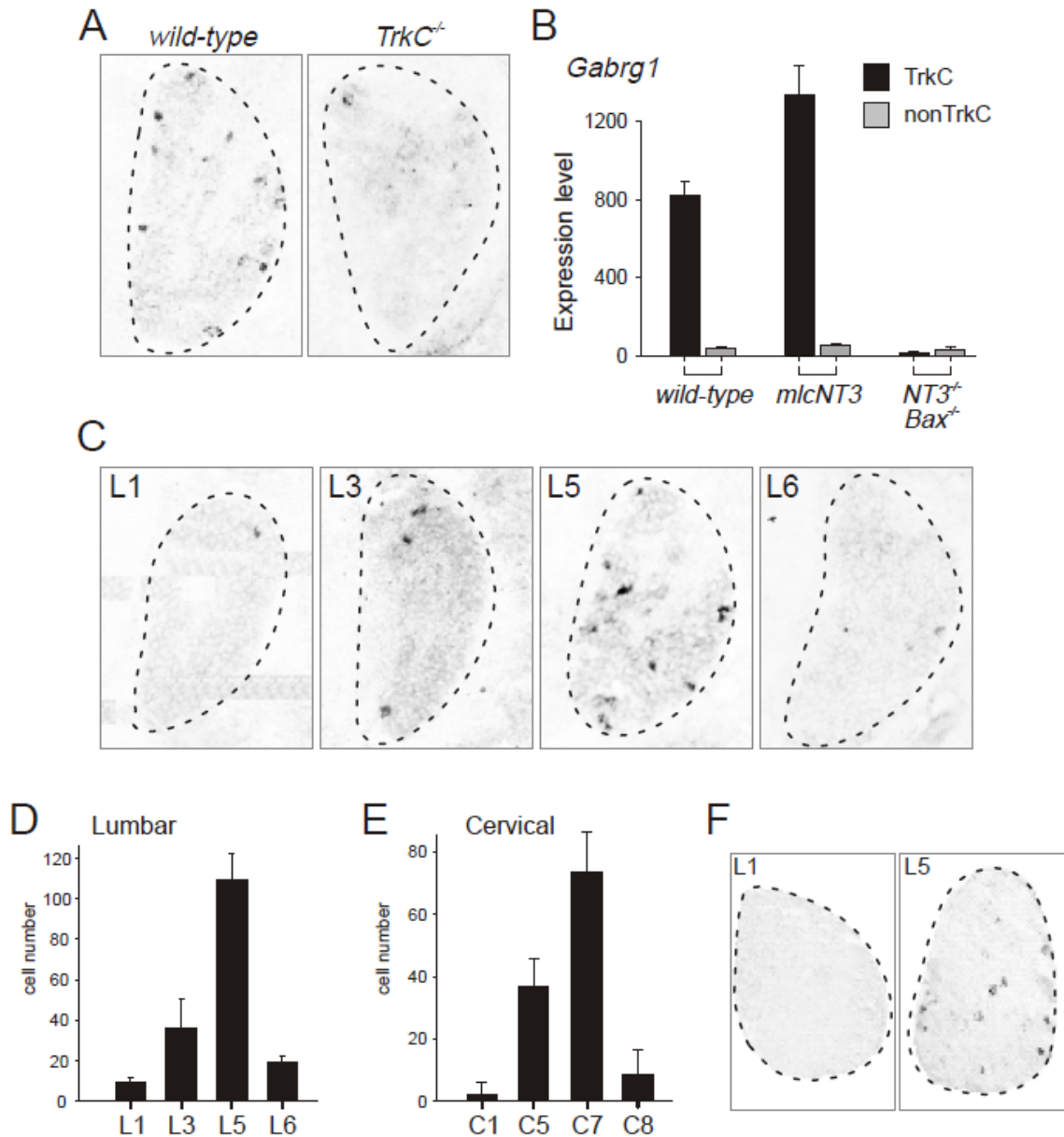
Fig. 16: Peculiar *Gabrg1* expression pattern
(**A**) In situ hybridization of Gabrg1 on wild type and *TrkC^-/-* tissue. In wild type *Gabrg1* seems to be confined to a subset of TrkC^{on} cells. In *TrkC^-/-* DRG most of the *Gabrg1* signal is gone. (**B**) Genechip expression data shows the NT3 dependent expression of *Gabrg1*. (**C**) Along the rostro-caudal axis *Gabrg1* displays a level specific expression pattern. (**D**) Quantification of *Gabrg1^{on}* cells at lumbar levels on p0 wild type tissue. (**E**) Quantification of *Gabrg1^{on}* cells at cervical levels on p0 wild type tissue. (**F**) *Gabrg1* maintains the level specific expression pattern also in adult tissue (p40).

While performing *in situ* hybridization experiments, we noticed an unequal density of *Gabrg1^{on}* cells along the rostro-caudal axis (**Fig. 16C**). Since L1-L6 DRG were pooled for Affymetrix microarray analysis, this observation prompted

51

us to perform *in situ* hybridization experiments to carefully quantify the number of cells detected at different segmental levels. We found a progressive increase in the number of $Gabrg1^{on}$ cells when comparing L1, L3 and L5, and a drop of expression at the L6 level (**Fig. 16D**). This rostro-caudal increase is not a simple reflection of the higher number of $TrkC^{on}$ neurons in more caudal lumbar DRG, since we observed differences of similar magnitude for expression values of *Gabrg1* measured from separately collected L1 and L5 $TrkC^{on}$ proprioceptors, using FACS in $TrkC^{GFP}$ mice ((Friese et al., 2009), data not shown), and *in situ* hybridization signal intensity of labeled cells did not obviously differ across DRG. We next determined whether *Gabrg1* expression is restricted to lumbar DRG levels or can also be detected at cervical levels. Quantitative assessment of $Gabrg1^{on}$ cell number across cervical level DRG C1-C8 revealed a similar gradient in expression as at lumbar levels, with low numbers of $Gabrg1^{on}$ cells at C1-C4, and gradually increasing numbers at C5-C7 (**Fig. 16E**).

To assess whether the subset restricted expression profile of *Gabrg1* is maintained in adult DRG, when GABA receptors are predicted to have a functional role, we first carried out *in situ* hybridization experiments at L1 and L5 DRG of adult mice (p40) (**Fig. 16F**). We found that also in the adult, *Gabrg1* expression in lumbar DRG was confined to sparsely scattered cells and exhibited rostro-caudal density differences between L1 and L5. Together, these findings provide evidence that *Gabrg1* expression in lumbar DRG exhibits pronounced rostro-caudal differences also at adult stages, a pattern likely maintained from early postnatal stages.

4.2.4 Functional analysis of Gabrg1: generation of mutant mice

Because only a small subset of TrkC cells expresses *Gabrg1*, the likelihood of finding the corresponding synapse within the spinal cord is quite low. However, the level specific expression pattern is interesting in a way that it indicates that *Gabrg1^{on}* TrkC neurons can be preferably found in DRG with neurons projecting to distal muscle groups (Landmesser and Morris, 1975; Prats-Galino et al., 1999). This suggests that the Gabrg1 could play a role in presynaptic inhibition of distinct muscular units.

Because the receptor is so sparsely expressed and subsequently locating and analyzing it with immunofluorecence would be time consuming and challenging we sought to generate a mutant mouse using a knock-In approach (Hippenmeyer et al., 2005). Inserting a Cre expressing cassette into the ATG start site of Gabrg1 would allow us to combine the heterozygous animal with a conditional reporter strain, which in turn would allow us to easily visualize and analyze the neurons of interests ((Hippenmeyer et al., 2005) and **Fig. 17**). The homozygous animal would further serve as a model to study the effects of Gabrg1 on motor behavior.

While we received chimeric animals with the cassette inserted into the correct site, we failed to get successful LacZ staining in offspring mice. Crossing the animals with Tau-LSL-GFP mice led to the expected ratio of offspring combinations, however only 50% of the double positive animals had a detectable GFP signal. Analyzing only animals with detectable GFP, we neither were able to identify the level specific pattern we found with using *in situ* hybridization nor were we able to recapitulate the number of cells we counted using in *in situ* hybridization.

Gabrg1 mutant construct
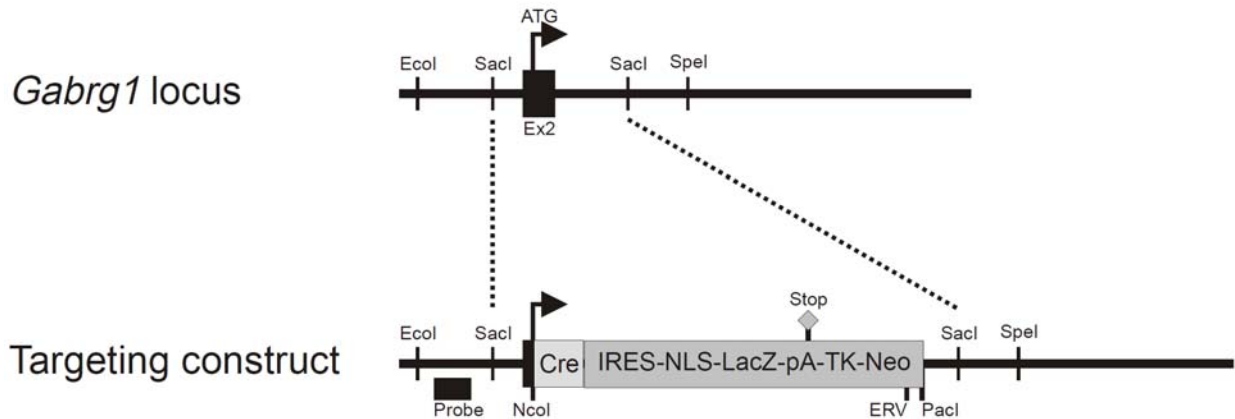
Fig. 17: Cloning scheme for a Gabrg1 knock-in construct

Aiming to generate homozygous animals for further analysis, we generated several intersectional breedings. We aimed at identifying the mutants using PCR and Southern Blot. In both cases, however, we never were able to obtain mutant offspring. To this date there is no report of a possible embryonic lethal knockout of GABA receptors, however we nevertheless checked at E16 and E12 for knockouts, without success.

In summary, the generation of *Gabrg1* mutant mice in the future will allow studying the role of this subunit in presynaptic inhibition, but our scheme of mutation unfortunately did not yield to a strain of mice for analysis, for reasons currently unknown.

4.3 Discussion

A striking feature revealed by our genome-wide expression profiling analysis was the observation that many genes encoding synaptic components were regulated by genetically altering NT3 signaling in proprioceptors. One of the most dramatic examples identified in our analysis was the gene encoding for the $GABA_A$ receptors subunit *Gabrg1*, a previously very poorly studied receptor subunit (Esmaeili et al., 2009). We found that *Gabrg1* expression is profoundly regulated in opposite directions by genetic NT3 level manipulations.

What could be possible roles for postsynaptic receptor components in neurons with purely axonal extensions? It is well-known that central branches of DRG sensory neurons not only establish synaptic contacts with a variety of central spinal neurons themselves, but that their synaptic terminals also provide postsynaptic substrates for inhibitory axo-axonal synapses (Eccles et al., 1962; Frank and Fuortes, 1957; Rudomin and Schmidt, 1999). It is thought that through these axo-axonal synapses, presynaptic inhibition or primary afferent depolarization (PAD) can selectively shunt incoming sensory information at the level of individual sensory synapses, thus preventing or significantly reducing a postsynaptic effect of sensory signals on spinal neurons (Eccles et al., 1962; Frank and Fuortes, 1957; Rudomin and Schmidt, 1999). Electrophysiological studies using pharmacological interventions provide evidence, that GABAA receptors are involved in presynaptic inhibition (Rudomin and Schmidt, 1999), but which receptor components contribute and whether perhaps different sensory afferents assemble receptors of different composition is currently unknown. Moreover, receptors for neurotransmitters other than GABA are also still being considered for their involvement in PAD regulation (Hochman et al., 2010; Rudomin and Schmidt, 1999), suggesting that also other proprioceptors-enriched and in part NT3 regulated postsynaptic receptor components identified here (e.g. *Htr2c*) may be relevant for this process.

Our findings show that *Gabrg1* is expressed preferentially by proprioceptors of more caudal level DRG both at lumbar and cervical spinal levels. These spinal segments are known to innervate distal limb muscles, in contrast to more rostral segments innervating proximal limb muscles (Landmesser and Morris, 1975; Prats-Galino et al., 1999). Our inability to generate antibodies or reporter mice to detect Gabrg1 protein in the spinal cord unfortunately prevented us from directly assessing whether only subsets of vGlut1^{on} proprioceptive terminals accumulate Gabrg1 protein centrally, as would be predicted from our *in situ* hybridization experiments. Analysis of Affymetrix gene expression profiles of other subunits of GABA$_A$ receptors in DRG sensory neurons support the idea that receptors of different subunit composition can be assembled in sensory neurons, but only *Gabrg1* exhibits profound transcriptional regulation in response to NT3 manipulations in both directions. GABA$_A$ receptors of different subunit composition are known to exhibit channel properties of different dynamics or magnitude (Levitan et al., 1988; Olsen, 1982) and alterations in subunit composition would therefore, in principle, be in a position to influence the effect of presynaptic inhibition at central proprioceptive synapses. A possible function of *Gabrg1* and other receptor component subunits in regulation of presynaptic inhibition will therefore be an important avenue to pursue in the future to understand the function of presynaptic inhibition in processing of motor output information.

Our work provides an entry point raising the interesting possibility that postsynaptic components of this presynaptic inhibitory circuit may not be expressed ubiquitously by all sensory neurons, and that NT3 signaling may influence the functionality of this pathway. On a broader scale, our data further confirms the involvement of target derived neurotrophins in the specification of synaptic identity and provides detailed genetic targets for additional detailed analysis.

5. Plasticity in adult spinal circuits

5.1 Introduction

One of the key factors for survival of an organism is its ability to adapt, to react appropriately to changes in its environment. At the level of the nervous system, these abilities are being displayed as the plastic properties of neurons. Initially thought to be hard wired, an undeniable amount of evidence has been provided within the last decades pointing towards the fact that neurons are indeed able to change their properties according to their activity, having led to important advances in the treatment of various neurological conditions such as stroke (Bach-y-Rita, 1983; Dombovy and Bach-y-Rita, 1988) and language deficits (Merzenich et al., 1996).

We now know that activity dependent plasticity can be observed at various levels. Neuronal plasticity can be observed during events such as gene activation (Demarque and Spitzer, 2010), neurogenesis (van Praag et al., 2005) and cellular morphology (Ruediger et al., 2011). Synaptic plasticity includes events such as long-term potentiation (LTP) and long-term depression (LTD) (Bear and Malenka, 1994). One remarkable finding is the physiological and histochemical effect of treadmill training on the spinal cord. Here, using treadmill training in combination with pharmacological and electrical stimulation in paralyzed rats led to a functional remodeling of the spinal locomotor circuits, ultimately allowing a coordinated function of the paralyzed hindlimbs (Courtine et al., 2009).

Again, the transcriptional pathways activated during these events are largely unknown. However there is evidence that exercise alone leads to increase in levels of neurotrophins: Within the spinal cord, bike- and step-training results in a significant increase of BDNF, NT3 and NT4 (Cote et al., 2011; Gomez-Pinilla et al., 2001; Sharma et al., 2010b). In addition, exercise also seems to lead to an increase of NT3 in the muscle (Gomez-Pinilla et al., 2001). Considering our work

introduced in the previous chapters, we therefore wondered whether exercise might also influence gene expression in DRG neurons transcriptionally, and perhaps thereby contribute to plasticity of sensory feedback circuits.

5.2 Results

5.2.1 Exercise dependent increase of *Gabrg1* expressing neurons

Among the NT3 dependent genes identified in our study, with a possible functional role (**Fig. 13**), four were known to be expressed at the postsynapse (**Fig. 13C**). This suggests that these proteins are not found at the axo-dendritic synapses between sensory neuron and motor neuron but at the axo-axonic synapse between interneuron and sensory neuron (Conradi et al., 1983; Fyffe and Light, 1984). We had chosen *Gabrg1* for further analysis and found its expression pattern to be quite peculiar, indicating that it might be specific for sensory neurons projecting preferably to the distal muscle groups. Hypothesizing that there, *Gabrg1* might play a role in presynaptic inhibition (Hochman et al., 2010; Rudomin and Schmidt, 1999), we assumed that it could play a role in fine-tuning of motor output.

Because expression of *Gabrg1* was strongly influenced by NT3 removal and surplus expression in muscles (**Fig. 16B**), we wondered whether the transcriptional regulation might be dynamically regulated through exercise. Past work had shown that exercise of mice leads to a rise of NT3 in muscle (Gomez-Pinilla et al., 2001). Because $GABA_A$ receptor levels might either be regulated at a cell autonomous level or at a population level, we first aimed to investigate whether we would notice a total change of $Gabrg1^{on}$ neurons in the DRG. Triplicates of mice were trained for several weeks in a voluntary running wheel,

DRG were then removed for ISH. Quantification of the ISH signal revealed indeed an increase in *Gabrg1* expressing DRG neurons (**Fig. 18A**), however only
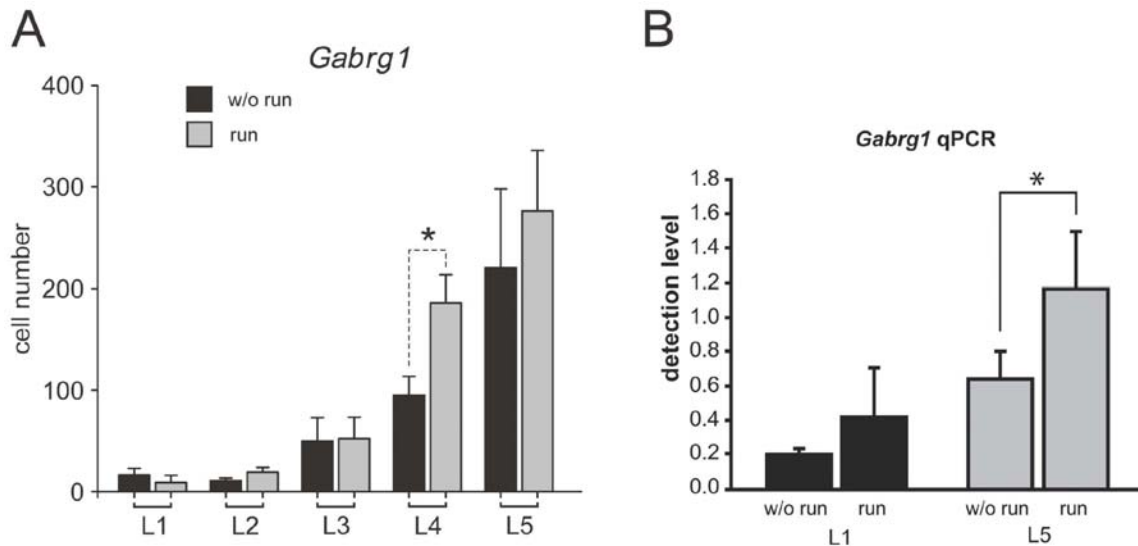
Fig. 18: Level specific increase of Gabrg1 expression after exercise
(**A**) DRG from trained and untrained mice (n = 4) were removed and prepared for ISH. All sections were kept for quantification. Black bar: wild type; grey bar: trained mice. Data for L4: wild type = 93.3 ± SEM; trained = 184.4 ± SEM.
(**B**) L1 and L5 DRG from trained (w/o run) and untrained mice (run) (n = 3) were removed and prepared for RNA extraction, cDNA synthesis and subsequent qPCR. Signals were normalized to TrkC qPCR signal. Black bars = L1; grey bars = L5

significant at L4. To assess whether there also might be a cell autonomous increase in *Gabrg1* levels, we took L1 and L5 DRG from trained mice for RT-PCR (**Fig. 18B**). Consistent with our previous findings we registered a stronger qPCR signal from the L5 DRG than from the L1 DRG in wild type. After exercise, we detect a significant increase of *Gabrg1* signal in the L5 DRG only, on the one hand confirming again that Gabrg1 expression is being upregulated by exercise, on the other hand suggesting that there also might be a cell internal increase of the transcript, since in L5 DRG we are not able to quantify an increase in Gabrg1 expressing neurons (**Fig. 18A**).

5.2.2 Effect of exercise on transcriptional regulation in DRG sensory neurons

Gabrg1 is regulated by NT3 signaling and pronounced expression differences were detected at birth in mutants genetically eliminating NT3 or raising NT3 levels. These findings prompted us to investigate whether exercise, which has previously been described to raise NT3 levels in skeletal muscles (Sharma et al., 2010b), may also influence gene expression in DRG neurons transcriptionally. For this purpose, p35 mice were kept in cages with running wheels, monitoring distances run for 5 weeks before L1 and L5 DRG were isolated and compared by Affymetrix gene expression profiling to DRG isolated from littermates kept in cages without running wheel (**Fig. 19**). We first assessed the number of genes with significantly different expression values between L1 and L5 of control mice (p≤0.02; regulation ≥1.5 fold) and found 15 genes with L1 enrichment and 88 genes with higher expression levels at L5 (**Fig. 19A-C**). Performing the same analysis on samples isolated from mice with running wheel experience yielded 122 genes with expression enriched at L5 when compared to L1 (**Fig. 19C**). Since these adult expression profiles were derived from whole DRG samples, we next determined how many of these genes with higher expression values at L5 also scored at proprioceptor-enriched in the p0 analysis. For mice without running experience, all (88/88) genes scored as p0 proprioceptor enriched (p≤0.02; regulation ≥2 fold) indicating that at least at adult stages (**Fig. 19C**), L1/L5 enriched ratios may be a feature specifically of proprioceptor but not of non-proprioceptor enriched genes. In contrast, only 141/450 genes expressed with L5 enrichment in DRG isolated from mice with running wheel experience were also proprioceptor-enriched in p0 DRG (**Fig. 19C**), suggesting that running wheel exercise also affects genes expression in non-proprioceptor populations. Lastly, we also analyzed how many of the isolated genes were regulated by NT3 signaling and found that 33/88 genes derived from animals without running and 64/141 genes from animals with running experience scored amongst the cohort of NT3 regulated genes.
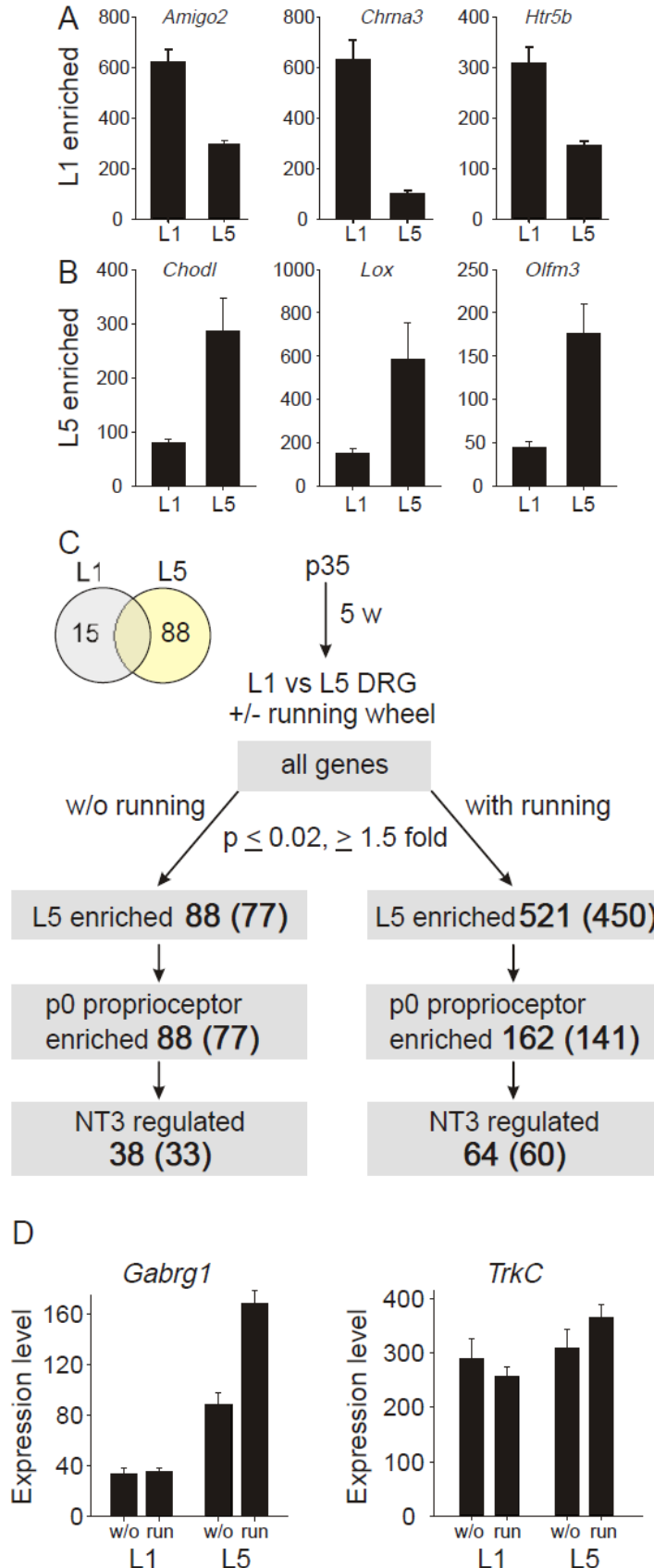
Fig. 19: Effect of exercise on DRG gene expression
(**A, B**) Examples for level specifc gene expression in adult DRG. (**C**) Comparison of gene expression between wild type L1 and L5 DRG led to the identification of 15 L1 enriched and 88 L5 enriched probe sets (p≤0.02; regulation ≥ 1.5 fold), notably all prbe sets had been identified as TrkC[on] marker in our wild type screen (**Fig. 6**). Focusing on the L5 population we found that all 38 of 88 probesets (33/77 genes) had been identified as NT3 dependent. After exercise, of the 521 probe sets (450 genes) enriched in L5, 162 probes (141 genes) had been identified as TrkC[on] marker. 64 of 162 probe sets (60/141 genes) had been previously identified as NT3 dependent.
(**D**) The array data confirms again the level specific expression of Gabrg1 and its increase after exercise.

Amongst the 33 NT3 regulated genes, *Gabrg1* exhibited a very clear Affymetrix gene expression profile. Running wheel experience at the L1 level did not significantly alter *Gabrg1* expression, but at the L5 segmental level, showed a significant increase in expression detected at the whole DRG level, a feature that was also confirmed using quantitative PCR (**Fig. 18B**). Wondering whether the increase in expression might be a general feature we checked the expression profile of TrkC. However, no difference in expression was detected (**Fig. 19D**). Together, these findings support the notion that *Gabrg1* is not only regulated by peripheral retrograde signaling in subpopulations of DRG neurons at embryonic and neonatal stages, but its expression can still be modulated by behavioral interventions in the adult.

Wondering whether exercise would further increase the already existing level specificity of a gene, we checked how many of the L1 and L5 enriched genes in WT would fall into this category. Interestingly, only *Gabrg1* fulfilled these conditions. All other level specific proprioceptor markers either lost their specificity or did not change significantly.

5.3 Discussion

Using a voluntary running paradigm, we provide evidence of exercise induced transcriptional regulation in unsorted DRG neurons. While the exact nature of this regulation is still unclear, previous work suggests that upregulation of neurotrophins in the target area might play a role, by retrogradely activating the transcriptional program of the cell (da Silva and Wang, 2011; Hippenmeyer et al., 2004; Huberman, 2006).

Considering the fact that target derived NT3 is necessary for survival of certain non proprioceptive afferents at adult stages, our findings regarding the influence of voluntary running on gene expression in DRG sensory neurons further support the notion that retrograde signals have life-long roles in adjusting gene expression programs. The fact that genes developmentally regulated by target-derived signals reappear in the behavioral paradigm carried out in our study in the adult suggests that expression of at least subsets of genes remains plastic also in the adult, a feature that may be important for the design of strategies interfering with pain or neuronal injury.

6. Supplementals
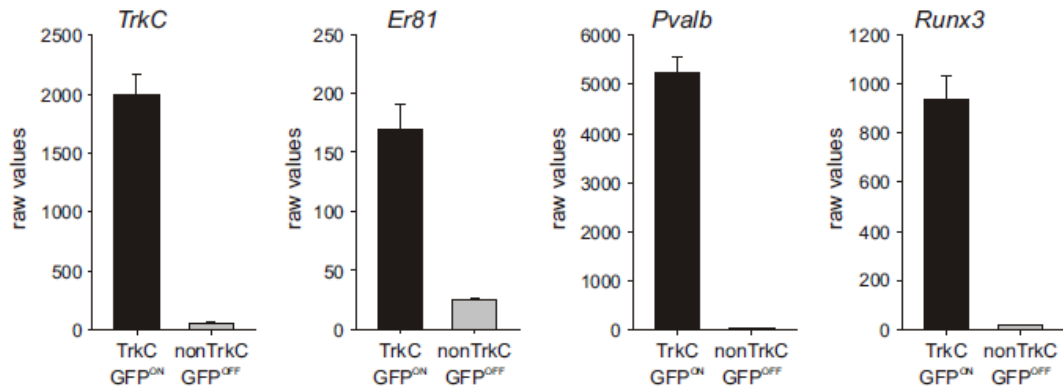
Supp. 1: Genechip expression data of four known proprioceptive marker marker genes in wild type p0 DRG. Black bar: expression in TrkCon cells; grey bar: expression in TrkCoff cells (n = 2)
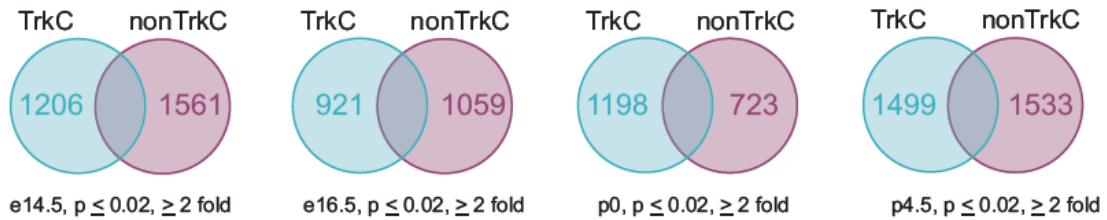
Supp. 2: Quantification of population specific marker at various time points

7. Material & Methods

Mouse genetics

Transgenic mice analyzed in this study were $TrkC^{GFP}$ (Gong et al., 2003), $Bax^{-/-}$ (Deckwerth et al., 1996), $NT3^{-/-}$ (Farinas et al., 1994), Mlc^{NT3} (Taylor et al., 2001).

Sample preparation and analysis for Affymetrix gene expression profiling experiments

For the study of the role of NT3 in the transcriptional regulation of DRG sensory neurons we used a total of 16 arrays representing 8 different groups (duplicates for each condition). For wild-type screens (e14.5, e16.5, p0.5 and p4.5) and the adult exercise screens, we used a total of 30 arrays representing 10 different groups (triplicates for each condition).

Dorsal Root Ganglia Dissection and Dissociation

1.) Isolation of DRG

- laminectomy was performed in ice cold HBSS medium w/o Ca2+/Mg2+, tissue should be covered in medium at all times
- coat FACS tube with sterile filtered, inactivated FCS (at least 15 min)
- remove FCS, refill FACS tube with 1ml ice cold HBSS medium w/o Ca2+/Mg2+, transfer isolated DRG into tube (use 1000 µl siliconized pipette tip to transfer DRG)

2.) Trypsin / Collagenase H Treatment

- centrifuge tubes for 7 min at 800 rpm. Remove HBSS medium with fire polished Pasteur pipette, take care not to lose any DRG

- add 1 ml 0.25% trypsin solution and 100 µl Collagenase H enzyme solution (final concentration 0.1%)
- mix gently by flipping with fingers the bottom of the tube
- incubate mix for 10 minutes at 37°C (15 min for p4 DRG). Flip the tube carefully every 5 min.
- stop digestion step by adding 2.5 ml HBSS medium. Mix gently and centrifuge the mix for 7 minutes at 800 rpm.
- Carefully discard the supernatant using a fire polished Pasteur pipette.
- Resuspend cell pellet in 1 ml ice cold HBSS medium. Tissue will appear as a lump.

3.) Trituration

- Dissociate cells by drawing them through a fire polished Pasteur pipette tip and expelling them along the Falcon tube. Repeat step approximately 20 times until the tissue is dissociated. The older the tissue, the more repetitions it will take.
- Check for single cell suspension under the binocular dissection microscope.
- Single cell solution was passed through a custom made gauze filter (40 µm mesh size) and transferred into a new previously FCS coated tube

Fluorescent Activated Cell Sorting

For Fluorescent Activated Cell Sorting a MoFlo (DAKO) high-speed 4-way cell sorter was used. It has a 3-laser set-up: two water-cooled Coherent Enterprise II lasers (Model610 emitting at 488nm and Model653 allowing UV excitation) and one air-cooled Spectra Physics Helium-Neon laser emitting at 633nm. To sort DRG sensory neurons, a 100µm nozzle was used at 20psi. Sorted cells were collected in 1 ml Eppendorff tubes filled with 50µl Trizol.

Microarray analysis

RNA extraction and amplification was performed by the FMI Microarray facility. For microarray analysis Affymetrix GeneChip Mouse Genome 430A 2.0 arrays were used.

Raw array data were read into R (v.2.9) and probeset condensation and RMA normalization were performed using the justRMA() function of the Affymetrix package from R/Bioconductor (2.3). Normalized probeset-level data was exported to a file and loaded into Genedata Analyst v2.2. Lists of differential genes were generated using the moderated ttest function (p ≤ 0.02) and an additional cut-off of an at least 2 fold change in expression levels. Heatmaps were generated in R using the heatmap function of the gplot package.

In situ hybridization and immunohistochemistry

Protocols: (Arber et al., 2000; Hippenmeyer et al., 2005)

Probe sequences:

(Friese, 2010); Gabrg1 and Grm3 from Allen Brain Atlas

Staining protocol for Cx36 staining

(For details check also (Ciolofan et al., 2007))

- Mice were deeply anesthetized with a rombutan/ketamin solution and transcardially perfused with 3 ml of cold 50 mM sodium phosphate buffer, pH 7.4, containing 0.9% NaCl, 0.1 M sodium nitrite and 1 U/ml heparin, followed by 40 ml of cold 0.16 M sodium phosphate buffer, pH 7.6, containing 1% formaldehyde and 0.2% picric acid.

- After perfusion fixation, tissue was removed and cryoprotected for 24–72h. Sections of spinal cord were cut (12 μm) on a cryostat and collected on coated glass slides.

- Sections were washed for 20 min in 50 mM Tris-HCl, pH 7.4, containing 1.5% sodium chloride (TBS) and 0.3% Triton X-100 (TBSTr). For double-immunofluorescence labeling, sections were incubated simultaneously with primary antibody for Cx36 (1:100 dilution) rabbit polyclonal (Life technologies) for 12h at 4°C, then washed for 1h in TBSTr, and incubated for 1.5h at room temperature simultaneously with appropriate combinations of secondary antibodies

- All antibodies were diluted in TBSTr containing 5% normal goat or normal donkey serum. After secondary antibody incubations, sections were washed in TBSTr for 20 min; in 50 mM Tris-HCl buffer, pH 7.4, for 30 min; covered with antifade medium; and coverslipped.

Southern Blot

Protocol: (Arber et al., 2000; Hippenmeyer et al., 2007; Hippenmeyer et al., 2005)

Probe sequence: Forward: 5`- ttcttatagctgctgtcagaacca-3'

Reverse: 5'-aaggattatttaacggtttcaca-3'

Digest with EcoRI

Voluntary running experiments with adult mice

5 weeks old male Bl6 mice were put into running wheels for 5 weeks. Distances were measured with a counter attached to the running wheel.

RNA isolation of DRG (for subsequent qPCR)

(adapted from http://www.ebi.ac.uk/arrayexpress/files/E-MEXP-976/E-MEXP-976.idf.txt)

1. Clean glass homogenizer first with detergent (Deacon). Rinse 3-4x with dH2O. Add 0.5ml Trizol and clean. Remove this.

2. Add 50µl Trizol to tissue and transfer to clean homogenizer. Homogenise for 2-3 min. Add another 50µl Trizol, homogenize and finally add 400µl Trizol. Transfer to clean 1.4ml tube and add another 750 µl of Trizol. Store on ice. Clean glass homogenizer as above and process second sample.

3. Load the lysate (maximum volume 700 µl) onto a QIAshredder spin column sitting in a 2 ml collection tube and spin for 2 min at maximum speed in a microfuge. Repeat with the remaining of the sample.

4. Transfer sample to a 1.5 ml tube and incubate 5 min at 15-30°C.

5. Add 0.2 volumes of chloroform (or chloroform-isoamyl alcohol). Cap tubes and shake vigorously for 15 seconds. Do not vortex!! Allow sample to stand at room temperature for 2-15 min.

6. Follow the protocol provided by the Qiagen RNeasy mini kit.

qPCR probes

gabrg1
forward 5'-cataaacatggagtatacaatag-'3
reverse 5'-gagttcctgaagaaagtgtc-'3

trkC
forward 5'-cagtcagtgtgatctcccag-'3
reverse 5'-gtccagttcagattggtc-'3

Material
- Binocular dissecting microscope
- Dissection tools
- Waterbath
- 1000 µl pipette with regular and siliconized tips
- Centrifuge for 15 ml reaction tubes, 800 rpm

- Fire polished Pasteur pipette

- Hank's modified solution, Hank's balanced salt solution (HBSS) medium w/o Ca2+/Mg2+, Gibco Nr. 14170-138

- Fetal Calf Serum, Amimed, Bioconcepts, 500 ml, heat inactivate for 30 minutes in 56°C, store at -20°C in appropriate aliquots

- Trypsin 0.25%, Amimed, Bioconcepts Nr. 5-50 F00-H07, 100 ml, or Sigma Nr. T-8253, store at -20°C in appropriate aliquots

- 1 g Collagenase H, Boehringer Mannheim Nr. 1074032, dilute to 1% in HBSS medium w/o Ca2+/Mg2+, sterilization of the medium through 0.45 μm filter under a laminar flow hood, store 100 μl aliquots at -20°C

- For generation of cDNA: ThermoScript RT-PCR System (Invitrogen no. 11146057)

- Platinum Sybr Green Super mix UDG with ROX (Invitrogen no. 11790-01K)

- Images were taken with either OLYMPUS BX61 Fluoview or Zeiss LSM700

List of Antibodies

- neurotrophin receptor tyrosine kinase antibodies (**Trks**) and the **islet1** used as described in (Kramer et al., 2006)

- Rabbit anti **Runx3**: (Kramer et al., 2006)

- Goat anti **p75**: Neuromics; cat #: GT15057; dilution 1:5.000

- Rabbit anti **p75**: (Reichert); dilution 1:8.000

- Rabbit anti **Cx36**: Invitrogen; cat #: 3646000; dilution 1:100

- Guinea pig anti **vGlut1**: Chemicon; cat. #: AB5905; dilution 1:20.000

- Chicken anti **GFP**: Molecular Probes; cat. #: A10262

6. Role of Fgf8 signalling in the specification of rostral Cajal-Retzius cells

Céline Zimmer1, Jun Lee, Amélie Griveau, Silvia Arber, Alessandra Pierani, Sonia Garel and François Guillemot

SUMMARY

Cajal-Retzius (CR) cells play a key role in the formation of the cerebral cortex. These pioneer neurons are distributed throughout the cortical marginal zone in distinct graded distributions. Fate mapping and cell lineage tracing studies have recently shown that CR cells arise from restricted domains of the pallial ventricular zone, which are associated with signalling centres involved in the early regionalisation of the telencephalic vesicles. In this study, we identified a subpopulation of CR cells in the rostral telencephalon that expresses Er81, a downstream target of Fgf8 signalling. We investigated the role of the rostral telencephalic patterning centre, which secretes FGF molecules, in the specification of these cells. Using pharmacological inhibitors and genetic inactivation of *Fgf8*, we showed that production of Fgf8 by the rostral telencephalic signalling centre is required for the specification of the Er81^{+} CR cell population. Moreover, the analysis of *Fgf8* gain-of-function in cultivated mouse embryos and of *Emx2* and *Gli3* mutant embryos revealed that ectopic Fgf8 signalling promotes the generation of CR cells with a rostral phenotype from the dorsal pallium. These data showed that Fgf8 signalling is both required and sufficient to induce rostral CR cells. Together, our results shed light on the mechanisms specifying rostral CR cells and further emphasise the crucial role of telencephalic signalling centres in the generation of distinct CR cell populations.

INTRODUCTION

The cerebral cortex contains different subclasses of excitatory projection neurons derived from the dorsal telencephalon or pallium, as well as inhibitory interneurons originating from the ventral telencephalon or subpallium (Marin and Rubenstein, 2003; Molyneaux et al., 2007). The cerebral cortex is subdivided into different regions with divergent evolutionary histories, i.e. the archicortex, neocortex and paleocortex, and into areas with distinct functions, i.e. the motor, somatosensory, visual and auditory cortical areas (O'Leary et al., 2007; Rakic, 1988; Rash and Grove, 2006; Sur and Rubenstein, 2005). The cortex is also organised into six layers containing neurons with different morphological, molecular and physiological characteristics and unique patterns of connectivity. This cytoarchitecture is tightly regulated, with a defined number of neurons adopting specific laminar features in each zone, which is crucial for the proper activity of the cerebral cortex. Cajal-Retzius (CR) cells are among the first neurons to be generated between E10.5 and E13.5 in mouse (Hevner et al., 2001; Takiguchi-Hayashi et al., 2004), and they die during the first postnatal weeks (Abraham and Meyer, 2003; del Rio et al., 1995; Derer and Derer, 1990; Marin-Padilla, 1990; Marin-Padilla, 1992; Zecevic and Rakic, 2001). This transient pioneer neuronal population was discovered more than a century ago, in humans by G. Retzius and in lagomorphs by S. Ramon y Cajal, but the features and functions of these cells remain largely unknown. They appear to play a key role in the radial migration of cortical neurons and in the laminar organisation of the mouse and human cortex, largely through the production of the extracellular glycoprotein reelin (D'Arcangelo et al., 1995; Ogawa et al., 1995; Rice and Curran, 2001; Super et al., 2000).

CR cells populate the marginal zone (MZ) of the cortex evenly in the prospective neocortex, but accumulate at distinct locations such as at the olfactory piriform cortex. Various CR cell subpopulations have been identified and shown to differentially express several molecular markers, including reelin, calretinin (calbindin 2 – Mouse Genome Informatics) and p73α (Trp73 – Mouse

Genome Informatics) (Bielle et al., 2005; Meyer et al., 2002; Takiguchi-Hayashi et al., 2004). CR cells have long been assumed to arise from the whole pallial ventricular zone (VZ) and to migrate radially to the cortical surface, similarly to other glutamatergic cortical neurons (del Rio et al., 1995; Hevner et al., 2003; Marin-Padilla, 1998). However, Meyer and colleagues identified restricted sites of generation of CR cells based on the expression of p73α, a transcription factor that is expressed by different CR cell subpopulations (Meyer et al., 2002). Consistently, fate mapping and cell lineage tracing studies have shown that CR cells arise from specific locations along the rostrocaudal and dorsoventral axes of the pallial VZ (Bielle et al., 2005; Garcia-Moreno et al., 2007; Imayoshi et al., 2008; Monuki et al., 2001; Takiguchi-Hayashi et al., 2004; Yoshida et al., 2006; Zhao et al., 2006). Four different sites of CR generation have been identified, comprising the pallial domain of the septum in the rostromedial (RM) pallium (Bielle et al., 2005), the ventral pallium (VP) laterally (Bielle et al., 2005), the prospective choroid plexus, and the cortical hem (CH) caudally (Garcia-Moreno et al., 2007; Imayoshi et al., 2008; Monuki et al., 2001; Takiguchi-Hayashi et al., 2004; Yoshida et al., 2006; Zhao et al., 2006). CR cells migrate tangentially from these focal sites to populate the entire cortical surface. Furthermore, fate mapping studies have shown that CR cells originating from different sources preferentially settle in distinct regions of the cortex (Bielle et al., 2005; Imayoshi et al., 2008; Takiguchi-Hayashi et al., 2004; Yoshida et al., 2006; Zhao et al., 2006). Indeed, ablation of the CH results in a substantial depletion of CR cells, except in the rostral cortex, thus demonstrating that CH-derived CR cells mainly populate the caudal cortex (Yoshida et al., 2006).

Intriguingly, the neuroepithelial domains that generate CR cells are closely associated with signalling centres involved in the early regionalisation of the telencephalic vesicles. These signaling centres secrete morphogens that provide positional and proliferative cues to the surrounding telencephalic neuroepithelium (O'Leary et al., 2007; Rash and Grove, 2006; Sur and Rubenstein, 2005). Recently, the signals produced by the CH in the caudomedial telencephalon, which include TGFβ molecules, were shown to be necessary for the generation

of caudal CR cells (Friedrichs et al., 2008; Hanashima et al., 2007; Siegenthaler and Miller, 2008; Theil, 2005). Morphogens produced by the commissural plate (CoP) in the RM telencephalon and by the putative anti-hem in the lateral telencephalon might similarly participate in CR cell generation. In contrast to the substantial progress that has been made in understanding how caudal CR cell populations are specified, the mechanisms underlying the specification of rostral CR cells have remained poorly characterised.

FGF signalling has been shown to play an essential role in patterning the rostral telencephalon (Cholfin and Rubenstein, 2007; Cholfin and Rubenstein, 2008; Fukuchi-Shimogori and Grove, 2001; Fukuchi-Shimogori and Grove, 2003; Garel et al., 2003; Paek et al., 2009; Shimogori et al., 2004; Storm et al., 2006). *Fgf8* is expressed early on at the rostral tip of the neural tube (called the anterior neural ridge or ANR) (Crossley and Martin, 1995; Crossley et al., 2001; Shimamura and Rubenstein, 1997) and its expression persists after fusion of the ANR to form the CoP at the rostrodorsal midline of the telencephalon (Crossley et al., 2001). Fgf8 is the main secreted factor produced by the rostral organising centre, where it regulates the expression of *Fgf17* and *Fgf18* and is involved in patterning both the dorsal and ventral telencephalon, as well as in promoting cell survival (Bachler and Neubuser, 2001; Borello et al., 2008; Chi et al., 2003; Cholfin and Rubenstein, 2008; Fukuchi-Shimogori and Grove, 2003; Gimeno and Martinez, 2007; Gutin et al., 2006; Lee et al., 2000; Ohkubo et al., 2002; Shanmugalingam et al., 2000; Storm et al., 2006; Storm et al., 2003).

In this study, we have examined the mechanisms engaged in the specification of rostral CR cells and asked specifically whether Fgf8 signalling from the rostral patterning centre is involved in this process. We found that Er81, an ETS transcription factor downstream of Fgf8 signalling, is specifically expressed at early stages by CR cells in the rostral cortex and not by caudal CH-derived CR cells. These rostral Er81^{+} CR cells derive largely from the RM pallium, as shown by their persistence in *Pax6* mutants. We used pharmacological inhibitors and genetic inactivation of *Fgf8* to demonstrate that the Fgf8 telencephalic signalling centre is required for the specification of Er81^{+}

CR cells. We have also used an *Fgf8* gain-of-function approach in vitro and analysed *Emx2* and *Gli3* mutant mouse embryos, which express *Fgf8* ectopically, to show that ectopic Fgf8 signalling promotes the generation of rostral-type CR cells from the dorsal pallium. Together, our results shed light on the mechanisms that specify rostral CR cells.

RESULTS

Rostral CR cells express Er81, a downstream target of FGF signaling

Genetic ablation of the CH-derived CR cell subpopulation has revealed the extent of the remaining CR cell subpopulations in the rostral telencephalon (Yoshida et al., 2006). The signalling activity of the CH during telencephalic patterning is balanced by the activity of the rostral CoP (O'Leary et al., 2007; Rash and Grove, 2006; Sur and Rubenstein, 2005). We thus hypothesised that rostral CR cells, which are spared by the ablation of the CH, might be induced by FGF signals emanating from the CoP.

To address this issue, we first mapped the domains of Fgf8 signalling activity by characterising the expression patterns of the ETS transcription factors *Erm*, *Pea3* and *Er81* (also known as *Etv5*, *Etv4* and *Etv1*, respectively), which are effectors of Fgf8 signalling (Cholfin and Rubenstein, 2008; Fukuchi-Shimogori and Grove, 2003). We conducted our analysis at different rostrocaudal levels of the mouse telencephalon at E11.5 (Fig. 1B-D'''). At rostral levels, *Erm* and *Pea3* were expressed medially throughout the dorsoventral extent of the telencephalic VZ (Fig. 1B,B',C,C'), whereas *Er81* expression was restricted to the MZ of the whole cortex at this level (Fig. 1D,D'). More caudally, *Erm* and *Pea3* were expressed at low levels in the CH (Fig. 1B'',C''), whereas *Er81* was absent (Fig. 1D''). Further caudally, expression of all three genes was absent
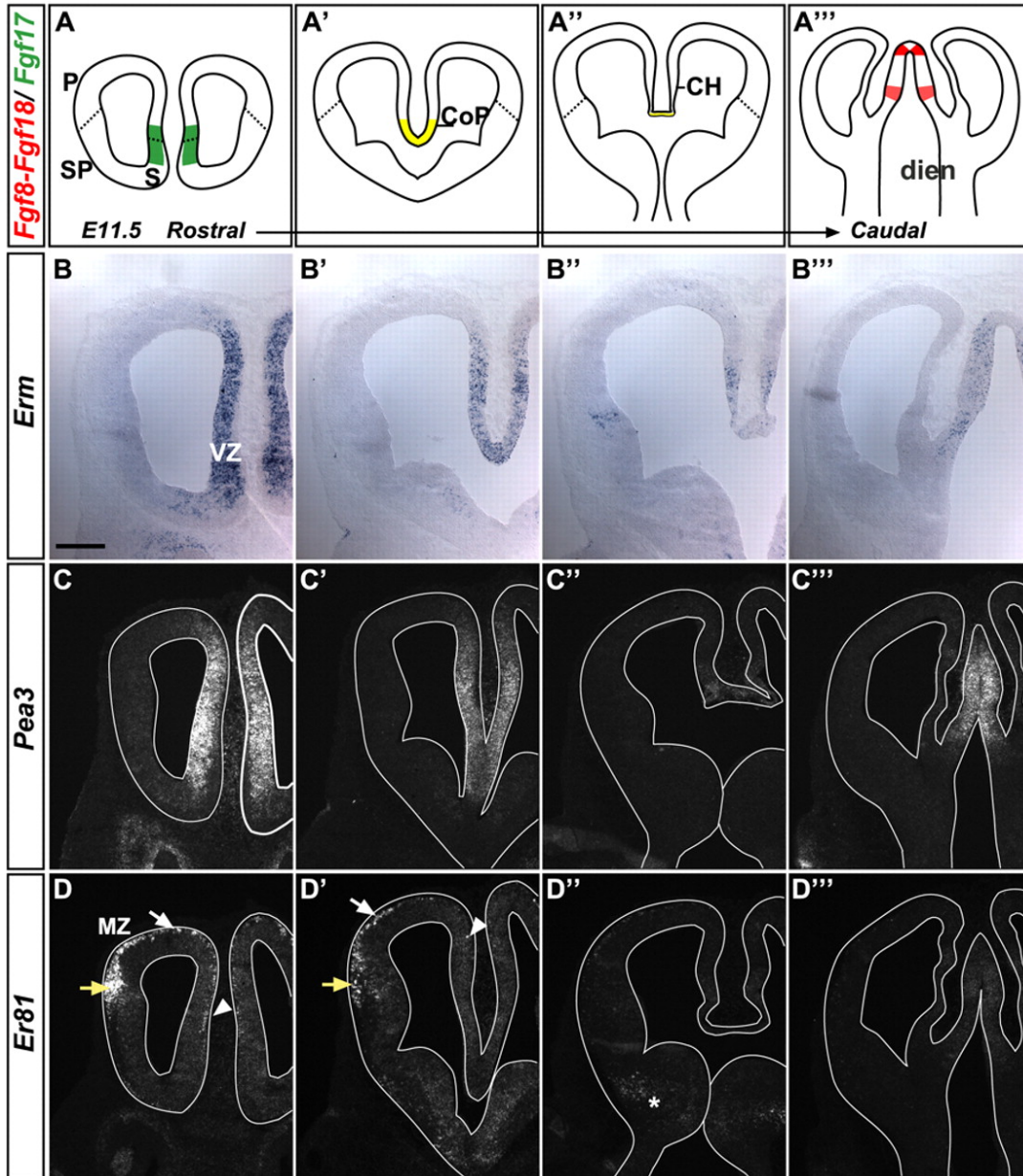
Fig. 1.: Expression patterns of FGF signalling-induced *ETS* factors in the mouse embryonic telencephalon. (**A-A‴**) Schemes of coronal sections of E11.5 telencephalon analysed at different rostral-caudal levels showing expression domains of *Fgf8* and *Fgf18* (red), *Fgf17* (green) and *Fgf8/17/18* (yellow). (**B-D‴**) *In situ* hybridisation of coronal sections of the telencephalon at E11.5. (B-B‴) *Erm* is expressed in the medial VZ of the telencephalon (B,B′), in the CH and the PSB (B″), and in the diencephalon but not the telencephalon at caudal levels (B‴). (C-C‴) *Pea3* shows a similar expression pattern to *Erm*, except in the PSB (C″). (D-D‴) *Er81* is expressed in the MZ of the medial (arrowhead) and dorsal (white arrow) cortex and in the olfactory piriform cortex (yellow arrow), where preplate cells are localised (D). Caudally, *Er81* is weakly expressed in the SP (asterisk in D″) and in the diencephalon (D‴). CH, cortical hem; CoP, commissural plate; dien, diencephalon; P, pallium; PSB, pallium-subpallium boundary; S, septum; SP, subpallium; VZ, ventricular zone; MZ, marginal zone. Scale bar: 210 µm.

from the telencephalon (Fig. 1B''',C''',D'''). FGF signalling activity thus correlated well with *Fgf* expression domains and was elevated within the RM pallium, which includes the pallial septum (Fig. 1A-A'''). Er81 expression was detected in the rostral cortex, where it started to decline at E12.5 and was absent at E13.5 (data not shown), suggesting a transient FGF signalling activity in postmitotic neurons.

We characterised the *Er81*-expressing cells of the rostral cortex by co-immunolabelling for Er81 and cell type-specific markers at E11.5. All Er81$^+$ cells expressed Tbr1, a T-box transcription factor that labels both CR and preplate neurons (see Fig. S1C-F in the supplementary material) (Hevner et al., 2001). Using reelin and calretinin as specific CR cell markers (Alcantara et al., 1998; del Rio et al., 1995), we further determined that ~75% of Er81$^+$ cells were positive for reelin or calretinin and had a similar distribution in the different cortical areas analysed (Fig. 2B-C''; see Fig. S2 in the supplementary material). Using p73α as a marker of CR cells derived from the pallial septum (A.G. and A.P., unpublished) (Hanashima et al., 2007), we also observed that some cells expressed both Er81 and p73α, representing more than 30% of the Er81$^+$ population in the medial cortex (Fig. 2D-D''). These data suggest that rostral CR cells are likely to represent two distinct CR cell types, one p73α+ and one p73α−. Together with the spatial analysis of Er81 expression (Fig. 1D,D'''), these data showed that rostral CR cells mainly express reelin, calretinin and the ETS transcription factor Er81 at E11.5. The co-expression of Er81 with reelin or calretinin can thus be used to discriminate rostral CR cells from CH-derived CR cells, which express neither Er81 nor calretinin at early developmental stages (E10.5-E12.5).
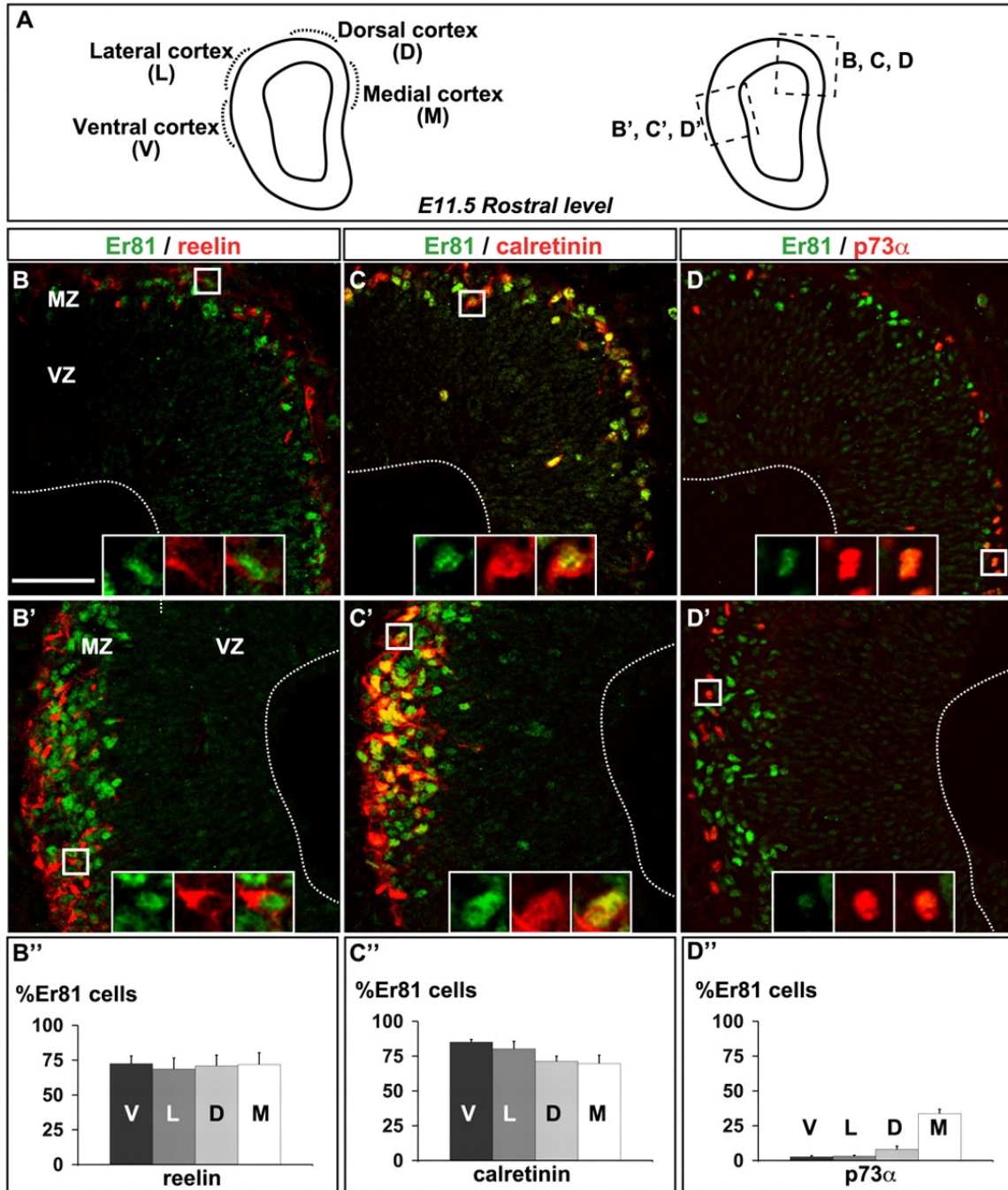
Fig. 2.: **Er81 expression in rostral Cajal-Retzius (CR) cells.** (**A**) Scheme of a coronal section of mouse E11.5 telencephalon at rostral level. (**B**,**B′**,**C**,**C′**,**D**,**D′**) Co-immunolabelling for Er81 and reelin (B,B′), Er81 and calretinin (C,C′), Er81 and p73α (D,D′) in the dorsal and medial cortex (B-D) and the lateral and ventral cortex (olfactory piriform cortex) (B′-D′). (**B″**,**C″**, **D″**) Cortical distribution of Er81^{+} cells that co-express reelin (V, 72.2±5.4%; L, 68.6±7.9%; D, 70.9±7.7%; M, 71.9±8.4%), calretinin (V, 85±2%; L, 81.2±5.3%; D, 71.2±3.8; M, 69.6±6%) and p73α (V, 2.6±0.9%; L, 3.1±0.8%; D, 8±2.4%; M, 33.8±3%). D, dorsal; L, lateral; M, medial; V, ventral. Scale bar: 50 µm.

The pallial septum gives rise to Er81$^+$ CR cells

We then examined which progenitor domains give rise to Er81$^+$ CR cells at E11.5. CR cells of the rostral cortex are mainly derived from the VP, located laterally, and from the pallial septum, located medially (A.G. and A.P., unpublished) (Bielle et al., 2005). *Dbx1* is expressed by progenitors of the VP and also by early postmitotic cells derivedfrom the pallial septum (A.G. and A.P., unpublished) (Bielle et al., 2005). We thus analysed the rostral cortex of heterozygous *Dbx1*$^{nls-lacZ}$ mice using co-immunolabelling for Er81 and β-galactosidase (β-gal), which can be used to trace the short-term progeny of *Dbx1*-expressing cells (Fig. 3A-A''). Most β-gal+ cells co-expressed Er81 (Fig. 3A''), indicating that a substantial fraction of Er81$^+$ CR cells derive from *Dbx1*-expressing cells located rostrally in the lateral pallium and the medial cortex.

To further assess whether Er81$^+$ cells were derived from the RM pallium domain, we analysed rostral CR cells in the *Pax6* mutant, in which the VP is not specified and no longer expresses *Dbx1* (data not shown) (Carney et al., 2009; Yun et al., 2001), whereas the pallial septum is unaffected and remains positive for *Dbx1* expression (data not shown). We found no significant difference in Er81 and reelin co-immunolabelling between wild-type and *Pax6* mutant embryos in medial, dorsal (Fig. 3B-E; see Table S1 in the supplementary material), lateral and ventral domains of the rostral cortex at E12.5 (see Fig. S3 in the supplementary material). These results indicate that Er81$^+$ CR cells are still specified in the absence of a lateral VP domain and must therefore originate from a medial location. Hence, the pallial septum gives rise to rostral Er81$^+$ CR cells populating the rostral cortex.
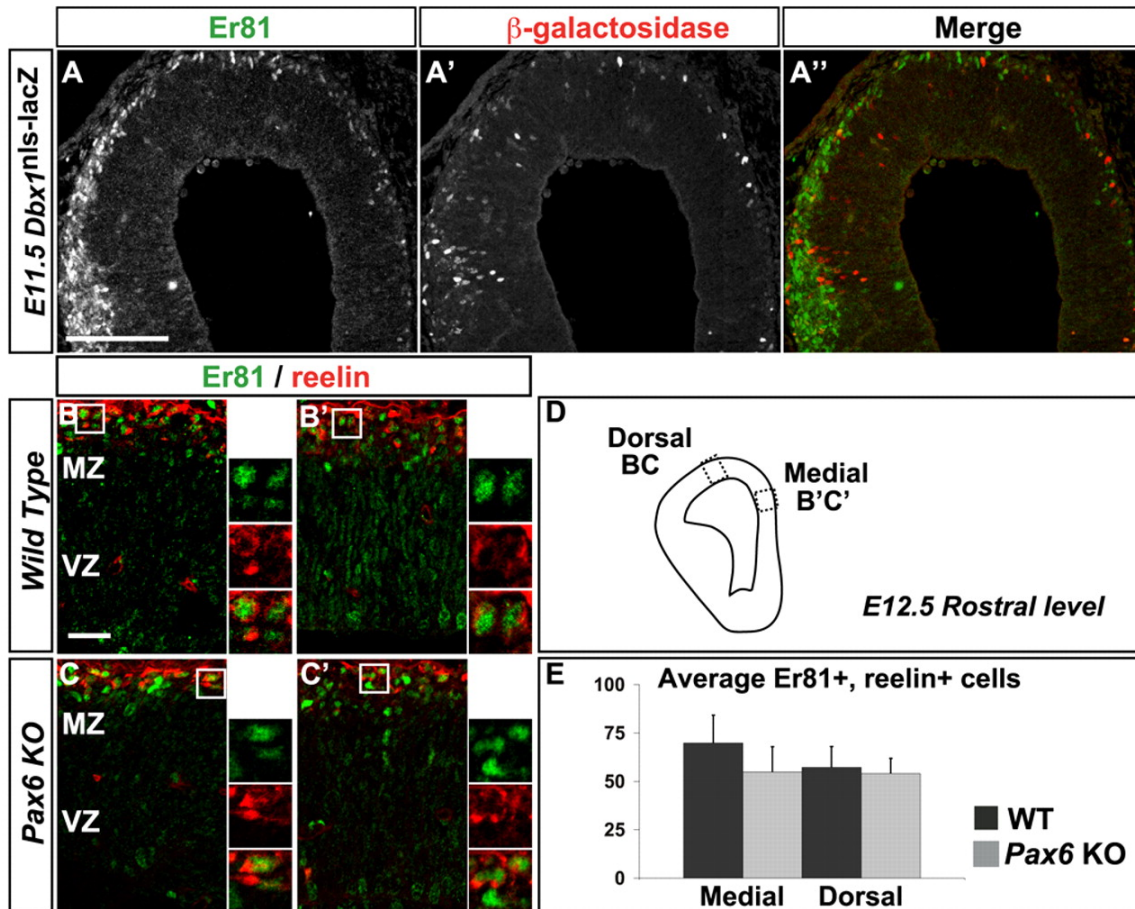
Fig. 3.: Er81⁺ CR cells originate particularly from the pallial septum. (**A-A″**) Co-immunolabelling for Er81 and β-galactosidase on sections of rostral telencephalon of heterozygous *Dbx1*[nls-lacZ] mouse embryos at E11.5, showing that some Er81⁺ cells derive from Dbx1⁺ cells. (**B-D**) Co-immunolabelling for Er81 and reelin in the dorsal (B,C) and medial (B′,C′) cortex of wild type (WT) or *Pax6* mutant (*Pax6 KO*) at E12.5 (see scheme in D). (**E**) Similar numbers (see Table S1 in the supplementary material) of rostral CR cells marked by double labelling for Er81 and reelin are found in the dorsal and medial cortex of both wild-type and *Pax6* mutant embryos. Scale bars: 100 μm in A-A″; 25 μm in B-C′.

Ectopic expression of Fgf8 induces rostral CR cells

Our previous observations suggested that the RM pallium, including the pallial septum, is exposed to the FGF signalling activity of the CoP and the septal VZ (Figs 1-3). We thus examined whether Fgf8, which is the main output of the rostral patterning centre, is involved in the generation of rostral CR cells. We first used a gain-of-function (GOF) approach, whereby a β-gal plasmid was co-

electroporated with an Fgf8 expression construct, or electroporated alone in control experiments, in the rostrodorsal pallium of E10.5 embryos, which were then cultivated for 2 days before analysis (see Fig. S4 in the supplementary material). As expected, Fgf8 electroporation resulted in the ectopic induction of several Fgf8 signalling targets, including *Er81*, *Pea3*, *Erm*, *Spry2* and *Fgfr1* (Fig. 4A-E). Although Fgf8 has a crucial role in patterning the rostral telencephalon (Cholfin and Rubenstein, 2008; Garel et al., 2003; Shimogori et al., 2004; Storm et al., 2006), ectopic Fgf8 did not affect the expression of pallial progenitor markers such as Lhx2, Pax6 or *Ngn2* (*Neurog2*) (Fig. 4G-I), nor that of the telencephalic marker *Foxg1* (Fig. 4F), as previously reported in an Fgf8 GOF study performed at E11.5 (Shimogori et al., 2004). Hence, the telencephalic identity of the electroporated tissue was maintained upon *Fgf8* GOF, but the dorsal pallium adopted a RM pallial identity as shown by the ectopic expression of *Erm*, *Pea3*, *Spry2* and *Fgfr1*.

Ectopic Fgf8 also markedly increased the number of reelinexpressing cells in the dorsal cortex as compared with the control electroporation or the non-electroporated side (Fig. 5A,B,C',D',E',F'). Co-immunolabelling experiments for β-gal, to mark the progeny of electroporated cells, and for rostral CR cellspecific markers showed that most β-gal$^+$, reelin$^+$ cells also expressed Tbr1 (Fig. 5D-D'''), Er81 (Fig. 5F-F''') and calretinin (see Fig. S5A,C-C''',E-E''' in the supplementary material), demonstrating that ectopic Fgf8 specifically induces CR cells of the rostral type. Moreover, we did not observe any change in Dbx1 or p73α labelling (data not shown; see Fig. S5B,D-D'' in the supplementarymaterial), indicating that Fgf8 is not sufficient to induce their expression. Coelectroporation of a constitutively active form of FGF receptor 1 (Fgfr1) with β-gal also resulted in the generation of β-gal$^+$ cells that co-expressed reelin and Er81 (see Fig. S6A-A''' in the supplementary material). Thus, Fgf8 signalling acts cell-autonomously to induce rostral CR cell generation in the rostrodorsal pallium.

	Er81	*Erm*
A		B
	Pea3	*Spry2*
C		D
	Fgfr1	*Foxg1*
E		F
	Lhx2	Pax6
G		H
	Ngn2	
I		

Fig. 5.: Overexpression of Fgf8 in the dorsal pallium induces the generation of Er81^{+} rostral CR cells. Immunolabelling of sections of mouse rostral telencephalon electroporated at E10.5 and cultivated for 2 DIV. (A) Control electroporation (*nls-lacZ*) does not affect reelin expression on the electroporated side (marked by +) as compared with the non-electroporated side (marked by –). (B) Co-electroporation of *Fgf8* and *nls-lacZ* leads to an increase in reelin expression (arrows). The yellow rectangles mark the dorsal cortex area shown at larger magnification in C-F*'''*. (C-D*'''*) Co-expression of reelin and Tbr1 in electroporated β-gal^{+} cells demonstrating that ectopic reelin^{+} cells are CR cells. The white rectangles outline the areas shown at higher magnification to the far right. (E-F*'''*) Co-expression of Er81 and reelin in electroporated β-gal^{+} cells shows that ectopic CR cells have a rostral identity. β-gal, β-galactosidase. For each condition for reelin, *n*>20, and for Er81/reelin or Tbr1/reelin, *n*=10. Scale bars: 210 µm in A,B; 25 µm in C-F*'''*.

Fgf8 promotes the neurogenesis of rostral CR cells

We further analysed the mechanisms by which ectopic Fgf8 expression promotes the generation of rostral CR cells. Ectopic expression of Fgf8 had no

significant effect on cell proliferation in electroporated embryos cultivated for 1 or 2 days (see Fig. S7 and Tables S2, S3 in the supplementary material). To determine whether Fgf8 promoted the generation of new neurons, we labeled progenitors in S phase 24 hours after electroporation by a 20-minute exposure of cultured embryos to BrdU, and examined the differentiation of BrdU-labelled progenitors 24 hours later by double labelling for BrdU and TUJ1 [βIII-tubulin (Tubb3) – Mouse Genome Informatics]. Fgf8 expression significantly increased the fraction of BrdU$^+$ cells that expressed TUJ1 (Fig. 6A-C; see Table S4 in the supplementary material), indicating that Fgf8 promotes the generation of new neurons from pallial progenitors.

To determine whether Fgf8 was specifically inducing CR cells or having a more general neurogenic effect, we examined the expression of reelin among Fgf8-induced neurons. Fgf8 expression significantly increased the fraction of TUJ1$^+$, β-gal$^+$ electroporated neurons that coexpressed reelin (Fig. 6D-F; see Table S5 in the supplementary material). Similar results were obtained when a construct expressing a constitutively active form of Fgfr1 was electroporated (see Fig. S6B-B''' in the supplementary material). Altogether, these results demonstrate that Fgf8 signalling specifically promotes the generation of CR cells from pallial progenitors in a cell-autonomous manner.
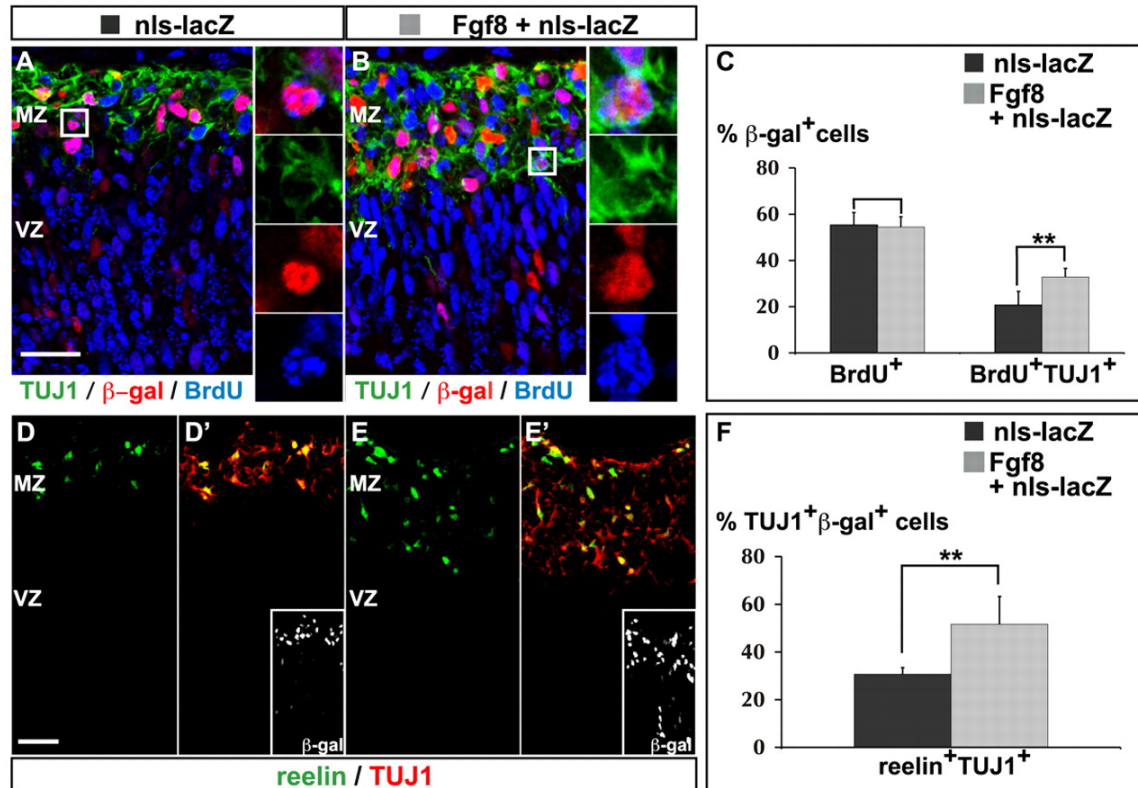
Fig. 6: Fgf8 overexpression promotes the differentiation of CR cells in the dorsal cortex. Immunolabelling of sections of mouse rostral telencephalon electroporated at E10.5 and cultivated for 2 DIV. (**A-C**) Triple labelling for BrdU, following a 20-minute pulse at 1 DIV and a 24-hour chase, and for β-gal and TUJ1 to mark newborn neurons. Ectopic Fgf8 significantly promotes neuronal differentiation in the dorsal cortex (Student's *t*-test, **P=0.002; see Table S4 in the supplementary material), whereas it does not significantly affect the rate of proliferation as measured by the fraction of cells double labelled for BrdU and β-gal (P=0.77). (**D-F**) Double labelling for reelin and TUJ1 to mark CR cells shows that ectopic Fgf8 specifically promotes the differentiation of this cell type (**P=0.004; see Table S5 in the supplementary material). Scale bars: 25 μm.

Ectopic expression of Fgf8 in vivo promotes the generation of rostral CR cells

To extend these findings to ectopic expression of endogenous Fgf8, we examined *Emx2* mutant mice, which present a caudal extension and persistence of the *Fgf8*, *Fgf17* and *Fgf18* rostral expression domains, and a concomitant reduction of the caudal Wnt/BMPsecreting telencephalic centre of the CH (Cholfin and Rubenstein, 2008; Fukuchi-Shimogori and Grove, 2003; Kimura et al., 2005; Shimogori et al., 2004). More cells expressed Pea3 within the RM

pallium in these mutants than in control embryos (Fig. 7C,C'), as previously described (Cholfin and Rubenstein, 2008; Fukuchi-Shimogori and Grove, 2003). We then found a significant increase in the number of Tbr1$^+$, reelin$^+$ CR cells in E12.5 *Emx2* mutant embryos at rostrodorsal and medial levels (Fig. 7A,B,D,D',G,G'; see Table S6 in the supplementary material). Co-labelling for Er81 and reelin showed that the majority of reelin$^+$ cells were of the rostral CR type (Fig. 7E,E',H,H') and that the population of p73α^+, Er81– CHderived CR cells was in fact reduced in the medial cortex of *Emx2* mutant embryos (Fig. 7I,I'). We also analysed *Gli3* mutant mice, in which an upregulation of Fgf8 signalling in the pallium and a loss of p73α^+ CH-derived CR cells have been reported (Kuschel et al., 2003; Okada et al., 2008; Rash and Grove, 2007; Theil et al., 1999). We found an increase in Pea3-expressing cells in the RM pallium at E12.5 (see Fig. S1B,B' in the supplementary material), as well as clusters of Er81$^+$, Tbr1$^+$, reelin$^+$ rostral CR cells in the medial cortex (see Fig. S1C-F' in the supplementary material). These data suggest that the enlarged *Fgf8* domain in *Emx2* or *Gli3* mutant pallium results in an expanded and persistent rostral CR cell progenitor domain, and supports the conclusion that ectopic Fgf8 signalling promotes the generation of rostral CR cells, both in embryo culture and in vivo.
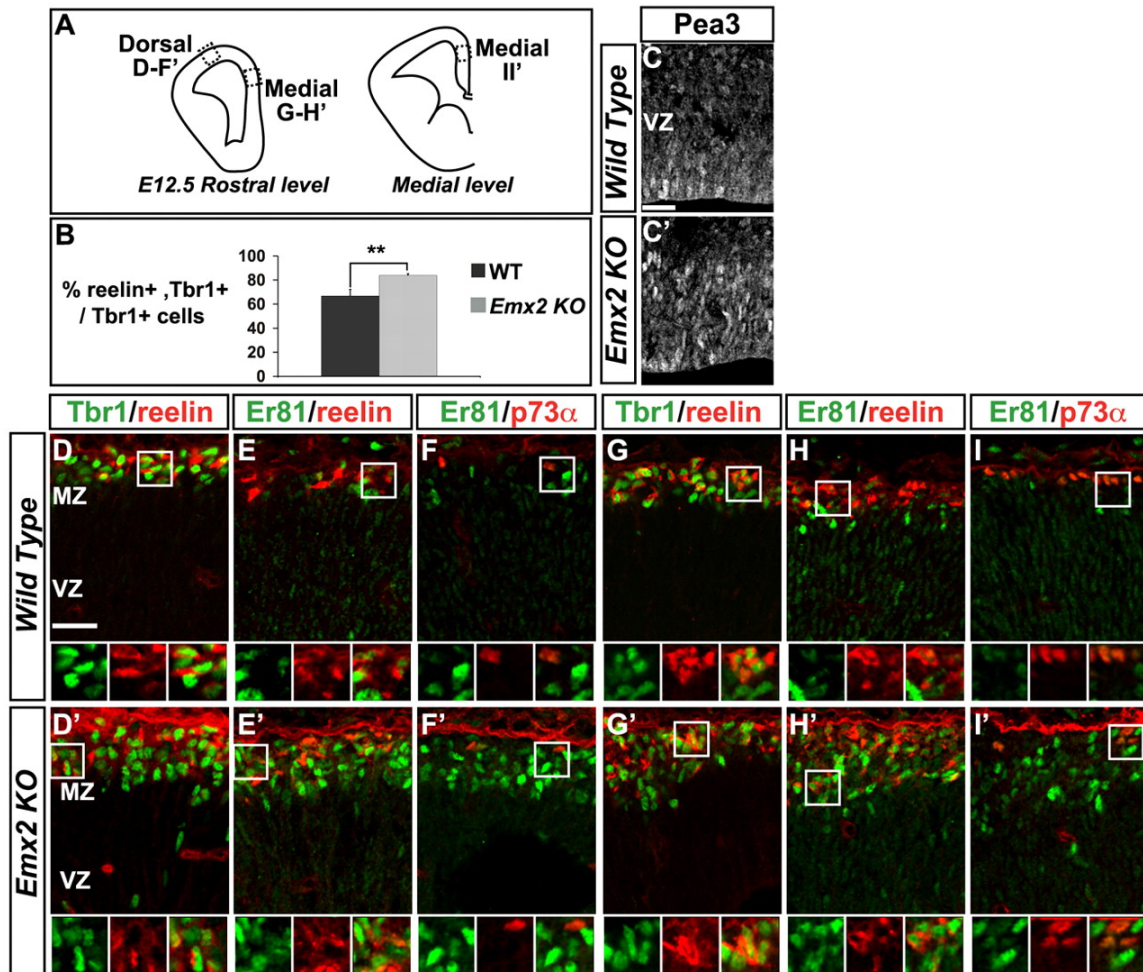
Fig. 7: Increased number of rostral CR cells in the dorsal cortex of *Emx2* mutant mouse embryos. (**A**) Schemes of coronal telencephalic sections showing the levels analysed at E12.5. (**B**) The proportion of CR cells is significantly increased in the rostrodorsal cortex of *Emx2* knockout (*KO*) embryos (Student's *t*-test, **P=0.006; see Table S6 in the supplementary material). (**C**,**C'**) More cells express Pea3 in the RM pallium of *Emx2* knockout than of wild-type embryos. (**D-I'**) The boxed areas are shown at high magnification beneath in single channel and merge. (D,D',G,G') Co-expression of Tbr1 and reelin identifies CR cells. (E,E',H,H') Mainly Er81 and reelin are co-expressed in the dorsal and medial cortex demonstrating that ectopic CR cells in *Emx2* KO cortex have a rostral identity. (F,F',I,I') p73α expression is decreased in the medial cortex, whereas Er81 expression is increased, even at more medial levels (see scheme in A). Scale bars: 25 μm.

In vitro inhibition of FGF signalling prevents the generation of rostral CR cells

To investigate whether Fgf8 signalling is not only sufficient, but also required for the generation of CR cells, we set up an explant culture system in

which Fgf8 signalling could be manipulated pharmacologically. The rostral head of E9.5 (21- to 23-somite) embryos was cultivated on a filter for 2 days in vitro (DIV), during which the explants maintained a dorsoventral organisation, as shown by labelling for *Mash1* (*Ascl1*) and *Ngn2* (see Fig. S8 in the supplementary material). TUJ1$^+$ neurons were only observed in the nasal placodes at the beginning of the culture, whereas TUJ1$^+$ neurons were found in the telencephalic part of the explant and particularly at its dorsal periphery after 2 DIV (see Fig. S8 in the supplementary material). Labelling for reelin, *Er81* and calretinin showed that most of the TUJ1$^+$ neurons generated during the culture were rostral CR cells (see Fig. S8 in the supplementary material). To assess the role of Fgf8 signalling, we used the pharmacological inhibitors SU5402, which inhibits signal transduction by FGF receptors (Mohammadi et al., 1997), and UO126, which prevents phosphorylation of MEK1/2 (Map2k1/2) kinases (Favata et al., 1998). Cultures exposed for 2 DIV to SU5402 (Fig. 8B-B''') or UO126 (Fig. 8D-D''') showed a strong decrease in TUJ1, calretinin and reelin labelling compared with DMSO-treated control explants in the dorsal part of the explants (Fig. 8A-A''',C-C''', arrows), whereas the lateral part of the explants was less affected. These results indicate that lowering Fgf8 signalling significantly reduces the rostral CR cell population.
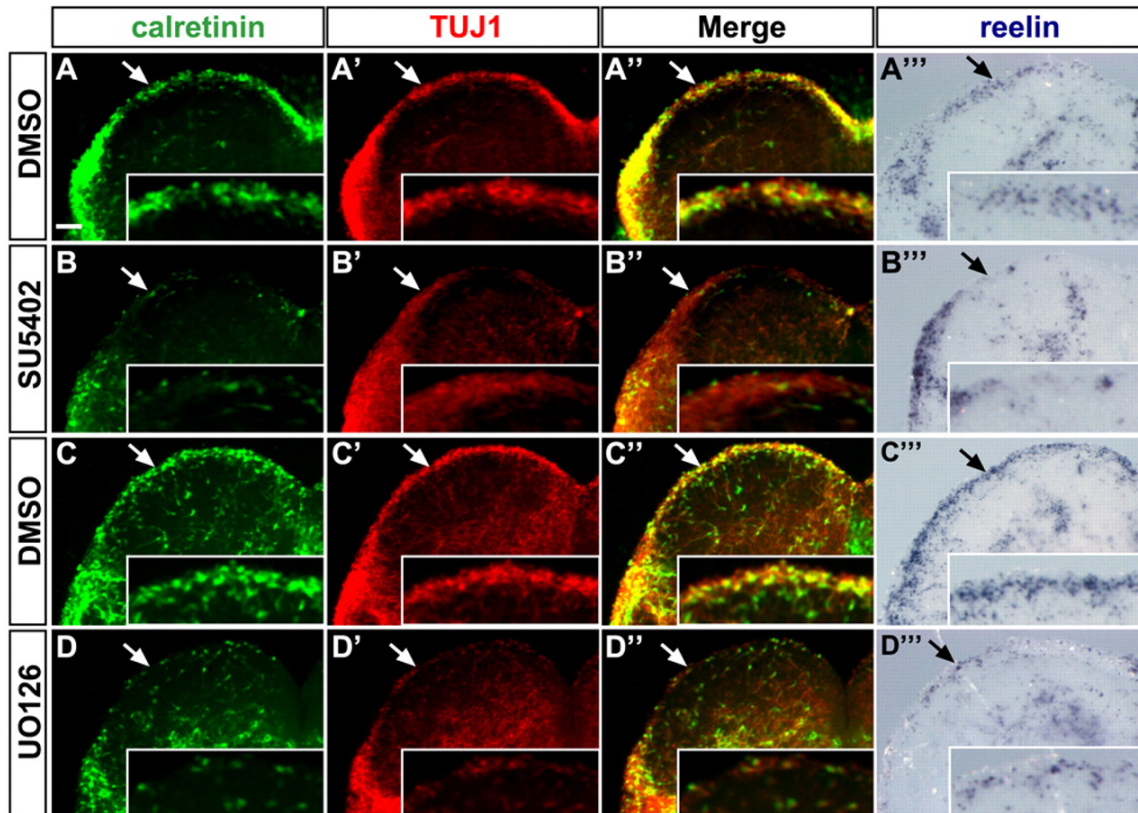
Fig. 8: Impairment of FGF signalling with pharmacological inhibitors decreases rostral CR cell generation in telencephalic explants. (**A-D'''**) Whole-mount immunohistochemistry for calretinin and TUJ1 and in situ hybridisation for reelin on mouse rostral telencephalic explants harvested at 22 somites and cultivated for 2 DIV (see Fig. S8 in the supplementary material). Exposure to SU5402 (B-B''' versus A-A''' control) or UO126 (D-D''' versus C-C''' control) leads to a decrease in the generation of CR cells (calretinin$^+$/TUJ1$^+$ or reelin$^+$) in the part of the explant that corresponds to the dorsal telencephalon (arrow), whereas the neuronal population (TUJ1$^+$ cells) is, overall, less affected. Neurogenesis appears to be less affected by exposure to FGF signalling inhibitors in the part of the explant that corresponds to the lateral cortex. For each condition for calretinin/TUJ1, $n \geq 15$, and for reelin, $n \geq 5$. Scale bar: 400 µm.

In vivo reduction in Fgf8 signalling decreases rostral CR cell generation

The requirement for Fgf8 signalling in the generation of CR cells was further examined in *Fgf8*$^{Null/Neo}$ mouse embryos, in which Fgf8 signalling activity in the rostral signalling centre is reduced (Storm et al., 2006; Storm et al., 2003), as a complete loss of *Fgf8* has drastic effects on telencephalic development that preclude examination of CR cells (Meyers et al., 1998). Tbr1$^+$,

reelin$^+$ CR cells were completely absent from the RM cortex in E11.5 *Fgf8*$^{Null/Neo}$ mutant embryos (Fig. 9C,C',J; see Table S7 in the supplementary material), and there was a reduction of this population in the rostrodorsal cortex and piriform cortex in these embryos (Fig. 9D-E',J; see Table S7 in the supplementary material). By contrast, Tbr1$^+$, reelin$^+$ CR cells were found in normal numbers in the caudal olfactory cortex (Fig. 9F,F'), indicating that Fgf8 signalling is required only rostrally for the generation of CR cells. In addition, Er81 expression was almost completely absent in *Fgf8*$^{Null/Neo}$ mutant embryos (Fig. 9G,G'), indicating that CR cells generated in the mutant have lost their rostral identity. Moreover, expression of the progenitor marker Pea3 was absent from the mutant RM pallium (Fig. 9I,I'), indicating that this territory was not properly specified in *Fgf8*$^{Null/Neo}$ embryos. We then analysed the *p73α* expression pattern at E12.5 to determine whether the decrease in rostral CR cells resulted in an expansion of CH-derived CR cells. However, we did not observe an increase in *p73α*-expressing cells (Fig. 9H,H'), suggesting that CH-derived CR cells had not invaded the rostroventral cortex in *Fgf8*$^{Null/Neo}$ embryos at the stage examined. We also asked whether eliminating the Fgf8-secreting rostral signalling centre would affect the generation of rostral CR cells by analyzing embryos with a telencephalon-specific deletion of Fgf8 (*Fgf8*^{TelKO}) (see Fig. S9 in the supplementary material) (Storm et al., 2006; Storm et al., 2003). We compared reelin expression in E12.5-13 whole telencephalon from wild-type, *Fgf8*$^{Null/Neo}$ and *Fgf8*^{TelKO} embryos and found a strong reduction in reelinexpressing cells in the medial and dorsal domains of the telencephalon of both *Fgf8* mutants as compared with the wild type (see Fig. S9 in the supplementary material). Altogether, these results establish that Fgf8 signalling activity is required for the specification of rostral CR cells originating from the RM pallium.
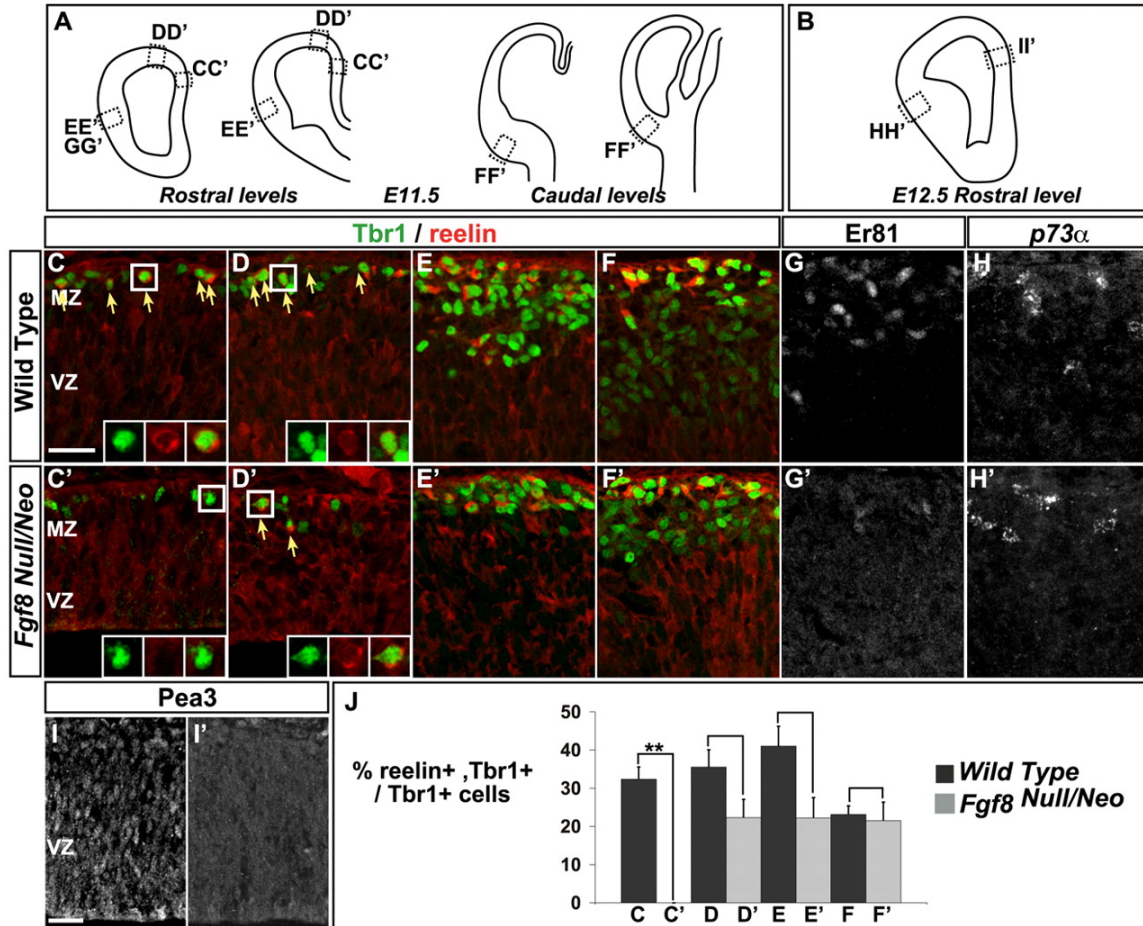
Fig. 9: Generation of rostral CR cells is reduced in _Fgf8_^{Null/Neo} mutant mouse embryos. (**A**,**B**) Schemes indicating the cortical regions analysed at E11.5 (A) and E12.5 (B). (**C-J**) Immunolabelling of coronal sections of different cortical regions in wild-type and _Fgf8_^{Null/Neo} mutant embryos. (C-F′,J) Tbr1 and reelin co-expression identifies CR cells. The proportion of CR cells is significantly decreased in the mutant RM cortex (C,C′,J; see Table S7 in the supplementary material) and is reduced in dorsal (D,D′,J; see Table S7 in the supplementary material) and piriform cortex (E,E′,J; see Table S7 in the supplementary material), but is not affected in the caudal cortex (F,F′,J; see Table S7 in the supplementary material), indicating that Fgf8 signalling is mainly required in the RM pallium. (G,G′) Er81 is only weakly expressed in the mutant cortex. (H,H′) At E12.5, there is no compensatory increase in _p73α_-expressing cells in the mutant piriform cortex. (I,I′) Pea3 expression is lost in the RM pallium, in agreement with the loss of CR cells in this area. Scale bars: 25 µm.

DISCUSSION

In this study, we have shown that rostral CR cells express the ETS transcription factor Er81, a downstream target of Fgf8 signalling, in addition to reelin, calretinin and p73α. We found that Er81$^+$ CR cells originate largely from the pallial septum, which is under the patterning influence of Fgf8 signalling, suggesting that this pathway could play a role in the specification of this rostral CR cell population. In agreement with this, we showed that ectopic activation of Fgf8 signalling in the dorsal pallium in vitro and in vivo results in ectopic generation of rostral CR cells. We also demonstrated that Fgf8 signalling activity is required in vitro and in vivo for the specification of the RM pallium, including the pallial septum, and for the generation of rostral CR cells. Altogether, our data establish a new role for the rostral signalling centre in the specification of rostral CR cells and further emphasise the involvement of telencephalic signalling centres in the generation of a diverse array of CR cells.

Er81$^+$ CR cells present unique defects in mutant mice

The existence of distinct origins and the fairly limited number of available markers might have complicated the analysis of CR cell subpopulations (Bielle et al., 2005; Garcia-Moreno et al., 2007; Imayoshi et al., 2008; Monuki et al., 2001; Takiguchi-Hayashi et al., 2004; Yoshida et al., 2006; Zhao et al., 2006). Expression of the ETS factor Er81 by rostral CR cells distinguishes them from CR cells located in the subpallium and the caudal pallium, where Er81 is not expressed. We thus used the co-expression of reelin and Er81 to identify rostral CR cells and re-examined the generation of CR cells in *Pax6*, *Emx2* and *Gli3* mutant mice.

Emx2 and Pax6, which cross-repress each other, are considered as positive and negative regulators of CR cell generation, respectively (Bishop et al.,

2003; Mallamaci et al., 2000; Shinozaki et al., 2002; Stoykova et al., 2003). We found, however, that a Er81⁺, reelin⁺ rostral CR cell population is still present in *Pax6* mutants, indicating that in contrast to other cell types (Tuoc and Stoykova, 2008), some *Er81*-expressing rostral CR cells are not dependent on Pax6 activity.

Our finding that loss of *Emx2* promotes the generation of rostral CR cells through derepression of Fgf8 signalling (Cholfin and Rubenstein, 2008; Fukuchi-Shimogori and Grove, 2003; Shimogori et al., 2004) is in agreement with the increase in reelin expression observed in *Emx2* mutant cortex (Mallamaci et al., 2000), although a loss of CR cells in *Emx2* mutants at later stages has been more widely documented (Bishop et al., 2003; Mallamaci et al., 2000; Yoshida et al., 1997). We can now associate this later phenotype with the loss of the CH-derived subpopulation, which we found already impaired at E12.5.

The generation of CR cells is impaired in *Gli3* mutant embryos, with the loss of caudal signals resulting in a substantial decrease in p73α⁺ CR cells and in a derepression of *Dbx1* in the dorsolateral pallium, which adopts a VP-like identity (Friedrichs et al., 2008; Hanashima et al., 2007; Theil, 2005). In agreement with these previous studies, we observed ectopic clusters of Er81⁺ CR cells in the lateral cortex in the *Gli3* mutant (data not shown). However, we also noted clusters of Er81⁺ CR cells in the medial cortex, as well as an increase in Pea3-expressing cells, reflecting the upregulation of Fgf8 signalling in these mutants (Okada et al., 2008; Rash and Grove, 2007; Theil, 2005; Theil et al., 1999). Thus, mutations in patterning genes differentially affect the subpopulations of CR cells because of their distinct effects on the different telencephalic signalling centres.

Multiple roles for Fgf8 signalling in the generation of rostral CR cells

The rostral signalling centre is characterised by the activity of FGF molecules, with Fgf8 playing the main role. We identified two distinct functions of Fgf8 signalling by challenging its activity in vitro and by analysing *Fgf8* gain- and loss-of-function phenotypes in mice. Firstly, Fgf8 signalling is involved in the specification of a progenitor domain within the RM pallium that gives rise to rostral CR cells, which is in line with its role in rostral telencephalic patterning. Secondly, Fgf8 signalling promotes the generation of rostral CR cells from mitotic progenitors.

Our GOF analysis showed that Fgf8 specifically promotes the generation of rostral CR cells. In contrast to a recent study in which ectopic Fgf8 expression resulted in re-patterning of the dorsal pallium into dorsal midline tissue (Okada et al., 2008), we observed that Fgf8-expressing cells maintained the expression of pallial progenitor markers such as Lhx2, Pax6 and *Ngn2*. These differences between the two studies can be explained by: (1) the competence of the tissue, as Okada et al. performed their experiment in younger embryos than we did (E9.5 as compared with E10.5); (2) the level of Fgf8 overexpression, as they used a stronger promoter to express *Fgf8* (the pCaggs vector versus pMiw in our study); and (3) the shorter time of exposure to Fgf8 (at 1 DIV versus 2 DIV). The importance of Fgf8 concentration and duration of action in determining its activity has been previously reported in various systems, including the CoP and the midhindbrain boundary (Basson et al., 2008; Liu et al., 2003; Sato et al., 2001). Altogether, these data lead us to suggest that a short exposure to a high Fgf8 concentration promotes a rostral midline identity (Okada et al., 2008), whereas a longer exposure to a lower Fgf8 concentration promotes RM pallial identity.

We have not detected any effect of ectopic Fgf8 on the proliferation of pallial progenitors, which is in agreement with previous studies demonstrating that Fgf8 regulates rostral telencephalic patterning but not cell proliferation (Crossley et al., 2001; Fukuchi-Shimogori and Grove, 2003; Okada et al., 2008;

Shimogori et al., 2004). However, we observed that Fgf8 induces neurogenesis, a function that has been previously reported in the eye, in the basal telencephalon (Crossley et al., 2001), and in the developing olfactory system (Bailey et al., 2006; Kawauchi et al., 2005).

CR cells originate from progenitor domains that are not only restricted spatially, but also short lived (e.g. (Imayoshi et al., 2008)). Our data show that the arrest of production of rostral CR cells after E12.5 might be a consequence of the reduction of Fgf8 signalling in the RM pallium at this stage. Hence, a longer exposure to Fgf8 signalling in Emx2 mutants or in electroporated embryos not only induced ectopic rostral CR cell production, but also extended the period of generation of this CR cell population.

In conclusion, our data establish that the rostral telencephalic signalling centre specifies a rostral CR cell population. Our study thus provides new evidence that CR cell progenitor domains are closely associated with telencephalic signalling centres and strengthens the hypothesis that CR cells participate in regional patterning of the cortex (Bielle et al., 2005; Meyer et al., 2004; Meyer et al., 2002). Because they migrate above progenitors at early developmental stages, CR cells are good candidates to provide telencephalic progenitors with instructive cues (Nomura et al., 2008; Soriano et al., 1997) (A.G. and A.P., unpublished). Thus, characterising CR cell subpopulations and their progenitor domains might help to unravel the mechanisms that control the early stages of development of the whole telencephalon.

MATERIALS AND METHODS

Mice

MF1, Parkes and F1 (CBA/CA _C57Bl/10) mice were used. All transgenic mouse lines were genotyped as previously described: *Dbx1*nls-lacZ (Bielle et al., 2005), *Pax6* (Stoykova et al., 1996), *Emx2* (Pellegrini et al., 1996), *Gli3* [Extra-toes/Extra-toes (Buscher et al., 1998)] *Fgf8*$^{Null/Neo}$ (Storm et al., 2003) and *Fgf8*^{TelKO} [*Foxg1*^{Cre}; *Fgf8*$^{Flox/Neo}$ (Storm et al., 2006)]. At least three

embryos were analysed per condition, unless specified otherwise. Midday of the day of vaginal plug discovery was considered as E0.5. All mouse experiments used protocols approved under the UK Animal (Scientific Procedures) Act.

Embryo culture and electroporation

E10.5 mouse embryos were dissected in Tyrode's solution, cultivated for 1 hour in rat serum at 37°C, 65% O_2/5% CO_2 (rolling incubator, BTC Engineering), injected (Femtojet, Eppendorf) and electroporated (chamber, CUY520P20; electroporator, Nepa Gene ECM830; 50 V, five pulses of 50 milliseconds, 1 second interval). Vectors: 1 mg/ml for pCaggs::IRES-nls- GFP (gift from J. Briscoe, NIMR, London, UK), pCaggs::IRES-nls-lacZ (gift from S. Price, UCL, London, UK) and pCDNA3::Fgfr1-DA (Freeman et al., 2003), or 0.8 mg/ml for pMiwIII::Fgf8 (b isoform, gift from A. Joyner, NYU, New York, USA); the vectors are referred to as nls-GFP, nls-lacZ, Pgfr1-DA and Fgf8, respectively, in the figures. Twenty-four hours after electroporation, embryos were transferred into fresh rat serum at 37°C, 100% O_2, and cultured for a further 24 hours. For cell cycle studies, 40 mM BrdU was added to the culture medium for 20 minutes.

Rostral telencephalic explants

E9.5 mouse embryos were dissected in Tyrode's solution. Only 22- to 24- somite embryos were used (see Fig. S8 in the supplementary material) (Storm et al., 2003). FGF signalling inhibitors (10 mM, DMSO diluted): SU5402 (#572630, Calbiochem); UO126 (#19-147, Millipore). Cell proliferation was only weakly affected by these inhibitors and could not account for the observed phenotypes. At 2 DIV, explants were: (1) washed in cold PBS, fixed for 30 minutes and washed in PBS for immunochemistry; or, (2) fixed overnight, washed in PBS, dehydrated in successive PBS/ethanol baths and kept in 100% ethanol at –20°C, for whole-mount in situ hybridisation.

Histology

Embryos were collected in PBS, heads fixed for 1 hour for immunohistochemistry or 3 hours for in situ hybridisation, washed with PBS, transferred into 15% sucrose in phosphate buffer (PB) pH 7.2 overnight, embedded in 7.5% gelatin, 15% sucrose in PB at 42°C, frozen in –40°C isopentane and stored at –80°C. Sections (10 mm) were prepared using a Microm cryostat (Zeiss).

For in situ hybridisation, tissues were processed as described by Hirsch et al. for sections (Hirsch et al., 2007) and by Bielle et al. for whole-mount (Bielle et al., 2005). Probes: Erm (IMAGE 4036564), Pea3, Er81, Mash1 (C. Goridis, ENS, Paris, France), Ngn2, reelin (Y. Hayashizaki, RIKEN, OSC, Kanagawa, Japan), p73a (IMAGE 6812399), Fgfr1 (J. Partanen, University of Helsinki, Finland), Spry2 (G. Martin, UCSF, San Francisco, USA) and Foxg1 (J. Mason, University of Edinburgh, UK). For immunohistochemistry, frozen sections were air dried, washed in PBS at 42°C to remove the gelatin and processed for immunofluorescence. Primary antibodies: mouse anti-reelin (1/375, #MAB5364, Chemicon), mouse antip73a (1/200, #MS762PO, LabVision), mouse (#6B3) or rabbit (#7699) anticalretinin (both at 1/2000, Swant), goat anti-b-galactosidase (1/1000, #ab12081, Abcam), sheep anti-GFP (1/750, #47451051, Biogenesis), mouse anti-TUJ1 (1/1000, #MMS435P, Babco), rat anti-BrdU (1/1000, #OBT0030CX, Serotec; denaturation in 2N HCl for 30 minutes at 37°C washes with 0.1 M sodium borate pH 8.0), mouse anti-Pax6 (1/20, Developmental Studies Hybridoma Bank), rabbit anti-Er81 and rabbit anti- Pea3, rabbit anti-Tbr1 (gift from R. Hevner, University of Washington, Seattle, USA) and rabbit anti-Lhx2 (gift from E. Monuki, University of California, Irvine, USA). Fluorescent secondary antibodies were Alexa 488 (Millipore) or Cy3 or Cy5 (Jackson ImmunoResearch) conjugated. Note that to perform the co-detection of Er81 and Tbr1, rabbit anti-Tbr1 was directly labelled with Cy5 using the Zenon Kit (Molecular Probes). For explant immunostaining, 1 hour blocking at room temperature was followed by incubation with antibody overnight at 4°C and washing in PBS.

Image analysis, quantifications and statistics

Images were captured using a ProgRes C14 camera (Jenoptik) linked to an Axioplan II microscope (Zeiss), a QImaging camera linked to MZ16/MZ16F scopes (Leica), or a Radiance 2100 confocal microscope (BioRad). Images were processed with Openlab (Perkin Elmer), ImageJ (NIH), Photoshop (Adobe) or FreeHand (Adobe). Quantifications were performed on confocal photographs (200 mm _200 mm; stack of 2 or 3 mm) using Photoshop. For example, in Fig. 2 the number of Er81+ cells was counted by marking the cells with a dot on a transparent layer linked to the Er81 staining layer in Photoshop. Then each Er81+ cell was assessed for its expression of either reelin, calretinin or p73a, using another transparent layer linked to each of these stainings. The same principle was used to perform all counts. In Fig. 2, four stacks per area from two wild-type embryos were analysed. For electroporated embryos, two to three stacks were analysed per embryo. Because of electroporation variability, results were normalised for each embryo before being gathered for statistical analysis using a paired Student's t-test (see tables in the supplementary material). For quantification in mutant embryos, three to four stacks were analysed per area.

Supplementals
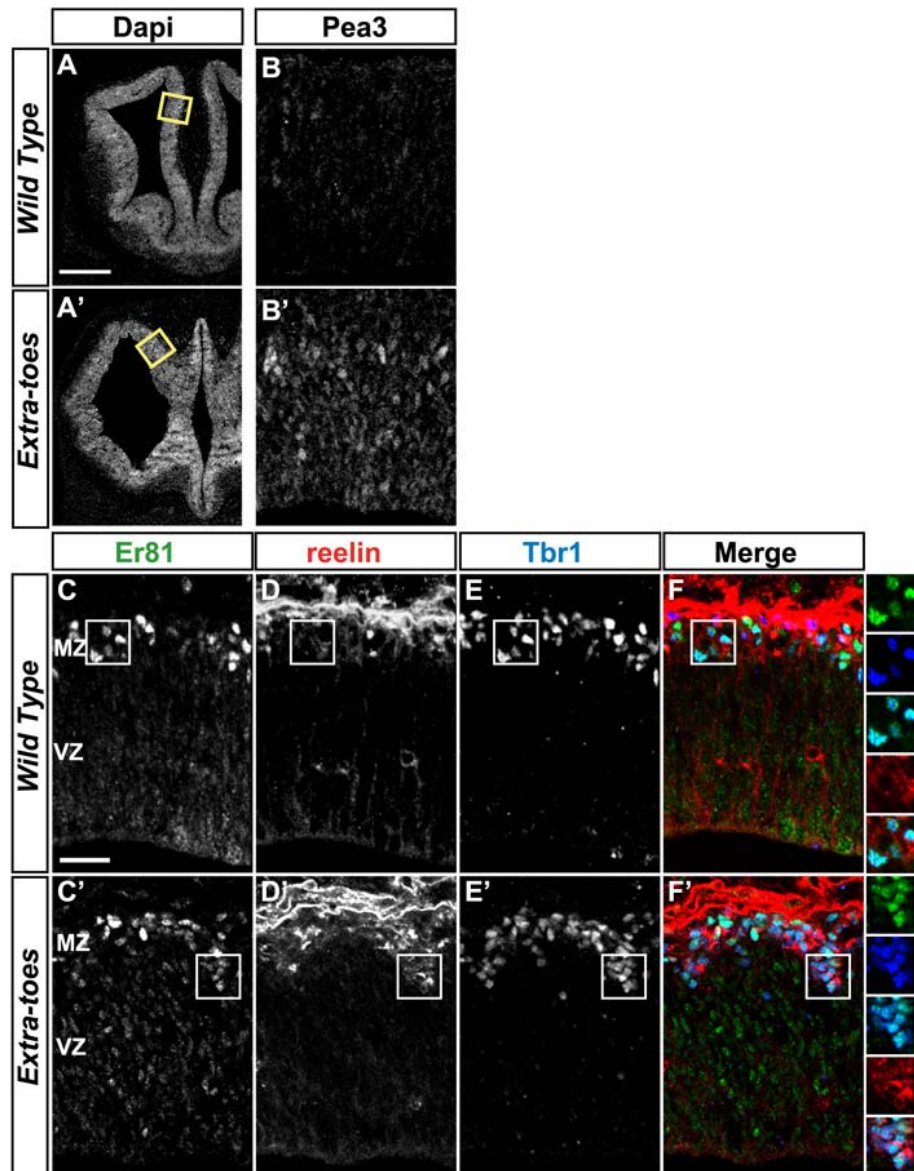
Fig. S1. Rostral Cajal-Retzius (CR) cells expressing Er81, reelin and Tbr1 accumulate in rostromedial *Gli3* mutant at E12.5. (**A**,**A'**) DAPI staining of coronal sections of wild-type (WT) and *Gli3* mutant (*Extra-toes*/*Extra-toes*) rostral telencephalon at E12.5, illustrating the morphological changes and the area depicted in B-F'. (**B**,**B'**) More Pea3$^+$ cells are detected in the RM pallium in the *Gli3* mutant. (**C-F'**) Triple immunolabelling of coronal sections of wild-type and *Gli3* mutants as indicated on the left. Co-expression of Er81 and Tbr1 shows that all Er81$^+$ cells express Tbr1 in wild type and *Gli3* mutant, indicating their pallial identity. Most Er81$^+$ cells co-express reelin, indicating their rostral CR cell identity. Scale bars: 210 µm for A,A'; 25 µm for B-F'.
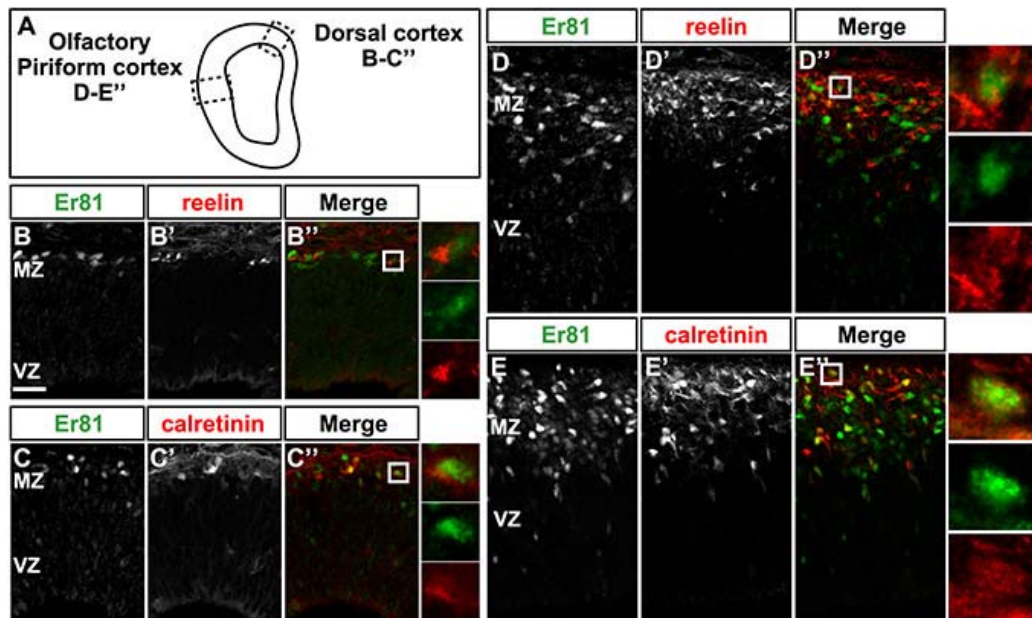
Fig. S2. Rostral Cajal-Retzius cells express Er81. (**A**) Scheme of a coronal section of E11.5 telencephalon at rostral level. Dashed rectangles indicate the areas analysed. (**B-E″**) Immunolabelling of coronal sections of E11.5 telencephalon. Er81 is co-expressed with reelin (B″,D″) and with calretinin (C″,E″), in the ventral cortex or olfactory piriform cortex (D″,E″) and the dorsal cortex (B″,C″). The boxed areas are shown at higher magnification to the right. Scale bars: 25 μm.
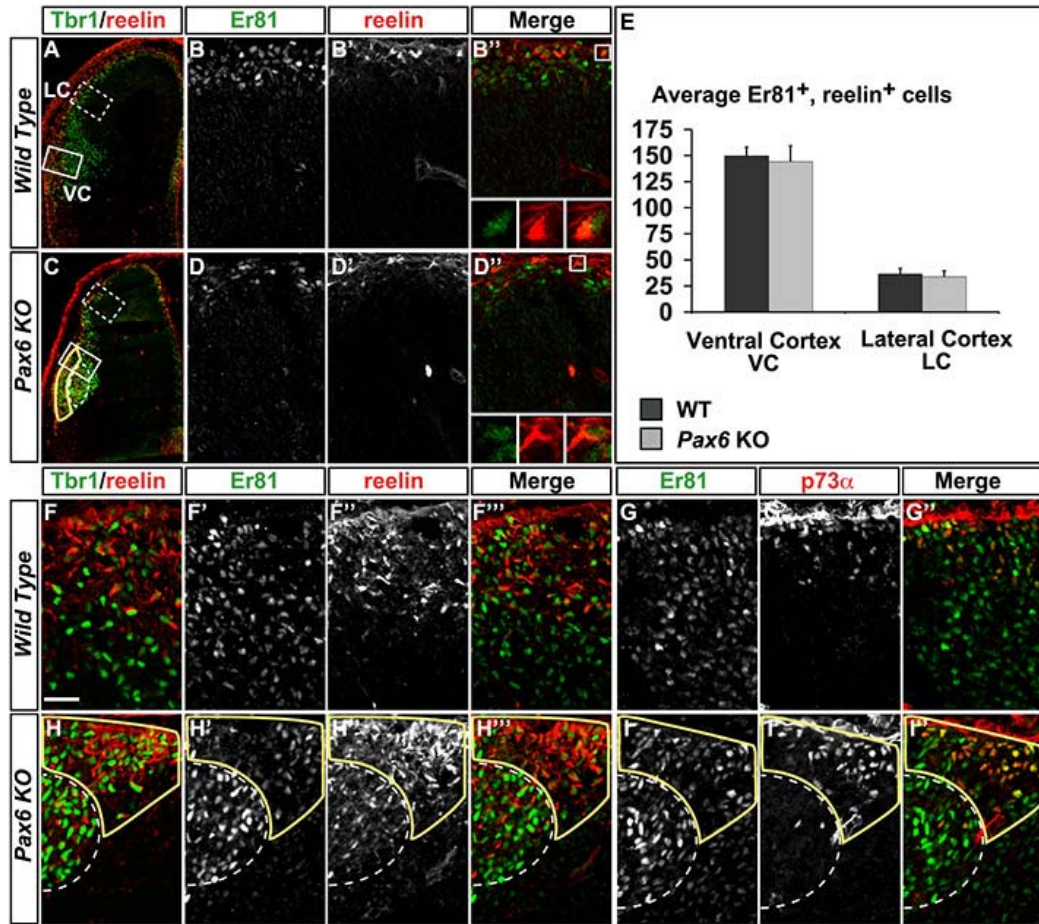
Fig. S3. Er81⁺ CR cells derive mainly from the pallial septum. (**A-I″**) Immunolabelling of coronal sections of E12.5 rostral telencephalon from wild type or *Pax6* mutant. (A,C) Co-immunolabelling for Tbr1 and reelin highlights CR cells. Dashed white rectangle shows the zone of the lateral cortex analyzed in B-D″ and white rectangle shows the zone of the ventral cortex analyzed in F-I″. Note that the ventral cortex (outlined in yellow, see also F,H) is compacted around the olfactory-like bulb structure (dashed circle), which is mislocalized in the mutant (see Jimenez et al., 2000; Tomura et al., 2004). (B-H‴) Er81⁺, reelin⁺ rostral CR cells are present in similar numbers in ventral (WT, 149.7±8.3; KO, 144.1±15.1; *t*-test, *P*=0.1) and lateral cortex (WT, 36.6±5.1; KO, 33.9±5.6; *t*-test, *P*=0.2) of wild-type and *Pax6* mutant telencephalon, showing that rostral Er81⁺ CR cells are mostly derived from the RM pallium. (G-I″) p73α⁺ CR cells of the ventral cortex co-express Er81 both in the wild type and *Pax6* mutant, showing that they derive from the RM pallium, which includes the pallial septum. Scale bar: 25 µm.
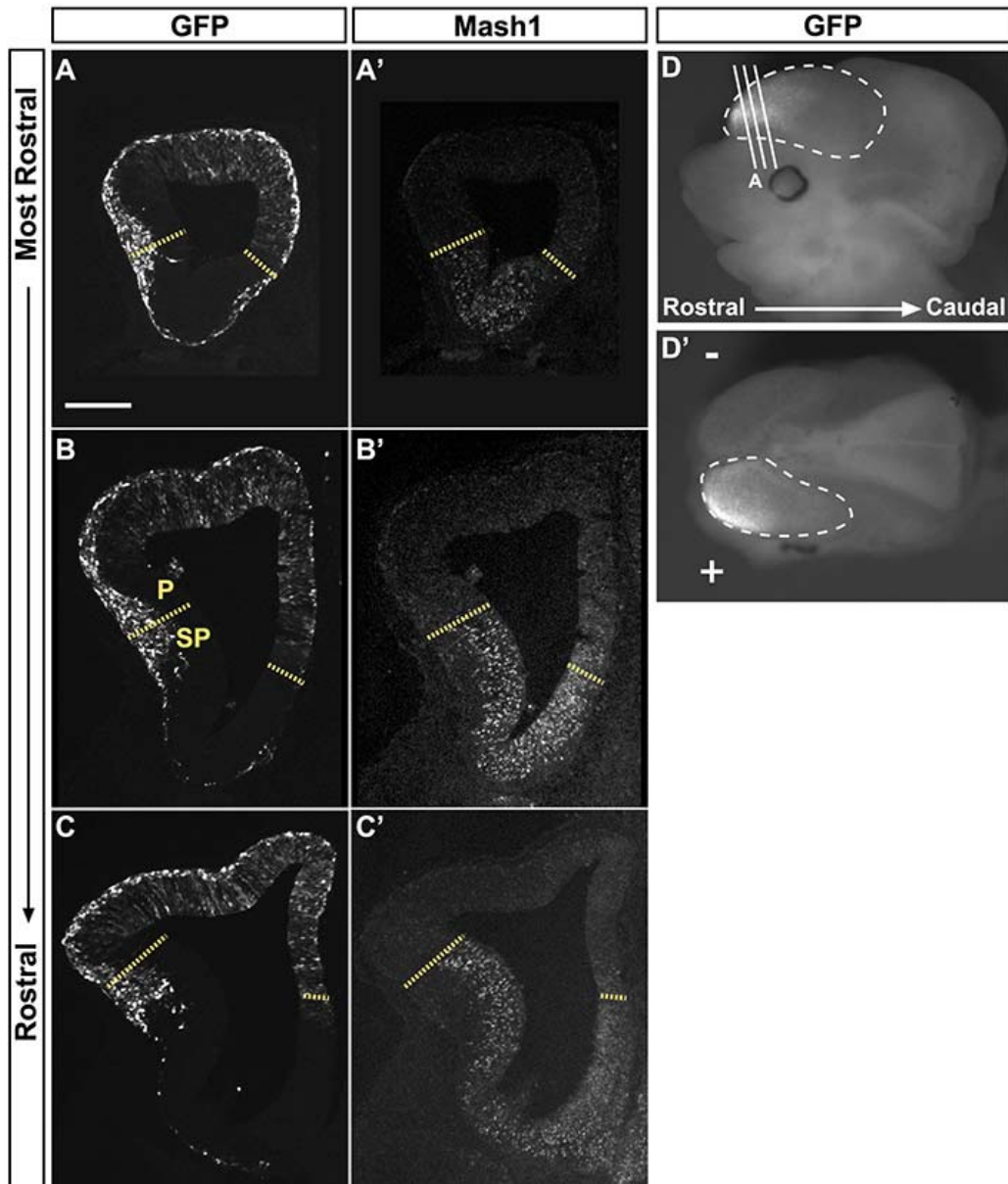
Fig. S4. Illustration of the electroporation procedure used in this study. (**A-C'**) Immunolabelling of coronal sections of rostral telencephalon electroporated with *nls-GFP* at E10.5 and cultivated for 2 DIV. Different rostral telencephalic levels of the electroporation are shown. GFP immunolabelling is compared with that for Mash1, which is highly expressed in the ventral telencephalon or subpallium (SP) at this stage (the pallium-subpallium boundary is delineated by a yellow dotted line). The electroporation targets dorsal or pallial (P) progenitors. Note that migrating cells, which express high levels of GFP, are detected all around the telencephalon. (**D,D'**) Head of an embryo electroporated at E10.5 and cultivated for 2 DIV. Profile (D) and dorsal (D') views are shown. The whole telencephalic vesicle is outlined with a white dashed line. Rostral levels depicted in A-C are indicated by solid white lines. Scale bar: 210 µm
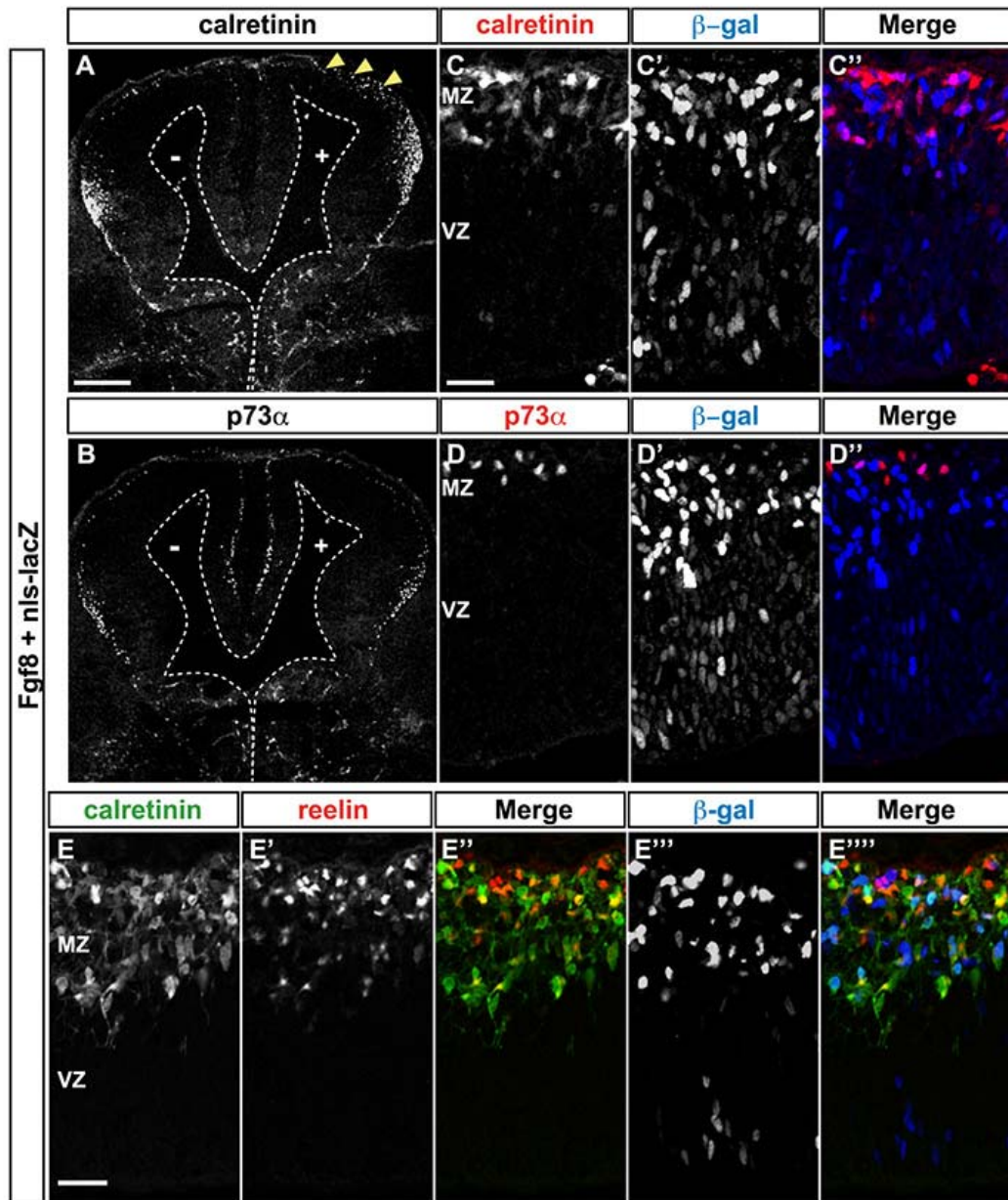
Fig. S5. Specific increase in the generation of rostral CR cells in Fgf8b gain-of-function experiments. (**A-E″″**) Immunolabelling of coronal telencephalic sections of embryos co-electroporated with *nls-lacZ* and *Fgf8b* at E10.5 and cultivated for 2 DIV. (A,C-C″) Rostral CR cells expressing calretinin are over-produced in the pallium (arrowheads); see also E-E″″ for co-expression of reelin and calretinin. (B,D-D″) No change in CR cells expressing p73α upon Fgf8b gain-of-function. *n*≥8. Scale bars: 210 μm for A,B; 25 μm for C-C″,D-D″,E-E″″.

103
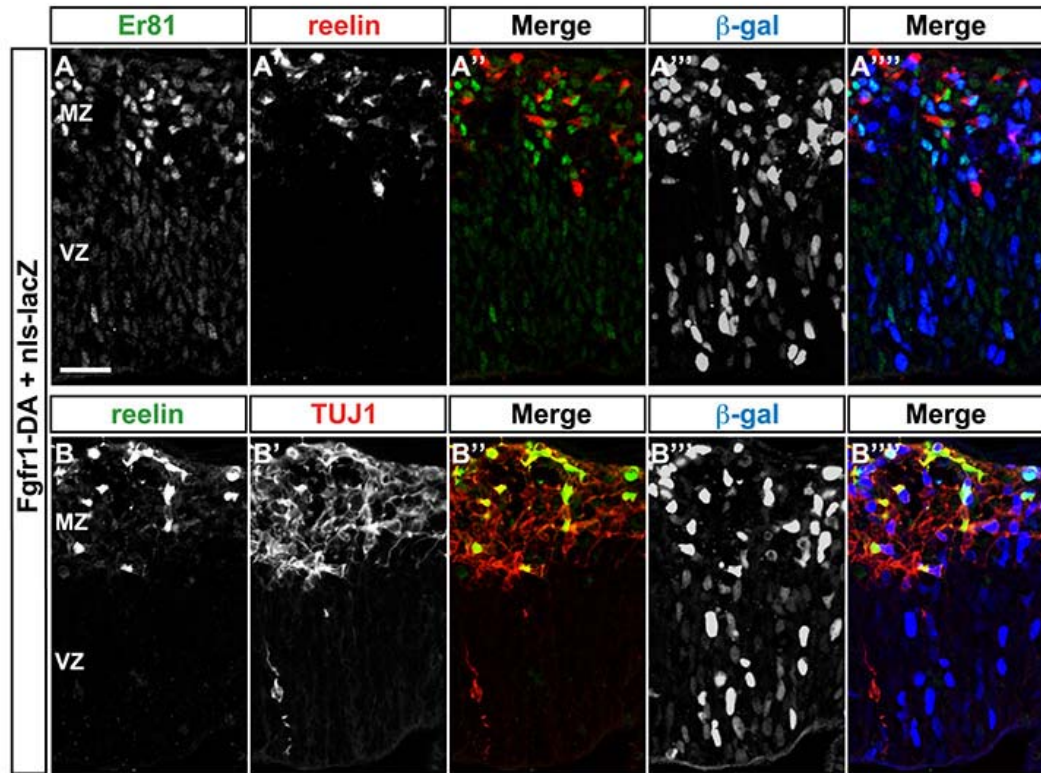
Fig. S6. Specific increase in the generation of rostral CR cells in Fgfr1-DA gain-of-function experiments. (**A-A''''**) Immunolabelling of coronal telencephalic sections of embryos co-electroporated with *nls-lacZ* and a dominant-active form of Fgfr1 (*FgfR1-DA*) at E10.5 and cultivated for 2 DIV. β-gal co-expression with Er81 and reelin shows that rostral CR cells are over-produced in the pallium upon Fgfr1-DA gain-of-function. (**B-B''''**) β-gal co-expression with reelin and TUJ1 shows that CR cells are specifically differentiated upon Fgfr1-DA gain-of-function. These data indicate that the effects observed upon Fgf8b gain-of-function are cell-autonomous. *n*≥8. Scale bar: 25 μm.
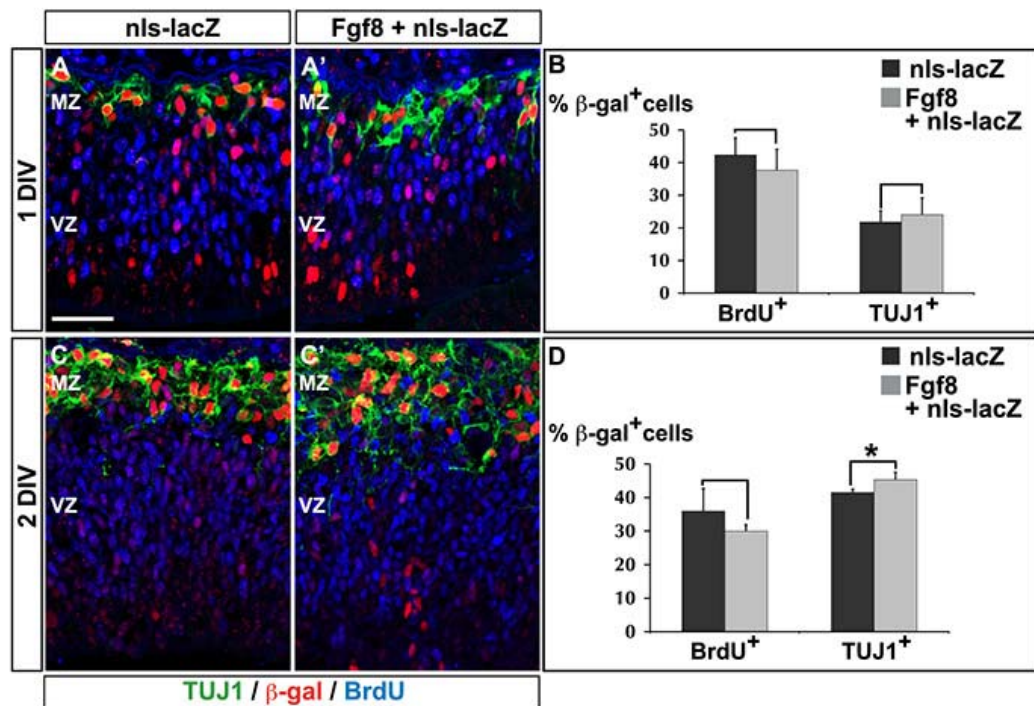
Fig. S7. Fgf8b gain-of-function at E10.5 does not promote cell proliferation in the dorsal pallium after 1 or 2 days. (**A**,**A′**,**C**,**C′**) Immunolabelling of coronal telencephalic sections of embryos co-electroporated with *nls-lacZ* and *Fgf8b* at E10.5 and cultivated for 1 or 2 DIV, as indicated on the left. Note that the images represent the dorsal pallium (boxed area in Fig. 4B). To analyse cell proliferation, BrdU was incubated for 20 minutes in the culture medium before arresting the culture at 1 DIV or 2 DIV. (A,C) Control electroporation with *nls-lacZ*. (A′,C′) Co-electroporation of *nls-lacZ* and *Fgf8b*. (**B**) At 1 DIV, similar proportions were obtained in control and Fgf8b-electroporated embryos for proliferative cells, labelled by BrdU[+], β-gal[+] (*t*-test, *P*=0.3, see Table S2) or for differentiated cells labelled as TUJ1^{+}, β-gal[+] (*t*-test, *P*=0.14, see Table S2). (**D**) At 2 DIV, similar proportions were obtained for proliferative cells labelled as BrdU[+], β-gal[+] (*t*-test, *P*=0.14, see Table S3). An increase in the proportion of differentiated cells labelled as TUJ1^{+}, β-gal[+] was observed upon Fgf8b gain-of-function (*t*-test, *P*=0.02, see Table S3), indicating that Fgf8b gain-of-function induces differentiation after 2 DIV. Scale bar: 25 μm.
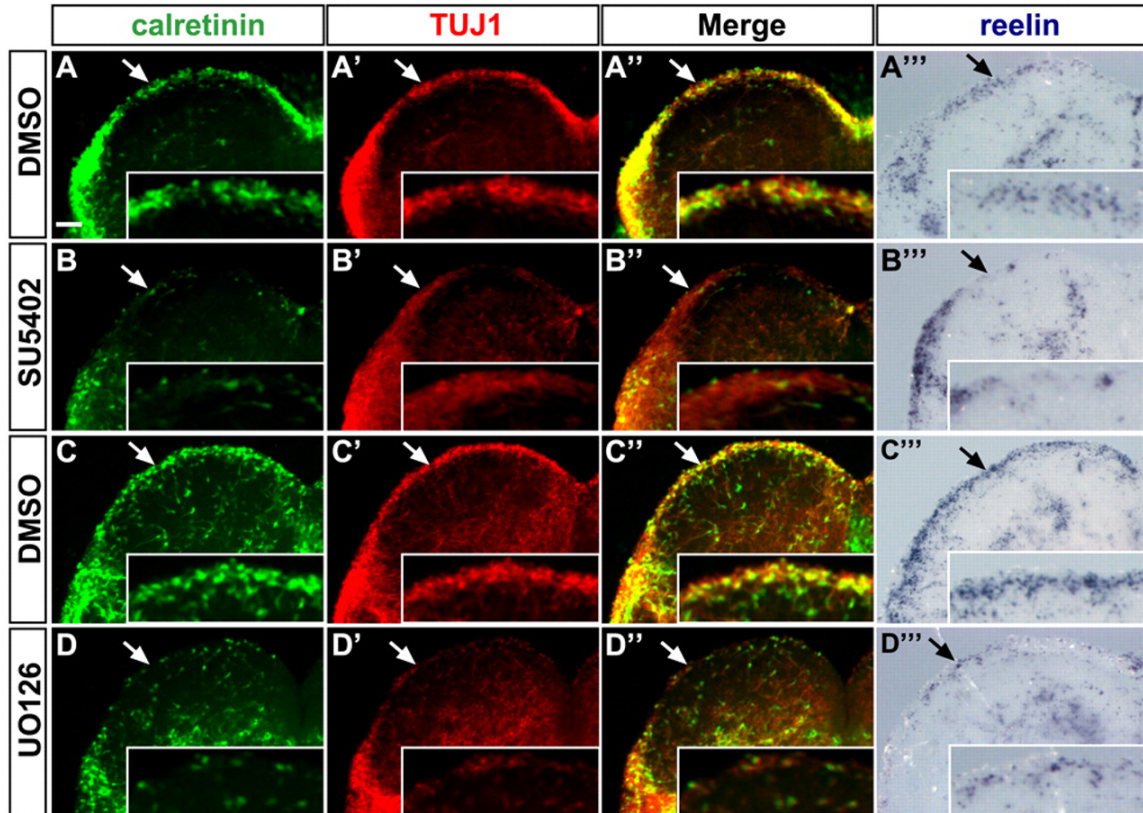
Fig. S8. Rostral telencephalic explant cultures at E9.5. Whole-mount in situ hybridisation on E9.5 mouse embryo (A,B) or rostral telencephalic explants (C,C′,E,F). (**A**) Head of E9.5 embryo showing the plan of section used to generate rostral telencephalic explants, which were flattened on a filter. (**B**,**B′**) At zero time point (t=0), *Fgf8* is expressed in the anterior neural ridge (anr) and in the nasal placodes (np), which are the only territories containing TUJ1^{+} neurons at that stage. (**C-C″**) After 2 DIV, the explants are well developed and present a normal dorsoventral organisation of the rostral telencephalon, with *Ngn2* expressed dorsally and *Mash1* highly expressed ventrally. Many neurons have been generated after 2 DIV. Neurons expressing both calretinin and TUJ1 are easily identifiable at the dorsal periphery of the explants. The boxed area in C″ is analysed in D-F. (**D-F**) TUJ1^{+}, calretinin^{+} neurons at the edge of the explant correspond to cells expressing reelin and *Er81*, and therefore to rostral CR cells. Scale bar: 170 µm.

106
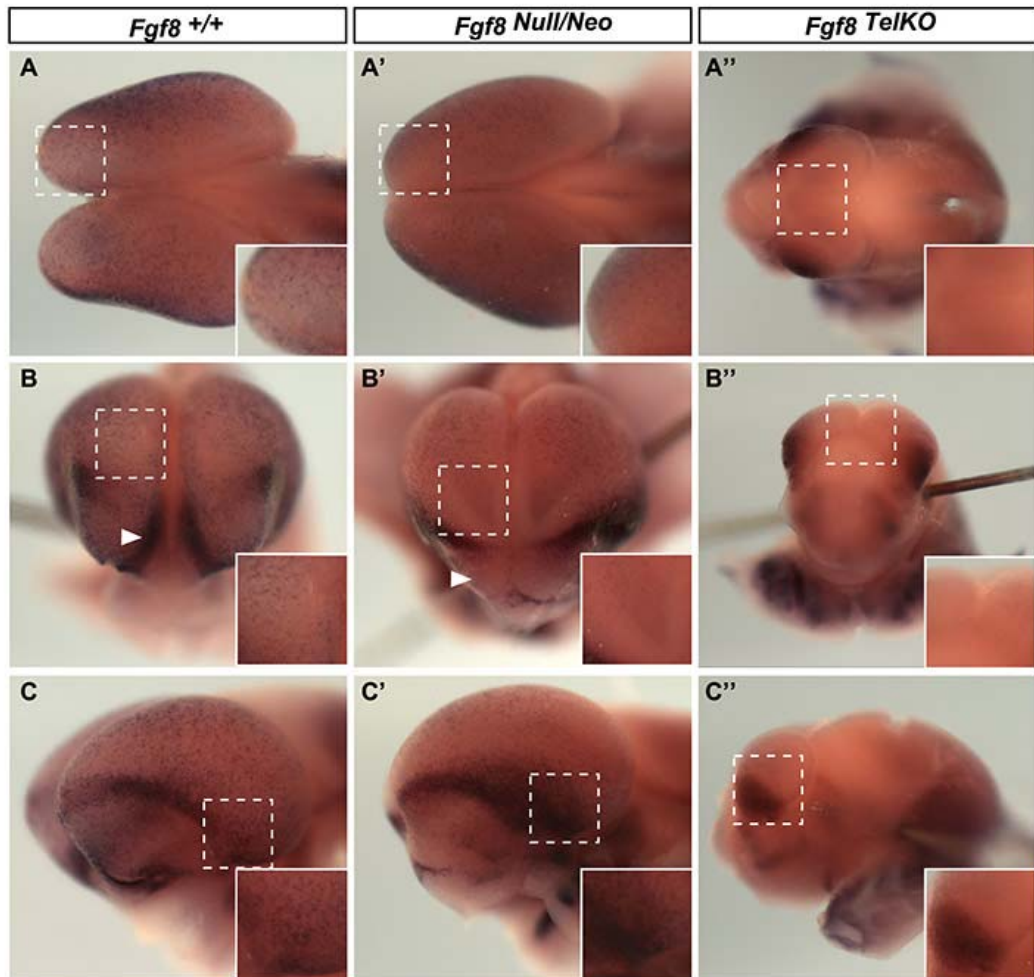
Fig. S9. Strong reduction in Cajal-Retzius cells generated from medial progenitor domains in *Fgf8*^{B>}TelKO mutant embryos. (A-C″) Telencephalon whole-mount in situ hybridization using reelin probe in wild type (*Fgf8*^{+/+}; A,B,C), *Fgf8* hypomorphic mutants (*Fgf8*^{Null/Neo}; A′,B′,C′) and conditional telencephalic *Fgf8* mutants (*Fgf8*^{TelKO}; A″,B″,C″) at E12.5-13. There is a strong reduction in CR cells located in dorsal and medial domains in both *Fgf8*^{Null/Neo} and *Fgf8*^{TelKO} compared with the wild type. CR cells could mainly be detected in the caudolateral domain in *Fgf8*^{TelKO}.

Table S1. Er81⁺, reelin⁺ CR cell population is not significantly affected in the E12.5 Pax6 mutant (Sey/Sey), which presents an absence of the VP progenitor domain

	Total medial	Av Er81⁺, reelin⁺ cells	Total dorsal	Av Er81⁺, reelin⁺ cells
Control (n=3)	395	65.8±9	343	57.2±6.5
Pax6 mutant (n=3)	329	54.8±8	324	54±2.8
t-test		P=0.2		P=0.5

Average (Av) is shown ± standard deviation.

Table S2. Fgf8b gain-of-function affects neither cell proliferation nor differentiation after 1 DIV

	Total β-gal⁺	Total BrdU⁺, β-gal⁺	Av % BrdU⁺, β-gal⁺ / β-gal⁺	Total TUJ1⁺, β-gal⁺	Av % TUJ1⁺, BrdU⁺, β-gal⁺ / β-gal⁺
Control (n=4)	1806	736	42.3±5.3	383	21.8±3.5
Fgf8b (n=4)	1179	462	37.7±6.5	285	24±5.2
t-test			P=0.3		P=0.49

Average (Av) is shown ± standard deviation.

Table S3. Fgf8b gain-of-function does not affect cell proliferation, but promotes cell differentiation after 2 DIV

	Total β-gal⁺	Total BrdU⁺, β-gal⁺	Av % BrdU⁺, β-gal⁺ / β-gal⁺	Total TUJ1⁺, β-gal⁺	Av % TUJ1⁺, BrdU⁺, β-gal⁺ / β-gal⁺
Control (n=4)	2907	1088	35.9±6.8	1204	41.5±1
Fgf8b (n=4)	2003	612	30±1.9	921	45.3±2.2
t-test			P=0.14		P=0.02

Average (Av) is shown ± standard deviation.

Table S4. Fgf8b gain-of-function promotes cell cycle exit at 2 DIV

	Total β-gal⁺	Total BrdU⁺, β-gal⁺	Av % BrdU⁺, β-gal⁺ / β-gal⁺	Total TUJ1⁺, β-gal⁺	Av % TUJ1⁺, BrdU⁺, β-gal⁺ / β-gal⁺
Control (n=4)	4111	2209	55.3±5.4	773	20.7±5.9
Fgf8b (n=6)	2807	1551	54.4±4.4	893	32.8±3.7
t-test			P=0.77		P=0.002

Average (Av) is shown ± standard deviation.

Table S6. Increased generation in CR cells in Emx2 mutant dorsal cortex

	Total Tbr1⁺	Total Tbr1⁺, reelin⁺	Av % reelin⁺, Tbr1⁺ / Tbr1⁺
Control (n=3)	514	340	66.8±5.4
Emx2 mutant (n=3)	958	805	83.9±1.3
t-test			P=0.006

Average (Av) is shown ± standard deviation.

Table S5. Fgf8b gain-of-function promotes CR cell differentiation at 2 DIV

	Total TUJ1⁺, β-gal⁺	Total reelin⁺ TUJ1⁺, β-gal⁺	Av % reelin⁺, TUJ1⁺, β-gal⁺ / TUJ1⁺, β-gal⁺
Control (n=5)	958	292	30.6±2.7
Fgf8b (n=5)	1051	559	51.6±11.6
t-test			P=0.004

Average (Av) is shown ± standard deviation.

Table S7. Decreased generation in CR cells in Fgf8ᴺᵉᵒ/ᴺᵉᵒ mutant

	Total Tbr1⁺ medial	Total Tbr1⁺, reelin⁺ medial	Av % reelin⁺, Tbr1⁺ / Tbr1⁺	Total Tbr1⁺ dorsal	Total Tbr1⁺, reelin⁺ dorsal	Av % reelin⁺, Tbr1⁺ / Tbr1⁺	Total Tbr1⁺ CxP	Total Tbr1⁺, reelin⁺ CxP	Av % reelin⁺, Tbr1⁺ / Tbr1⁺	Total Tbr1⁺ caudal	Total Tbr1⁺, reelin⁺ caudal	Av % reelin⁺, Tbr1⁺ / Tbr1⁺
Control*	159	51	32.4±3.2	184	65	35.5±4.5	699	233	41±5.2	1098	236	23.1±2.2
Fgf8ᴺᵉᵒ/ᴺᵉᵒ*	82	0	0	134	31	22.3±4.8	262	63	22.2±5.3	732	158	21.5±4.9
t-test			0.004			0.1			0.07			0.7

Average (Av) is shown ± standard deviation.
*, n=2.

7. Abbreviations

ANR	anterior neural ridge
BAC	Bacterial Artificial Chromosome
BDNF	braind derived neurotrophic factor
BrdU	Bromodeoxyuridine
CR cells	Cajal-Retzius cell
CNS	central nervous system
CoP	commissural plate
CH	cortical hem
DIV	days in vitro
DMSO	Dimethylsulfoxid
DRG	dorsal root ganglion
EPSP	excitatory postsynaptic potential
FACS	Fluorescent Activated Cell Sorting
GOF	gain of function
GABA	gamma aminobutyric acid
GDNF	glia cell line derived neurotrophic factor
GTO	Golgi tendon organ
GFP	Green Fluorescent Protein
ISH	in sity Hybridization
KO	knock out
LTD	long term depression
LTP	long term potentation
LOF	Loss of function
LSL	lox-STOP-lox
MZ	marginal zone
mlc	myosin light chain
NGF	nerve growth factor
NMJ	neuromuscular juction
NT3	neurotrophin 3
NT4	neurotrophin 4
PAD	primary afferent depolarization
RM	rostromedial
SEM	Standard Error of the Mean
Trk	tyrosine receptor kinase
VP	ventral pallium
VZ	ventricular zone

8. Acknowledgements

I would like to my supervisor Prof. Silvia Arber for giving me the opportunity to do my Ph. D. research work in her lab. I am especially grateful for her support and generosity in the last months of my thesis.

I would like to thank Prof. Pico Caroni for being my "Korreferent" on my Ph. D. thesis committee.

Many thanks to Prof. Yves-Alain Barde, who had kindly agreed to chair my thesis exam. His constant support and advice during the end of my project gave me the welcome opportunity to think outside the box.

I owe a lot to Dr. Edward Oakeley and Dr. Tim Roloff from the FMI Affymetrix microarray service facility for performing the data analysis of all the microarray experiments as well as for their endless patience. Hubertus Kohler from the FACS facility was essential for my experiments as well as Dr. Erik Cabuy.

With Dr. David Ladle, Dr. Simon Dalla Torre and Dr. Celine Jean-Xavier I enjoyed many fruitful discussions about my project and science in general.

Dr. Jorge Cham and Dr. Mike Slackenerny, I salute you.

Sarah, I thank you for being there and keeping me sane.

9. References

Abraham, H. and Meyer, G. (2003). Reelin-expressing neurons in the postnatal and adult human hippocampal formation. *Hippocampus* **13**, 715-27.

Airaksinen, M. S., Koltzenburg, M., Lewin, G. R., Masu, Y., Helbig, C., Wolf, E., Brem, G., Toyka, K. V., Thoenen, H. and Meyer, M. (1996). Specific subtypes of cutaneous mechanoreceptors require neurotrophin-3 following peripheral target innervation. *Neuron* **16**, 287-95.

Albright, T. D., Jessell, T. M., Kandel, E. R. and Posner, M. I. (2000). Neural science: a century of progress and the mysteries that remain. *Neuron* **25 Suppl**, S1-55.

Alcantara, S., Ruiz, M., D'Arcangelo, G., Ezan, F., de Lecea, L., Curran, T., Sotelo, C. and Soriano, E. (1998). Regional and cellular patterns of reelin mRNA expression in the forebrain of the developing and adult mouse. *J Neurosci* **18**, 7779-99.

Allen, K., Fuchs, E. C., Jaschonek, H., Bannerman, D. M. and Monyer, H. (2011). Gap Junctions between Interneurons Are Required for Normal Spatial Coding in the Hippocampus and Short-Term Spatial Memory. *J Neurosci* **31**, 6542-52.

Arber, S., Ladle, D. R., Lin, J. H., Frank, E. and Jessell, T. M. (2000). ETS gene Er81 controls the formation of functional connections between group Ia sensory afferents and motor neurons. *Cell* **101**, 485-98.

Avivi, C. and Goldstein, R. S. (1999). Differential expression of Islet-1 in neural crest-derived ganglia: Islet-1 + dorsal root ganglion cells are post-mitotic and Islet-1 + sympathetic ganglion cells are still cycling. *Brain Res Dev Brain Res* **115**, 89-92.

Bach-y-Rita, P. (1983). Rehabilitation versus passive recovery of motor control following central nervous system lesions. *Adv Neurol* **39**, 1085-92.

Bachler, M. and Neubuser, A. (2001). Expression of members of the Fgf family and their receptors during midfacial development. *Mech Dev* **100**, 313-6.

Bailey, A. P., Bhattacharyya, S., Bronner-Fraser, M. and Streit, A. (2006). Lens specification is the ground state of all sensory placodes, from which FGF promotes olfactory identity. *Dev Cell* **11**, 505-17.

Barde, Y. A., Edgar, D. and Thoenen, H. (1982). Purification of a new neurotrophic factor from mammalian brain. *EMBO J* **1**, 549-53.

Basson, M. A., Echevarria, D., Ahn, C. P., Sudarov, A., Joyner, A. L., Mason, I. J., Martinez, S. and Martin, G. R. (2008). Specific regions within the embryonic midbrain and cerebellum require different levels of FGF signaling during development. *Development* **135**, 889-98.

Bear, M. F. and Malenka, R. C. (1994). Synaptic plasticity: LTP and LTD. *Curr Opin Neurobiol* **4**, 389-99.

Betley, J. N., Wright, C. V., Kawaguchi, Y., Erdelyi, F., Szabo, G., Jessell, T. M. and Kaltschmidt, J. A. (2009). Stringent specificity in the construction of a GABAergic presynaptic inhibitory circuit. *Cell* **139**, 161-74.

Bibel, M. and Barde, Y. A. (2000). Neurotrophins: key regulators of cell fate and cell shape in the vertebrate nervous system. *Genes Dev* **14**, 2919-37.

Bielle, F., Griveau, A., Narboux-Neme, N., Vigneau, S., Sigrist, M., Arber, S., Wassef, M. and Pierani, A. (2005). Multiple origins of Cajal-Retzius cells at the borders of the developing pallium. *Nat Neurosci* **8**, 1002-12.

Bishop, K. M., Garel, S., Nakagawa, Y., Rubenstein, J. L. and O'Leary, D. D. (2003). Emx1 and Emx2 cooperate to regulate cortical size, lamination, neuronal differentiation, development of cortical efferents, and thalamocortical pathfinding. *J Comp Neurol* **457**, 345-60.

Boiko, T., Rasband, M. N., Levinson, S. R., Caldwell, J. H., Mandel, G., Trimmer, J. S. and Matthews, G. (2001). Compact myelin dictates the differential targeting of two sodium channel isoforms in the same axon. *Neuron* **30**, 91-104.

Bonanomi, D. and Pfaff, S. L. (2010). Motor axon pathfinding. *Cold Spring Harb Perspect Biol* **2**, a001735.

Borello, U., Cobos, I., Long, J. E., McWhirter, J. R., Murre, C. and Rubenstein, J. L. (2008). FGF15 promotes neurogenesis and opposes FGF8 function during neocortical development. *Neural Dev* **3**, 17.

Brown, A. G. (1981). Organization in the Spinal Cord. *(New York, Springer).*

Buscher, D., Grotewold, L. and Ruther, U. (1998). The XtJ allele generates a Gli3 fusion transcript. *Mamm Genome* **9**, 676-8.

Carney, R. S., Cocas, L. A., Hirata, T., Mansfield, K. and Corbin, J. G. (2009). Differential regulation of telencephalic pallial-subpallial boundary patterning by Pax6 and Gsh2. *Cereb Cortex* **19**, 745-59.

Chen, A. I., de Nooij, J. C. and Jessell, T. M. (2006). Graded activity of transcription factor Runx3 specifies the laminar termination pattern of sensory axons in the developing spinal cord. *Neuron* **49**, 395-408.

Chen, H. H., Hippenmeyer, S., Arber, S. and Frank, E. (2003). Development of the monosynaptic stretch reflex circuit. *Curr Opin Neurobiol* **13**, 96-102.

Chi, C. L., Martinez, S., Wurst, W. and Martin, G. R. (2003). The isthmic organizer signal FGF8 is required for cell survival in the prospective midbrain and cerebellum. *Development* **130**, 2633-44.

Cholfin, J. A. and Rubenstein, J. L. (2007). Patterning of frontal cortex subdivisions by Fgf17. *Proc Natl Acad Sci U S A* **104**, 7652-7.

Cholfin, J. A. and Rubenstein, J. L. (2008). Frontal cortex subdivision patterning is coordinately regulated by Fgf8, Fgf17, and Emx2. *J Comp Neurol* **509**, 144-55.

Ciolofan, C., Lynn, B. D., Wellershaus, K., Willecke, K. and Nagy, J. I. (2007). Spatial relationships of connexin36, connexin57 and zonula occludens-1 in the outer plexiform layer of mouse retina. *Neuroscience* **148**, 473-88.

Conradi, S., Cullheim, S., Gollvik, L. and Kellerth, J. O. (1983). Electron microscopic observations on the synaptic contacts of group Ia muscle spindle afferents in the cat lumbosacral spinal cord. *Brain Res* **265**, 31-9.

Cote, M. P., Azzam, G. A., Lemay, M. A., Zhukareva, V. and Houle, J. D. (2011). Activity-dependent increase in neurotrophic factors is associated with an enhanced modulation of spinal reflexes after spinal cord injury. *J Neurotrauma* **28**, 299-309.

Courtine, G., Gerasimenko, Y., van den Brand, R., Yew, A., Musienko, P., Zhong, H., Song, B., Ao, Y., Ichiyama, R. M., Lavrov, I. et al. (2009). Transformation of nonfunctional spinal circuits into functional states after the loss of brain input. *Nat Neurosci* **12**, 1333-42.

Crossley, P. H. and Martin, G. R. (1995). The mouse Fgf8 gene encodes a family of polypeptides and is expressed in regions that direct outgrowth and patterning in the developing embryo. *Development* **121**, 439-51.

Crossley, P. H., Martinez, S., Ohkubo, Y. and Rubenstein, J. L. (2001). Coordinate expression of Fgf8, Otx2, Bmp4, and Shh in the rostral prosencephalon during development of the telencephalic and optic vesicles. *Neuroscience* **108**, 183-206.

Crowley, C., Spencer, S. D., Nishimura, M. C., Chen, K. S., Pitts-Meek, S., Armanini, M. P., Ling, L. H., McMahon, S. B., Shelton, D. L., Levinson, A. D. et al. (1994). Mice lacking nerve growth factor display perinatal loss of sensory and sympathetic neurons yet develop basal forebrain cholinergic neurons. *Cell* **76**, 1001-11.

D'Arcangelo, G., Miao, G. G., Chen, S. C., Soares, H. D., Morgan, J. I. and Curran, T. (1995). A protein related to extracellular matrix proteins deleted in the mouse mutant reeler. *Nature* **374**, 719-23.

da Silva, S. and Wang, F. (2011). Retrograde neural circuit specification by target-derived neurotrophins and growth factors. *Curr Opin Neurobiol* **21**, 61-7.

Dalla Torre di Sanguinetto, S. A. (2009). Identification of Motor Neuron Pool Marker Genes and Analysis of their Roles in Motor Circuit Assembly. *PhD thesis*.

Dasen, J. S. (2009). Transcriptional networks in the early development of sensory-motor circuits. *Curr Top Dev Biol* **87**, 119-48.

de Quervain, D. J. and Papassotiropoulos, A. (2006). Identification of a genetic cluster influencing memory performance and hippocampal activity in humans. *Proc Natl Acad Sci U S A* **103**, 4270-4.

Deans, M. R., Gibson, J. R., Sellitto, C., Connors, B. W. and Paul, D. L. (2001). Synchronous activity of inhibitory networks in neocortex requires electrical synapses containing connexin36. *Neuron* **31**, 477-85.

Deckwerth, T. L., Elliott, J. L., Knudson, C. M., Johnson, E. M., Jr., Snider, W. D. and Korsmeyer, S. J. (1996). BAX is required for neuronal death after trophic factor deprivation and during development. *Neuron* **17**, 401-11.

del Rio, J. A., Martinez, A., Fonseca, M., Auladell, C. and Soriano, E. (1995). Glutamate-like immunoreactivity and fate of Cajal-Retzius cells in the murine cortex as identified with calretinin antibody. *Cereb Cortex* **5**, 13-21.

Demarque, M. and Spitzer, N. C. (2010). Activity-dependent expression of Lmx1b regulates specification of serotonergic neurons modulating swimming behavior. *Neuron* **67**, 321-34.

Derer, P. and Derer, M. (1990). Cajal-Retzius cell ontogenesis and death in mouse brain visualized with horseradish peroxidase and electron microscopy. *Neuroscience* **36**, 839-56.

Destombes, J., Horcholle-Bossavit, G., Simon, M. and Thiesson, D. (1996). Gaba-like immunoreactive terminals on lumbar motoneurons of the adult cat. A quantitative ultrastructural study. *Neurosci Res* **24**, 123-30.

Dickson, B. J. (2002). Molecular mechanisms of axon guidance. *Science* **298**, 1959-64.

Dombovy, M. L. and Bach-y-Rita, P. (1988). Clinical observations on recovery from stroke. *Adv Neurol* **47**, 265-76.

Eccles, J. C., Eccles, R. M. and Lundberg, A. (1957). The convergence of monosynaptic excitatory afferents on to many different species of alpha motoneurones. *J Physiol* **137**, 22-50.

Eccles, J. C., Eccles, R. M. and Magni, F. (1961). Central inhibitory action attributable to presynaptic depolarization produced by muscle afferent volleys. *J Physiol* **159**, 147-66.

Eccles, J. C., Kostyuk, P. G. and Schmidt, R. F. (1962). Central pathways responsible for depolarization of primary afferent fibres. *J Physiol* **161**, 237-57.

Ernfors, P., Lee, K. F., Kucera, J. and Jaenisch, R. (1994). Lack of neurotrophin-3 leads to deficiencies in the peripheral nervous system and loss of limb proprioceptive afferents. *Cell* **77**, 503-12.

Ernsberger, U. (2009). Role of neurotrophin signalling in the differentiation of neurons from dorsal root ganglia and sympathetic ganglia. *Cell Tissue Res* **336**, 349-84.

Esmaeili, A., Lynch, J. W. and Sah, P. (2009). GABAA receptors containing gamma1 subunits contribute to inhibitory transmission in the central amygdala. *J Neurophysiol* **101**, 341-9.

Farinas, I. (1999). Neurotrophin actions during the development of the peripheral nervous system. *Microsc Res Tech* **45**, 233-42.

Farinas, I., Jones, K. R., Backus, C., Wang, X. Y. and Reichardt, L. F. (1994). Severe sensory and sympathetic deficits in mice lacking neurotrophin-3. *Nature* **369**, 658-61.

Farinas, I., Wilkinson, G. A., Backus, C., Reichardt, L. F. and Patapoutian, A. (1998). Characterization of neurotrophin and Trk receptor functions in developing sensory ganglia: direct NT-3 activation of TrkB neurons in vivo. *Neuron* **21**, 325-34.

Favata, M. F., Horiuchi, K. Y., Manos, E. J., Daulerio, A. J., Stradley, D. A., Feeser, W. S., Van Dyk, D. E., Pitts, W. J., Earl, R. A., Hobbs, F. et al. (1998). Identification of a novel inhibitor of mitogen-activated protein kinase kinase. *J Biol Chem* **273**, 18623-32.

Frank, E. and Sanes, J. R. (1991). Lineage of neurons and glia in chick dorsal root ganglia: analysis in vivo with a recombinant retrovirus. *Development* **111**, 895-908.

Frank, E. and Wenner, P. (1993). Environmental specification of neuronal connectivity. *Neuron* **10**, 779-85.

Frank, K. and Fuortes, M. (1957). Presynaptic and postsynaptic inhibition of monosynaptic reflexes. *Fed Proc*, 39–40.

Friedrichs, M., Larralde, O., Skutella, T. and Theil, T. (2008). Lamination of the cerebral cortex is disturbed in Gli3 mutant mice. *Dev Biol* **318**, 203-14.

Friese, A. (2010). Gene profiling of identified neurons to dissect molecular mechanisms involved in spinal reflex assembly. . *PhD thesis.*

Friese, A., Kaltschmidt, J. A., Ladle, D. R., Sigrist, M., Jessell, T. M. and Arber, S. (2009). Gamma and alpha motor neurons distinguished by expression of transcription factor Err3. *Proc Natl Acad Sci U S A* **106**, 13588-93.

Fritschy, J. M. and Mohler, H. (1995). GABAA-receptor heterogeneity in the adult rat brain: differential regional and cellular distribution of seven major subunits. *J Comp Neurol* **359**, 154-94.

Fukuchi-Shimogori, T. and Grove, E. A. (2001). Neocortex patterning by the secreted signaling molecule FGF8. *Science* **294**, 1071-4.

Fukuchi-Shimogori, T. and Grove, E. A. (2003). Emx2 patterns the neocortex by regulating FGF positional signaling. *Nat Neurosci* **6**, 825-31.

Fyffe, R. E. and Light, A. R. (1984). The ultrastructure of group Ia afferent fiber synapses in the lumbosacral spinal cord of the cat. *Brain Res* **300**, 201-9.

Garcia-Moreno, F., Lopez-Mascaraque, L. and De Carlos, J. A. (2007). Origins and migratory routes of murine Cajal-Retzius cells. *J Comp Neurol* **500**, 419-32.

Garel, S., Huffman, K. J. and Rubenstein, J. L. (2003). Molecular regionalization of the neocortex is disrupted in Fgf8 hypomorphic mutants. *Development* **130**, 1903-14.

Gimeno, L. and Martinez, S. (2007). Expression of chick Fgf19 and mouse Fgf15 orthologs is regulated in the developing brain by Fgf8 and Shh. *Dev Dyn* **236**, 2285-97.

Glasgow, S. M., Henke, R. M., Macdonald, R. J., Wright, C. V. and Johnson, J. E. (2005). Ptf1a determines GABAergic over glutamatergic neuronal cell fate in the spinal cord dorsal horn. *Development* **132**, 5461-9.

Glover, J. C. (2000). Development of specific connectivity between premotor neurons and motoneurons in the brain stem and spinal cord. *Physiol Rev* **80**, 615-47.

Gomez-Pinilla, F., Ying, Z., Opazo, P., Roy, R. R. and Edgerton, V. R. (2001). Differential regulation by exercise of BDNF and NT-3 in rat spinal cord and skeletal muscle. *Eur J Neurosci* **13**, 1078-84.

Gong, S., Zheng, C., Doughty, M. L., Losos, K., Didkovsky, N., Schambra, U. B., Nowak, N. J., Joyner, A., Leblanc, G., Hatten, M. E. et al. (2003). A gene expression atlas of the central nervous system based on bacterial artificial chromosomes. *Nature* **425**, 917-25.

Gross, M. K., Dottori, M. and Goulding, M. (2002). Lbx1 specifies somatosensory association interneurons in the dorsal spinal cord. *Neuron* **34**, 535-49.

Guo, J., Chung, U. I., Kondo, H., Bringhurst, F. R. and Kronenberg, H. M. (2002). The PTH/PTHrP receptor can delay chondrocyte hypertrophy in vivo without activating phospholipase C. *Dev Cell* **3**, 183-94.

Guo, T., Mandai, K., Condie, B. G., Wickramasinghe, S. R., Capecchi, M. R. and Ginty, D. D. (2011). An evolving NGF-Hoxd1 signaling pathway mediates development of divergent neural circuits in vertebrates. *Nat Neurosci* **14**, 31-6.

Gutin, G., Fernandes, M., Palazzolo, L., Paek, H., Yu, K., Ornitz, D. M., McConnell, S. K. and Hebert, J. M. (2006). FGF signalling generates ventral telencephalic cells independently of SHH. *Development* **133**, 2937-46.

Haase, G., Dessaud, E., Garces, A., de Bovis, B., Birling, M., Filippi, P., Schmalbruch, H., Arber, S. and deLapeyriere, O. (2002). GDNF acts through PEA3 to regulate cell body positioning and muscle innervation of specific motor neuron pools. *Neuron* **35**, 893-905.

Haeberle, H., Fujiwara, M., Chuang, J., Medina, M. M., Panditrao, M. V., Bechstedt, S., Howard, J. and Lumpkin, E. A. (2004). Molecular profiling reveals synaptic release machinery in Merkel cells. *Proc Natl Acad Sci U S A* **101**, 14503-8.

Hanashima, C., Fernandes, M., Hebert, J. M. and Fishell, G. (2007). The role of Foxg1 and dorsal midline signaling in the generation of Cajal-Retzius subtypes. *J Neurosci* **27**, 11103-11.

Hantman, A. W. and Jessell, T. M. (2010). Clarke's column neurons as the focus of a corticospinal corollary circuit. *Nat Neurosci* **13**, 1233-9.

Hevner, R. F., Daza, R. A., Rubenstein, J. L., Stunnenberg, H., Olavarria, J. F. and Englund, C. (2003). Beyond laminar fate: toward a molecular classification of cortical projection/pyramidal neurons. *Dev Neurosci* **25**, 139-51.

Hevner, R. F., Shi, L., Justice, N., Hsueh, Y., Sheng, M., Smiga, S., Bulfone, A., Goffinet, A. M., Campagnoni, A. T. and Rubenstein, J. L. (2001). Tbr1 regulates differentiation of the preplate and layer 6. *Neuron* **29**, 353-66.

Hippenmeyer, S., Kramer, I. and Arber, S. (2004). Control of neuronal phenotype: what targets tell the cell bodies. *Trends Neurosci* **27**, 482-8.

Hippenmeyer, S., Vrieseling, E., Sigrist, M., Portmann, T., Laengle, C., Ladle, D. R. and Arber, S. (2005). A developmental switch in the response of DRG neurons to ETS transcription factor signaling. *PLoS Biol* **3**, e159.

Hirsch, M. R., Glover, J. C., Dufour, H. D., Brunet, J. F. and Goridis, C. (2007). Forced expression of Phox2 homeodomain transcription factors induces a branchio-visceromotor axonal phenotype. *Dev Biol* **303**, 687-702.

Hochman, S., Shreckengost, J., Kimura, H. and Quevedo, J. (2010). Presynaptic inhibition of primary afferents by depolarization: observations supporting nontraditional mechanisms. *Ann N Y Acad Sci* **1198**, 140-52.

Hodge, L. K., Klassen, M. P., Han, B. X., Yiu, G., Hurrell, J., Howell, A., Rousseau, G., Lemaigre, F., Tessier-Lavigne, M. and Wang, F. (2007). Retrograde BMP signaling regulates trigeminal sensory neuron identities and the formation of precise face maps. *Neuron* **55**, 572-86.

Hofer, M. M. and Barde, Y. A. (1988). Brain-derived neurotrophic factor prevents neuronal death in vivo. *Nature* **331**, 261-2.

Hohn, A., Leibrock, J., Bailey, K. and Barde, Y. A. (1990). Identification and characterization of a novel member of the nerve growth factor/brain-derived neurotrophic factor family. *Nature* **344**, 339-41.

Holstege, J. C. and Calkoen, F. (1990). The distribution of GABA in lumbar motoneuronal cell groups. A quantitative ultrastructural study in rat. *Brain Res* **530**, 130-7.

Huang, E. J. and Reichardt, L. F. (2001). Neurotrophins: roles in neuronal development and function. *Annu Rev Neurosci* **24**, 677-736.

Huber, A. B., Kolodkin, A. L., Ginty, D. D. and Cloutier, J. F. (2003). Signaling at the growth cone: ligand-receptor complexes and the control of axon growth and guidance. *Annu Rev Neurosci* **26**, 509-63.

Huberman, A. D. (2006). Target-derived cues instruct synaptic differentiation. *J Neurosci* **26**, 1063-4.

Hughes, D. I., Mackie, M., Nagy, G. G., Riddell, J. S., Maxwell, D. J., Szabo, G., Erdelyi, F., Veress, G., Szucs, P., Antal, M. et al. (2005). P boutons in lamina IX of the rodent spinal cord express high levels of glutamic acid decarboxylase-65 and originate from cells in deep medial dorsal horn. *Proc Natl Acad Sci U S A* **102**, 9038-43.

Imayoshi, I., Shimogori, T., Ohtsuka, T. and Kageyama, R. (2008). Hes genes and neurogenin regulate non-neural versus neural fate specification in the dorsal telencephalic midline. *Development* **135**, 2531-41.

Ip, N. Y., Ibanez, C. F., Nye, S. H., McClain, J., Jones, P. F., Gies, D. R., Belluscio, L., Le Beau, M. M., Espinosa, R., 3rd, Squinto, S. P. et al. (1992). Mammalian neurotrophin-4: structure, chromosomal localization, tissue distribution, and receptor specificity. *Proc Natl Acad Sci U S A* **89**, 3060-4.

Jessell, T. M. and Sanes, J. R. (2000). Development. The decade of the developing brain. *Curr Opin Neurobiol* **10**, 599-611.

Kaplan, M. R., Cho, M. H., Ullian, E. M., Isom, L. L., Levinson, S. R. and Barres, B. A. (2001). Differential control of clustering of the sodium channels Na(v)1.2 and Na(v)1.6 at developing CNS nodes of Ranvier. *Neuron* **30**, 105-19.

Kawauchi, S., Shou, J., Santos, R., Hebert, J. M., McConnell, S. K., Mason, I. and Calof, A. L. (2005). Fgf8 expression defines a morphogenetic center required for olfactory neurogenesis and nasal cavity development in the mouse. *Development* **132**, 5211-23.

Kimura, J., Suda, Y., Kurokawa, D., Hossain, Z. M., Nakamura, M., Takahashi, M., Hara, A. and Aizawa, S. (2005). Emx2 and Pax6 function in cooperation with Otx2 and Otx1 to develop caudal forebrain primordium that includes future archipallium. *J Neurosci* **25**, 5097-108.

Klein, R., Silos-Santiago, I., Smeyne, R. J., Lira, S. A., Brambilla, R., Bryant, S., Zhang, L., Snider, W. D. and Barbacid, M. (1994). Disruption of the neurotrophin-3 receptor gene trkC eliminates la muscle afferents and results in abnormal movements. *Nature* **368**, 249-51.

Kralic, J. E., Korpi, E. R., O'Buckley, T. K., Homanics, G. E. and Morrow, A. L. (2002a). Molecular and pharmacological characterization of GABA(A) receptor alpha1 subunit knockout mice. *J Pharmacol Exp Ther* **302**, 1037-45.

Kralic, J. E., O'Buckley, T. K., Khisti, R. T., Hodge, C. W., Homanics, G. E. and Morrow, A. L. (2002b). GABA(A) receptor alpha-1 subunit deletion alters receptor subtype assembly, pharmacological and behavioral responses to benzodiazepines and zolpidem. *Neuropharmacology* **43**, 685-94.

Kralic, J. E., Sidler, C., Parpan, F., Homanics, G. E., Morrow, A. L. and Fritschy, J. M. (2006). Compensatory alteration of inhibitory synaptic circuits in cerebellum and thalamus of gamma-aminobutyric acid type A receptor alpha1 subunit knockout mice. *J Comp Neurol* **495**, 408-21.

Kramer, I., Sigrist, M., de Nooij, J. C., Taniuchi, I., Jessell, T. M. and Arber, S. (2006). A role for Runx transcription factor signaling in dorsal root ganglion sensory neuron diversification. *Neuron* **49**, 379-93.

Krimm, R. F., Davis, B. M., Woodbury, C. J. and Albers, K. M. (2004). NT3 expressed in skin causes enhancement of SA1 sensory neurons that leads to postnatal enhancement of Merkel cells. *J Comp Neurol* **471**, 352-60.

Kuschel, S., Ruther, U. and Theil, T. (2003). A disrupted balance between Bmp/Wnt and Fgf signaling underlies the ventralization of the Gli3 mutant telencephalon. *Dev Biol* **260**, 484-95.

Ladle, D. R., Pecho-Vrieseling, E. and Arber, S. (2007). Assembly of motor circuits in the spinal cord: driven to function by genetic and experience-dependent mechanisms. *Neuron* **56**, 270-83.

Landmesser, L. and Morris, D. G. (1975). The development of functional innervation in the hind limb of the chick embryo. *J Physiol* **249**, 301-26.

Landmesser, L. T. (2001). The acquisition of motoneuron subtype identity and motor circuit formation. *Int J Dev Neurosci* **19**, 175-82.

Lee, H. Y., Kleber, M., Hari, L., Brault, V., Suter, U., Taketo, M. M., Kemler, R. and Sommer, L. (2004). Instructive role of Wnt/beta-catenin in sensory fate specification in neural crest stem cells. *Science* **303**, 1020-3.

Lee, S. M., Tole, S., Grove, E. and McMahon, A. P. (2000). A local Wnt-3a signal is required for development of the mammalian hippocampus. *Development* **127**, 457-67.

Levi-Montalcini, R. and Booker, B. (1960). DESTRUCTION OF THE SYMPATHETIC GANGLIA IN MAMMALS BY AN ANTISERUM TO A NERVE-GROWTH PROTEIN. *Proc Natl Acad Sci U S A* **46**, 384-91.

Levitan, E. S., Schofield, P. R., Burt, D. R., Rhee, L. M., Wisden, W., Kohler, M., Fujita, N., Rodriguez, H. F., Stephenson, A., Darlison, M. G. et al. (1988). Structural and functional basis for GABAA receptor heterogeneity. *Nature* **335**, 76-9.

Lin, J. H., Saito, T., Anderson, D. J., Lance-Jones, C., Jessell, T. M. and Arber, S. (1998). Functionally related motor neuron pool and muscle sensory afferent subtypes defined by coordinate ETS gene expression. *Cell* **95**, 393-407.

Liu, A., Li, J. Y., Bromleigh, C., Lao, Z., Niswander, L. A. and Joyner, A. L. (2003). FGF17b and FGF18 have different midbrain regulatory properties from FGF8b or activated FGF receptors. *Development* **130**, 6175-85.

Livet, J., Sigrist, M., Stroebel, S., De Paola, V., Price, S. R., Henderson, C. E., Jessell, T. M. and Arber, S. (2002). ETS gene Pea3 controls the central position and terminal arborization of specific motor neuron pools. *Neuron* **35**, 877-92.

Lu, B., Pang, P. T. and Woo, N. H. (2005). The yin and yang of neurotrophin action. *Nat Rev Neurosci* **6**, 603-14.

Luo, W., Wickramasinghe, S. R., Savitt, J. M., Griffin, J. W., Dawson, T. M. and Ginty, D. D. (2007). A hierarchical NGF signaling cascade controls Ret-dependent and Ret-independent events during development of nonpeptidergic DRG neurons. *Neuron* **54**, 739-54.

Luscher, B., Fuchs, T. and Kilpatrick, C. L. (2011). GABA(A) Receptor Trafficking-Mediated Plasticity of Inhibitory Synapses. *Neuron* **70**, 385-409.

Ma, Q., Fode, C., Guillemot, F. and Anderson, D. J. (1999). Neurogenin1 and neurogenin2 control two distinct waves of neurogenesis in developing dorsal root ganglia. *Genes Dev* **13**, 1717-28.

Maier, A. (1997). Development and regeneration of muscle spindles in mammals and birds. *Int J Dev Biol* **41**, 1-17.

Maisonpierre, P. C., Belluscio, L., Squinto, S., Ip, N. Y., Furth, M. E., Lindsay, R. M. and Yancopoulos, G. D. (1990). Neurotrophin-3: a neurotrophic factor related to NGF and BDNF. *Science* **247**, 1446-51.

Mallamaci, A., Mercurio, S., Muzio, L., Cecchi, C., Pardini, C. L., Gruss, P. and Boncinelli, E. (2000). The lack of Emx2 causes impairment of Reelin signaling and defects of neuronal migration in the developing cerebral cortex. *J Neurosci* **20**, 1109-18.

Marin-Padilla, M. (1990). Three-dimensional structural organization of layer I of the human cerebral cortex: a Golgi study. *J Comp Neurol* **299**, 89-105.

Marin-Padilla, M. (1992). Ontogenesis of the pyramidal cell of the mammalian neocortex and developmental cytoarchitectonics: a unifying theory. *J Comp Neurol* **321**, 223-40.

Marin-Padilla, M. (1998). Cajal-Retzius cells and the development of the neocortex. *Trends Neurosci* **21**, 64-71.

Marin, O. and Rubenstein, J. L. (2003). Cell migration in the forebrain. *Annu Rev Neurosci* **26**, 441-83.

Marmigere, F. and Ernfors, P. (2007). Specification and connectivity of neuronal subtypes in the sensory lineage. *Nat Rev Neurosci* **8**, 114-27.

Maro, G. S., Vermeren, M., Voiculescu, O., Melton, L., Cohen, J., Charnay, P. and Topilko, P. (2004). Neural crest boundary cap cells constitute a source of neuronal and glial cells of the PNS. *Nat Neurosci* **7**, 930-8.

McIlwrath, S. L., Lawson, J. J., Anderson, C. E., Albers, K. M. and Koerber, H. R. (2007). Overexpression of neurotrophin-3 enhances the mechanical response properties of slowly adapting type 1 afferents and myelinated nociceptors. *Eur J Neurosci* **26**, 1801-12.

Mendelson, B. and Frank, E. (1991). Specific monosynaptic sensory-motor connections form in the absence of patterned neural activity and motoneuronal cell death. *J Neurosci* **11**, 1390-403.

Meng, Y., Zhang, Y. and Jia, Z. (2003). Synaptic transmission and plasticity in the absence of AMPA glutamate receptor GluR2 and GluR3. *Neuron* **39**, 163-76.

Merzenich, M. M., Jenkins, W. M., Johnston, P., Schreiner, C., Miller, S. L. and Tallal, P. (1996). Temporal processing deficits of language-learning impaired children ameliorated by training. *Science* **271**, 77-81.

Meyer, G., Cabrera Socorro, A., Perez Garcia, C. G., Martinez Millan, L., Walker, N. and Caput, D. (2004). Developmental roles of p73 in Cajal-Retzius cells and cortical patterning. *J Neurosci* **24**, 9878-87.

Meyer, G., Perez-Garcia, C. G., Abraham, H. and Caput, D. (2002). Expression of p73 and Reelin in the developing human cortex. *J Neurosci* **22**, 4973-86.

Meyers, E. N., Lewandoski, M. and Martin, G. R. (1998). An Fgf8 mutant allelic series generated by Cre- and Flp-mediated recombination. *Nat Genet* **18**, 136-41.

Minichiello, L., Piehl, F., Vazquez, E., Schimmang, T., Hokfelt, T., Represa, J. and Klein, R. (1995). Differential effects of combined trk receptor mutations on dorsal root ganglion and inner ear sensory neurons. *Development* **121**, 4067-75.

Mirnics, K. and Koerber, H. R. (1995). Prenatal development of rat primary afferent fibers: II. Central projections. *J Comp Neurol* **355**, 601-14.

Mohammadi, M., McMahon, G., Sun, L., Tang, C., Hirth, P., Yeh, B. K., Hubbard, S. R. and Schlessinger, J. (1997). Structures of the tyrosine kinase domain of fibroblast growth factor receptor in complex with inhibitors. *Science* **276**, 955-60.

Molliver, D. C., Radeke, M. J., Feinstein, S. C. and Snider, W. D. (1995). Presence or absence of TrkA protein distinguishes subsets of small sensory neurons with unique cytochemical characteristics and dorsal horn projections. *J Comp Neurol* **361**, 404-16.

Molliver, D. C. and Snider, W. D. (1997). Nerve growth factor receptor TrkA is down-regulated during postnatal development by a subset of dorsal root ganglion neurons. *J Comp Neurol* **381**, 428-38.

Molyneaux, B. J., Arlotta, P., Menezes, J. R. and Macklis, J. D. (2007). Neuronal subtype specification in the cerebral cortex. *Nat Rev Neurosci* **8**, 427-37.

Monuki, E. S., Porter, F. D. and Walsh, C. A. (2001). Patterning of the dorsal telencephalon and cerebral cortex by a roof plate-Lhx2 pathway. *Neuron* **32**, 591-604.

Muller, T., Brohmann, H., Pierani, A., Heppenstall, P. A., Lewin, G. R., Jessell, T. M. and Birchmeier, C. (2002). The homeodomain factor lbx1 distinguishes two major programs of neuronal differentiation in the dorsal spinal cord. *Neuron* **34**, 551-62.

Nomura, T., Takahashi, M., Hara, Y. and Osumi, N. (2008). Patterns of neurogenesis and amplitude of Reelin expression are essential for making a mammalian-type cortex. *PLoS One* **3**, e1454.

O'Leary, D. D., Chou, S. J. and Sahara, S. (2007). Area patterning of the mammalian cortex. *Neuron* **56**, 252-69.

Oakley, R. A., Garner, A. S., Large, T. H. and Frank, E. (1995). Muscle sensory neurons require neurotrophin-3 from peripheral tissues during the period of normal cell death. *Development* **121**, 1341-50.

Ogawa, M., Miyata, T., Nakajima, K., Yagyu, K., Seike, M., Ikenaka, K., Yamamoto, H. and Mikoshiba, K. (1995). The reeler gene-associated antigen on Cajal-Retzius neurons is a crucial molecule for laminar organization of cortical neurons. *Neuron* **14**, 899-912.

Ohkubo, Y., Chiang, C. and Rubenstein, J. L. (2002). Coordinate regulation and synergistic actions of BMP4, SHH and FGF8 in the rostral prosencephalon regulate morphogenesis of the telencephalic and optic vesicles. *Neuroscience* **111**, 1-17.

Okada, T., Okumura, Y., Motoyama, J. and Ogawa, M. (2008). FGF8 signaling patterns the telencephalic midline by regulating putative key factors of midline development. *Dev Biol* **320**, 92-101.

Okaty, B. W., Sugino, K. and Nelson, S. B. (2011). A quantitative comparison of cell-type-specific microarray gene expression profiling methods in the mouse brain. *PLoS One* **6**, e16493.

Olsen, R. W. (1982). Drug interactions at the GABA receptor-ionophore complex. *Annu Rev Pharmacol Toxicol* **22**, 245-77.

Ornung, G., Shupliakov, O., Linda, H., Ottersen, O. P., Storm-Mathisen, J., Ulfhake, B. and Cullheim, S. (1996). Qualitative and quantitative analysis of glycine- and GABA-immunoreactive nerve terminals on motoneuron cell bodies in the cat spinal cord: a postembedding electron microscopic study. *J Comp Neurol* **365**, 413-26.

Ozaki, S. and Snider, W. D. (1997). Initial trajectories of sensory axons toward laminar targets in the developing mouse spinal cord. *J Comp Neurol* **380**, 215-29.

Paek, H., Gutin, G. and Hebert, J. M. (2009). FGF signaling is strictly required to maintain early telencephalic precursor cell survival. *Development* **136**, 2457-65.

Patel, T. D., Jackman, A., Rice, F. L., Kucera, J. and Snider, W. D. (2000). Development of sensory neurons in the absence of NGF/TrkA signaling in vivo. *Neuron* **25**, 345-57.

Patel, T. D., Kramer, I., Kucera, J., Niederkofler, V., Jessell, T. M., Arber, S. and Snider, W. D. (2003). Peripheral NT3 signaling is required for ETS protein expression and central patterning of proprioceptive sensory afferents. *Neuron* **38**, 403-16.

Pellegrini, M., Mansouri, A., Simeone, A., Boncinelli, E. and Gruss, P. (1996). Dentate gyrus formation requires Emx2. *Development* **122**, 3893-8.

Pfaff, S. L., Mendelsohn, M., Stewart, C. L., Edlund, T. and Jessell, T. M. (1996). Requirement for LIM homeobox gene Isl1 in motor neuron generation reveals a motor neuron-dependent step in interneuron differentiation. *Cell* **84**, 309-20.

Pierce, J. P. and Mendell, L. M. (1993). Quantitative ultrastructure of Ia boutons in the ventral horn: scaling and positional relationships. *J Neurosci* **13**, 4748-63.

Prats-Galino, A., Puigdellivol-Sanchez, A., Ruano-Gil, D. and Molander, C. (1999). Representations of hindlimb digits in rat dorsal root ganglia. *J Comp Neurol* **408**, 137-45.

Rakic, P. (1988). Specification of cerebral cortical areas. *Science* **241**, 170-6.

Rash, B. G. and Grove, E. A. (2006). Area and layer patterning in the developing cerebral cortex. *Curr Opin Neurobiol* **16**, 25-34.

Rash, B. G. and Grove, E. A. (2007). Patterning the dorsal telencephalon: a role for sonic hedgehog? *J Neurosci* **27**, 11595-603.

Reichardt, L. F. (2006). Neurotrophin-regulated signalling pathways. *Philos Trans R Soc Lond B Biol Sci* **361**, 1545-64.

Rice, D. S. and Curran, T. (2001). Role of the reelin signaling pathway in central nervous system development. *Annu Rev Neurosci* **24**, 1005-39.

Rudomin, P. and Schmidt, R. F. (1999). Presynaptic inhibition in the vertebrate spinal cord revisited. *Exp Brain Res* **129**, 1-37.

Ruediger, S., Vittori, C., Bednarek, E., Genoud, C., Strata, P., Sacchetti, B. and Caroni, P. (2011). Learning-related feedforward inhibitory connectivity growth required for memory precision. *Nature* **473**, 514-8.

Sanes, J. R. and Yamagata, M. (1999). Formation of lamina-specific synaptic connections. *Curr Opin Neurobiol* **9**, 79-87.

Sato, T., Araki, I. and Nakamura, H. (2001). Inductive signal and tissue responsiveness defining the tectum and the cerebellum. *Development* **128**, 2461-9.

Shanmugalingam, S., Houart, C., Picker, A., Reifers, F., Macdonald, R., Barth, A., Griffin, K., Brand, M. and Wilson, S. W. (2000). Ace/Fgf8 is required for forebrain commissure formation and patterning of the telencephalon. *Development* **127**, 2549-61.

Sharma, N., Deppmann, C. D., Harrington, A. W., St Hillaire, C., Chen, Z. Y., Lee, F. S. and Ginty, D. D. (2010a). Long-distance control of synapse assembly by target-derived NGF. *Neuron* **67**, 422-34.

Sharma, N. K., Ryals, J. M., Gajewski, B. J. and Wright, D. E. (2010b). Aerobic exercise alters analgesia and neurotrophin-3 synthesis in an animal model of chronic widespread pain. *Phys Ther* **90**, 714-25.

Sharrocks, A. D. (2001). The ETS-domain transcription factor family. *Nat Rev Mol Cell Biol* **2**, 827-37.

Sherrington, C. S. (1906). The Integrative Action of the Nervous System. *2nd Edition (New Haven,NJ: Yale University Press).*

Sherrington, C. S. (1910). Flexion-reflex of the limb, crossed extension-reflex, and reflex stepping and standing. *J Physiol* **40**, 28-121.

Shimamura, K. and Rubenstein, J. L. (1997). Inductive interactions direct early regionalization of the mouse forebrain. *Development* **124**, 2709-18.

Shimogori, T., Banuchi, V., Ng, H. Y., Strauss, J. B. and Grove, E. A. (2004). Embryonic signaling centers expressing BMP, WNT and FGF proteins interact to pattern the cerebral cortex. *Development* **131**, 5639-47.

Shinozaki, K., Miyagi, T., Yoshida, M., Miyata, T., Ogawa, M., Aizawa, S. and Suda, Y. (2002). Absence of Cajal-Retzius cells and subplate neurons associated with defects of tangential cell migration from ganglionic eminence in Emx1/2 double mutant cerebral cortex. *Development* **129**, 3479-92.

Siegenthaler, J. A. and Miller, M. W. (2008). Generation of Cajal-Retzius neurons in mouse forebrain is regulated by transforming growth factor beta-Fox signaling pathways. *Dev Biol* **313**, 35-46.

Smith, C. L. and Frank, E. (1988). Specificity of sensory projections to the spinal cord during development in bullfrogs. *J Comp Neurol* **269**, 96-108.

Snider, W. D. (1994). Functions of the neurotrophins during nervous system development: what the knockouts are teaching us. *Cell* **77**, 627-38.

Soriano, E., Alvarado-Mallart, R. M., Dumesnil, N., Del Rio, J. A. and Sotelo, C. (1997). Cajal-Retzius cells regulate the radial glia phenotype in the adult and developing cerebellum and alter granule cell migration. *Neuron* **18**, 563-77.

Storm, E. E., Garel, S., Borello, U., Hebert, J. M., Martinez, S., McConnell, S. K., Martin, G. R. and Rubenstein, J. L. (2006). Dose-dependent functions of Fgf8 in regulating telencephalic patterning centers. *Development* **133**, 1831-44.

Storm, E. E., Rubenstein, J. L. and Martin, G. R. (2003). Dosage of Fgf8 determines whether cell survival is positively or negatively regulated in the developing forebrain. *Proc Natl Acad Sci U S A* **100**, 1757-62.

Stoykova, A., Fritsch, R., Walther, C. and Gruss, P. (1996). Forebrain patterning defects in Small eye mutant mice. *Development* **122**, 3453-65.

Stoykova, A., Hatano, O., Gruss, P. and Gotz, M. (2003). Increase in reelin-positive cells in the marginal zone of Pax6 mutant mouse cortex. *Cereb Cortex* **13**, 560-71.

Sung, K. W., Kirby, M., McDonald, M. P., Lovinger, D. M. and Delpire, E. (2000). Abnormal GABAA receptor-mediated currents in dorsal root ganglion neurons isolated from Na-K-2Cl cotransporter null mice. *J Neurosci* **20**, 7531-8.

Super, H., Del Rio, J. A., Martinez, A., Perez-Sust, P. and Soriano, E. (2000). Disruption of neuronal migration and radial glia in the developing cerebral cortex following ablation of Cajal-Retzius cells. *Cereb Cortex* **10**, 602-13.

Sur, C., Wafford, K. A., Reynolds, D. S., Hadingham, K. L., Bromidge, F., Macaulay, A., Collinson, N., O'Meara, G., Howell, O., Newman, R. et al. (2001). Loss of the major GABA(A) receptor subtype in the brain is not lethal in mice. *J Neurosci* **21**, 3409-18.

Sur, M. and Rubenstein, J. L. (2005). Patterning and plasticity of the cerebral cortex. *Science* **310**, 805-10.

Takiguchi-Hayashi, K., Sekiguchi, M., Ashigaki, S., Takamatsu, M., Hasegawa, H., Suzuki-Migishima, R., Yokoyama, M., Nakanishi, S. and Tanabe, Y. (2004). Generation of reelin-positive marginal zone cells from the caudomedial wall of telencephalic vesicles. *J Neurosci* **24**, 2286-95.

Taylor, M. D., Vancura, R., Patterson, C. L., Williams, J. M., Riekhof, J. T. and Wright, D. E. (2001). Postnatal regulation of limb proprioception by muscle-derived neurotrophin-3. *J Comp Neurol* **432**, 244-58.

Tessarollo, L., Vogel, K. S., Palko, M. E., Reid, S. W. and Parada, L. F. (1994). Targeted mutation in the neurotrophin-3 gene results in loss of muscle sensory neurons. *Proc Natl Acad Sci U S A* **91**, 11844-8.

Tessier-Lavigne, M. and Goodman, C. S. (1996). The molecular biology of axon guidance. *Science* **274**, 1123-33.

Theil, T. (2005). Gli3 is required for the specification and differentiation of preplate neurons. *Dev Biol* **286**, 559-71.

Theil, T., Alvarez-Bolado, G., Walter, A. and Ruther, U. (1999). Gli3 is required for Emx gene expression during dorsal telencephalon development. *Development* **126**, 3561-71.

Tucker, K. L., Meyer, M. and Barde, Y. A. (2001). Neurotrophins are required for nerve growth during development. *Nat Neurosci* **4**, 29-37.

Tuoc, T. C. and Stoykova, A. (2008). Er81 is a downstream target of Pax6 in cortical progenitors. *BMC Dev Biol* **8**, 23.

Van Der Giessen, R. S., Koekkoek, S. K., van Dorp, S., De Gruijl, J. R., Cupido, A., Khosrovani, S., Dortland, B., Wellershaus, K., Degen, J.,

Deuchars, J. et al. (2008). Role of olivary electrical coupling in cerebellar motor learning. *Neuron* **58**, 599-612.

van Praag, H., Shubert, T., Zhao, C. and Gage, F. H. (2005). Exercise enhances learning and hippocampal neurogenesis in aged mice. *J Neurosci* **25**, 8680-5.

Vrieseling, E. and Arber, S. (2006). Target-induced transcriptional control of dendritic patterning and connectivity in motor neurons by the ETS gene Pea3. *Cell* **127**, 1439-52.

Wang, Z., Li, L. Y., Taylor, M. D., Wright, D. E. and Frank, E. (2007). Prenatal exposure to elevated NT3 disrupts synaptic selectivity in the spinal cord. *J Neurosci* **27**, 3686-94.

Watson, A. H. and Bazzaz, A. A. (2001). GABAAnd glycine-like immunoreactivity at axoaxonic synapses on 1a muscle afferent terminals in the spinal cord of the rat. *J Comp Neurol* **433**, 335-48.

Wenner, P. and Frank, E. (1995). Peripheral target specification of synaptic connectivity of muscle spindle sensory neurons with spinal motoneurons. *J Neurosci* **15**, 8191-8.

Yoshida, M., Assimacopoulos, S., Jones, K. R. and Grove, E. A. (2006). Massive loss of Cajal-Retzius cells does not disrupt neocortical layer order. *Development* **133**, 537-45.

Yoshida, M., Suda, Y., Matsuo, I., Miyamoto, N., Takeda, N., Kuratani, S. and Aizawa, S. (1997). Emx1 and Emx2 functions in development of dorsal telencephalon. *Development* **124**, 101-11.

Yun, K., Potter, S. and Rubenstein, J. L. (2001). Gsh2 and Pax6 play complementary roles in dorsoventral patterning of the mammalian telencephalon. *Development* **128**, 193-205.

Zecevic, N. and Rakic, P. (2001). Development of layer I neurons in the primate cerebral cortex. *J Neurosci* **21**, 5607-19.

Zelena, J. (1994). Nerves and Mechanoreceptors: the role of innervation in the development and
maintenance of mammalian mechanoreceptors. *London, Chapman & Hall*.

Zelena, J. and Soukup, T. (1977). The development of Golgi tendon organs. *J Neurocytol* **6**, 171-94.

Zhao, C., Guan, W. and Pleasure, S. J. (2006). A transgenic marker mouse line labels Cajal-Retzius cells from the cortical hem and thalamocortical axons. *Brain Res* **1077**, 48-53.

10. Curriculum vitae

Name: Jun Lee
Birthdate: 16 July 1979
Place of Birth: Wiesbaden / Germany
Nationality: German

Klingnaustr.26
4058 Basel
Switzerland
Email: junlee@fmi.ch

Education

Sept 2005 until present

PhD student in the Lab of Prof. Silvia Arber, Friedrich Miescher Institute (FMI) for Biomedical Research, Basel/Switzerland

Oct 1999 to Feb 2005

Johannes Gutenberg University, Mainz/Germany, Diploma in Biology

1990 to 1999

Bischöfliches Willigis Gymnasium Mainz/Germany

Research Experience

09/2005 to 06/2011: PhD thesis in the lab of Prof. Silvia Arber, Friedrich Miescher Institute (FMI) for Biomedical Research, Basel/Switzerland
"Scaling Proprioceptor Gene Transcription by Retrograde NT3 Signaling"

06/2004 to 02/2005: Diploma thesis under supervision of Prof. Stephan Kröger, Johannes Gutenberg University, Mainz/Germany (now at Ludwig Maximilians University, Munich/Germany)
"**Analysis of the Role of the Dytrophin-associated Protein Complex in the Developing CNS using RNAi"**
Final mark: 1 (1 = best, 6 = worst), within top 10% of that year`s graduates

09/2003 to 12/2003: Voluntary internship at BioSpring (www.biospring-online.de), Frankfurt a.M./Germany
Internal project: **Mutagensis and subsequent characterization of selected enzymes**

Publications

Lee J, Arber S (in preparation) **Scaling Proprioceptor Gene Transcription by Retrograde NT3 Signaling.**

Zimmer C, **Lee J**, Griveau A, Arber S, Pierani A, Garel S, Guillemot F (2010) **Role of Fgf8 signalling in the specification of rostral Cajal-Retzius cells.** Development 137:293 - 302.

Schröder JE, Tegeler MR, Grosshans U, Porten E, Blank M, **Lee J**, Esapa C, Blake DJ, Kröger S (2007) **Dystroglycan regulates structure, proliferation and differentiation of neuroepithelial cells in the developing vertebrate CNS.** Dev Biol 307:62 - 78.

Posters

Lee J & Arber S, **Effect of target-derived NT3 on transcriptional regulation in the spinal monosynaptic reflex circuit.** Soc.Neurosci. San Diego, CA, November 13-17 2010

Lee J & Arber S, **Influence of target-derived NT3 on transcriptional regulation in the spinal monosynaptic reflex circuit.** FENS Amsterdam, July 3-7 2010, Abstr. 129.4

Scholarships

2004 Scholarship of the Johannes Gutenberg University, Mainz/Germany

Additional activities

- 2009 Organizer for the Joint PhD Meeting between FMI and UC London
- Since 2008, FMI student representative, responsible for the organization of the Student Science Colloquia and the Student Career Seminars
- 2007 tutor for 1st semester students, University of Basel
- 2007 German representative for the Young Generation Forum, Seoul/South Korea
- Since 2000 mentor for Juforum (German association for pupils and young students interested in Science and Engineering, www.juforum.de)

Additional Skills

- Adobe Products, CorelDraw, Bitplane Imaris, ImageJ
- VectorNTI
- Ingenuity Pathway Analysis
- Genedata Expressionist
- Basics in SigmaPlot
- Basics in R
- Languages: German, English, Korean (intermediate), French (basics)

Reference contacts

Prof. Silvia Arber (PhD thesis adivsor)
Biozentrum Basel & FMI Basel
Switzerland
Email: Silvia.Arber@fmi.ch
Phone: +41 – 61 267 2057

Prof. Stephan Kröger (Diploma thesis advisor)
Ludwig Maximillians University
Munich
Switzerland
Email: stephan.kroeger@lrz.uni-muenchen.de
Phone: +49 – 89 2180 75526